ADDITIONAL MATERIALS AVAILABLE ON THE HEI WEBSITE

Research Report 210

Global Burden of Disease from Major Air Pollution Sources (GBD MAPS): A Global Approach

Erin McDuffie et al.

Additional Materials 1: McDuffie EE, Smith SJ, O'Rourke P, Tibrewal K, Venkataraman C, Marais EA, et al. 2020. A global anthropogenic emission inventory of atmospheric pollutants from sector- and fuel-specific sources (1970–2017): An application of the Community Emissions Data System (CEDS). Earth Syst Sci Data 12:3413–3442; doi:10.5194/essd-12-3413-2020.

Correspondence concerning the Investigators' Report may be addressed to Dr. Michael Brauer, The University of British Columbia, School of Population and Public Health, 366A – 2206 East Mall, Vancouver, BC V6T1Z3, Canada; e-mail: *michael.brauer@ubc.camonica.guxens@isglobal.org*.

Earth Syst. Sci. Data, 12, 3413–3442, 2020
https://doi.org/10.5194/essd-12-3413-2020

Open Access Earth System Science Data

A global anthropogenic emission inventory of atmospheric pollutants from sector- and fuel-specific sources (1970–2017): an application of the Community Emissions Data System (CEDS)

Erin E. McDuffie[1,2], **Steven J. Smith**[3], **Patrick O'Rourke**[3], **Kushal Tibrewal**[4], **Chandra Venkataraman**[4], **Eloise A. Marais**[5,a], **Bo Zheng**[6], **Monica Crippa**[7], **Michael Brauer**[8,9], and **Randall V. Martin**[2,1]

[1]Department of Physics and Atmospheric Science, Dalhousie University, Halifax, NS, Canada
[2]Department of Energy, Environmental, and Chemical Engineering, Washington University in St. Louis, St. Louis, MO, USA
[3]Joint Global Change Research Institute, Pacific Northwest National Laboratory, College Park, MD, USA
[4]Department of Chemical Engineering, Indian Institute of Technology Bombay, Mumbai, Maharashtra, India
[5]School of Physics and Astronomy, University of Leicester, Leicester, UK
[6]Institute of Environment and Ecology, Tsinghua Shenzhen International Graduate School, Tsinghua University, Shenzhen 518055, China
[7]European Commission, Joint Research Centre (JRC), Via E. Fermi 2749 (T.P. 123), 21027 Ispra, Varese, Italy
[8]School of Population and Public Health, University of British Columbia, Vancouver, BC, Canada
[9]Institute for Health Metrics and Evaluation, University of Washington, Seattle, WA, USA
[a]now at: Department of Geography, University College London, London, UK

Correspondence: Erin E. McDuffie (erin.mcduffie@wustl.edu)

Received: 27 April 2020 – Discussion started: 3 June 2020
Revised: 4 October 2020 – Accepted: 27 October 2020 – Published: 15 December 2020

Abstract. Global anthropogenic emission inventories remain vital for understanding the sources of atmospheric pollution and the associated impacts on the environment, human health, and society. Rapid changes in today's society require that these inventories provide contemporary estimates of multiple atmospheric pollutants with both source sector and fuel type information to understand and effectively mitigate future impacts. To fill this need, we have updated the open-source Community Emissions Data System (CEDS) (Hoesly et al., 2019) to develop a new global emission inventory, $\mathrm{CEDS_{GBD\text{-}MAPS}}$. This inventory includes emissions of seven key atmospheric pollutants (NO_x; CO; SO_2; NH_3; non-methane volatile organic compounds, NMVOCs; black carbon, BC; organic carbon, OC) over the time period from 1970–2017 and reports annual country-total emissions as a function of 11 anthropogenic sectors (agriculture; energy generation; industrial processes; on-road and non-road transportation; separate residential, commercial, and other sectors (RCO); waste; solvent use; and international shipping) and four fuel categories (total coal, solid biofuel, the sum of liquid-fuel and natural-gas combustion, and remaining process-level emissions). The $\mathrm{CEDS_{GBD\text{-}MAPS}}$ inventory additionally includes monthly global gridded ($0.5° \times 0.5°$) emission fluxes for each compound, sector, and fuel type to facilitate their use in earth system models. $\mathrm{CEDS_{GBD\text{-}MAPS}}$ utilizes updated activity data, updates to the core CEDS default scaling procedure, and modifications to the final procedures for emissions gridding and aggregation. Relative to the previous CEDS inventory (Hoesly et al., 2018), these updates extend the emission estimates from 2014 to 2017 and improve the overall agreement between CEDS and two widely used global bottom-up emission inventories. The

$CEDS_{GBD-MAPS}$ inventory provides the most contemporary global emission estimates to date for these key atmospheric pollutants and is the first to provide global estimates for these species as a function of multiple fuel types and source sectors. Dominant sources of global NO_x and SO_2 emissions in 2017 include the combustion of oil, gas, and coal in the energy and industry sectors as well as on-road transportation and international shipping for NO_x. Dominant sources of global CO emissions in 2017 include on-road transportation and residential biofuel combustion. Dominant global sources of carbonaceous aerosol in 2017 include residential biofuel combustion, on-road transportation (BC only), and emissions from the waste sector. Global emissions of NO_x, SO_2, CO, BC, and OC all peak in 2012 or earlier, with more recent emission reductions driven by large changes in emissions from China, North America, and Europe. In contrast, global emissions of NH_3 and NMVOCs continuously increase between 1970 and 2017, with agriculture as a major source of global NH_3 emissions and solvent use, energy, residential, and the on-road transport sectors as major sources of global NMVOCs. Due to similar development methods and underlying datasets, the $CEDS_{GBD-MAPS}$ emissions are expected to have consistent sources of uncertainty as other bottom-up inventories. The $CEDS_{GBD-MAPS}$ source code is publicly available online through GitHub: https://github.com/emcduffie/CEDS/tree/CEDS_GBD-MAPS (last access: 1 December 2020). The $CEDS_{GBD-MAPS}$ emission inventory dataset (both annual country-total and monthly global gridded files) is publicly available under https://doi.org/10.5281/zenodo.3754964 (McDuffie et al., 2020c).

1 Introduction

Human activities emit a complex mixture of chemical compounds into the atmosphere, impacting air quality, the environment, and population health. For instance, direct emissions of nitric oxide (NO) rapidly oxidize to form nitrogen dioxide (NO_2) and can lead to net ozone (O_3) production in the presence of sunlight and oxidized volatile organic compounds (VOCs) (e.g., Chameides, 1978; Crutzen, 1970). In addition, direct emissions of particles containing organic carbon (OC) and black carbon (BC) as well as secondary reactions involving gaseous sulfur dioxide (SO_2), NO, ammonia (NH_3), and VOCs can lead to atmospheric fine particulate matter less than 2.5 µm in diameter ($PM_{2.5}$) (e.g., Mozurkewich, 1993; Jimenez et al., 2009; Saxena and Seigneur, 1987; Brock et al., 2002). $PM_{2.5}$ concentrations were estimated to account for nearly 3 million deaths worldwide in 2017 (GBD 2017 Risk Factor Collaborators, 2018), while surface O_3 concentrations were associated with nearly 500 000 deaths in 2017 (GBD 2017 Risk Factor Collaborators, 2018) and significant global crop losses, valued at USD 11 billion in 2000 (USD_{2000}) (Avnery et al., 2011; Ainsworth, 2017). In addition, atmospheric O_3 and aerosol both impact earth's radiative budget (e.g., Bond et al., 2013; Haywood and Boucher, 2000; US EPA, 2018). Other pollutants, including carbon monoxide (CO), NO_2, and SO_2, are also directly hazardous to human health (US EPA, 2018), while NO_2 and SO_2 can additionally contribute to acid rain (Saxena and Seigneur, 1987; US EPA, 2018) and indirectly impact human health via their contributions to secondary $PM_{2.5}$ formation. In addition, NH_3 deposition and nitrification can also cause nutrient imbalances and eutrophication in terrestrial and marine ecosystems (e.g., Behera et al., 2013; Stevens et al., 2004). While these reactive gases and aerosol have both anthropogenic and natural sources, dominant global sources of NO_x ($= NO + NO_2$), SO_2, CO, and VOCs include fuel transformation and use in the energy sector, industrial activities, and on-road and off-road transportation (Hoesly et al., 2018). Global NH_3 emissions are predominantly from agricultural activities such as animal husbandry and fertilizer application (e.g., Behera et al., 2013), and OC and BC have large contributions from incomplete or uncontrolled combustion in residential and commercial settings (e.g., Bond et al., 2013). Emissions of these compounds and the distribution of their chemical products vary spatially and temporally, with atmospheric lifetimes that allow for their transport across political boundaries, continuously driving changes in the composition of the global atmosphere.

Global emission inventories of these major atmospheric pollutants, with both sectoral and fuel type information, are paramount (1) for understanding the range of emission impacts on the environment and human health and (2) for developing effective strategies for pollution mitigation. For example, spatially gridded emission inventories are used as inputs in general circulation climate (GCM) and chemical transport models (CTM), which are used to predict the evolution of atmospheric constituents over space and time. By perturbing emission sources or historical emission trends, such models can quantify the impact of emissions on the environment, economy, and human health (e.g., Mauzerall et al., 2005; Lelieveld et al., 2019; IPCC, 2013; Liang et al., 2018; Lacey and Henze, 2015); provide mitigation-relevant information for polluted regions (e.g., GBD MAPS Working Group, 2016, 2018; RAQC, 2019; Lacey et al., 2017); and anchor future projections (e.g., Shindell and Smith, 2019; Venkataraman et al., 2018; Gidden et al., 2019; Mickley et al., 2004).

Three global emission inventories have been widely used for these purposes, including the Emissions Database for

Global Atmospheric Research (EDGAR) from the European Commission Joint Research Centre (Crippa et al., 2018), the ECLIPSE (Evaluating the Climate and Air Quality Impacts of Short-Lived Pollutants) inventory from the Greenhouse Gas–Air Pollution Interactions and Synergies (GAINS) model at the International Institute for Applied Systems Analysis (IIASA) (Amann et al., 2011; Klimont et al., 2017), and the CEDS (v2016-07-26) inventory from the newly developed Community Emissions Data System (CEDS) from the Joint Global Change Research Institute at the Pacific Northwest National Laboratory and University of Maryland (Hoesly et al., 2018). All three inventories are derived using a bottom-up approach where emissions are estimated using reported activity data (e.g., amount of fuel consumed) and source- and region-specific (where available) emission factors (mass of emitted pollutant per mass of fuel consumed) for each emitted compound. All three inventories are similar in that they use this bottom-up approach to provide historical, source-specific gridded emission estimates of major atmospheric pollutants (NO_x (as NO_2); SO_2; CO; non-methane volatile organic compounds, NMVOCs; NH_3; BC; and OC). Table 1 provides a comparison of the key features between these inventories, which provide emissions from multiple source sectors over the collective time period from 1750–2014. In contrast to EDGAR and GAINS, the CEDS system implements an increasingly utilized mosaic approach, which, in this case, incorporates activity and emission input data from other sources such as EDGAR, GAINS, and regional- and national-level inventories to produce global emissions that are both historically consistent and reflective of contemporary country-level estimates (Hoesly et al., 2018). The CEDS source code has been publicly released (https://github.com/JGCRI/CEDS/tree/master, last access: 1 December 2020), increasing both the reproducibility and public accessibility to quality emission estimates of global- and national-level air pollutants.

Due to the long development times of global bottom-up inventories, current versions of the EDGAR, ECLIPSE, and CEDS inventories are limited in their ability to capture emission trends over recent years (Table 1), particularly the last 6–10 years in regions undergoing rapid change such as China, North America, Europe, India, and Africa. For example, China implemented the Action Plan on the Prevention and Control of Air Pollution in 2013, which has targeted specific emission sectors, fuels, and species and resulted in reductions in ambient $PM_{2.5}$ concentrations by up to 40 % in metropolitan regions between 2013 and 2017 (reviewed in Zheng et al., 2018). Similarly, over the past 10–20 years in the US and Europe, the reduction in coal-fired power plant emissions and phase-in of stricter vehicle emission standards have resulted in emission reductions in SO_2 and NO_x across these regions (Krotkov et al., 2016; Duncan et al., 2013; Castellanos and Boersma, 2012; de Gouw et al., 2014). Over this same time period, however, oil and gas production in key regions in the US has more than tripled between 2007 and 2017 (EIA, 2020). In addition, the absence of widespread regulations targeting NH_3 from agricultural practices has led to continuous increases in global NH_3 emissions (Behera et al., 2013). Global energy consumption also increased by an average of 1.5 % each year between 2008 and 2018 (BP, 2019), and the global consumption of coal increased for the first time in 2017 since its peak in 2013 (BP, 2019). Many of these energy changes have been attributed to the growth of energy generation in rapidly growing regions, such as India (BP, 2019). Africa is also experiencing rapid growth, with increasing emissions from diffuse and inefficient combustion sources, which may not be accurately accounted for in current global inventories (Marais and Wiedinmyer, 2016). Therefore, to capture recent trends around the globe as well as quantify the resulting economic, health, and environmental impacts and mitigate future burdens, computational models require emission inventories with regionally accurate estimates, global coverage, and the most up-to-date information possible. Though global bottom-up inventories can lag in time due to data collection and reporting requirements, the incorporation of smaller regional inventories provides the opportunity to improve the timeliness and regional accuracy of global estimates.

To further increase the policy relevance of such data, it is also important that global emission inventories not only provide contemporary estimates but report emissions as a function of detailed source sector and fuel type. For example, the recent air quality policies in China have included emission reductions targeting coal-fired power plants within the larger energy generation sector (e.g., Zheng et al., 2018). Decisions to implement such policies require accurate predictions of the air quality benefits, which in turn depend on simulations that use accurate estimates of contemporary sector- and fuel-specific emissions. While the EDGAR, ECLIPSE, and CEDS inventories all provide varying degrees of sectoral information (Table 1), there are no global inventories to date that provide public datasets of multiple atmospheric pollutants with both detailed source sector and fuel type information. Crippa et al. (2019) do describe estimates of biofuel use from the residential sector in Europe using emissions from the EDGAR v4.3.2 inventory (EC-JRC, 2018) but do not report global estimates or regional emissions from other fuel types. Similarly, Hoesly et al. (2018) describe fuel-specific activity data and emission factors used to develop the global CEDS v2016-07-26 inventory but do not publicly report final global emissions as a function of fuel type. In contrast, a limited number of regional inventories have provided both fuel- and sector-specific emissions. These inventories, for example, have been applied to earth system models to attribute the mortality associated with outdoor air pollution to dominant sources of ambient $PM_{2.5}$ mass, such as residential biofuel combustion in India and coal combustion in China (GBD MAPS Working Group, 2018, 2016). As countries undergo rapid changes that impact fluxes of their emitted pollutants, including population, emission capture technologies, and the

Table 1. Comparison of three historical, gridded, source-specific emission inventories of atmospheric pollutants (NO_x, SO_2, CO, NMVOCs, NH_3, BC, OC).

Inventory name (version)	Temporal coverage	Number of reported gridded sectors	Detailed fuels	Spatial resolution	Reference
CEDS (v2016_07_26)	1750–2014	9	Total only	0.5° × 0.5°	Hoesly et al. (2018)
EDGAR (v4.3.2)	1970–2012	26	Biofuel (Europe only)[b]	0.1° × 0.1°	Crippa et al. (2018)
ECLIPSE (v5a)	1990, 1995, 2000, 2005, 2010 (projections to 2050)[a]	8	Total only	0.5° × 0.5°	Klimont et al. (2017), Amann et al. (2011)

[a] Projections assume current air pollution legislation (CLE) in the GAINS model. [b] Described in Crippa et al. (2019).

mix of fuels used, fuel- and source-specific estimates are vital for capturing these contemporary changes and understanding the air quality impacts across multiple scales.

As part of the Global Burden of Disease – Major Air Pollution Sources (GBD-MAPS) project, which aims to quantify the disease burden associated with dominant country-specific sources of ambient $PM_{2.5}$ mass (https://sites.wustl.edu/acag/datasets/gbd-maps/, last access: 1 December 2020), we have updated and utilized the CEDS open-source emissions system to produce a new global anthropogenic emission inventory ($CEDS_{GBD\text{-}MAPS}$). $CEDS_{GBD\text{-}MAPS}$ includes country-level and global gridded (0.5° × 0.5°) emissions of seven major atmospheric pollutants (NO_x (as NO_2), CO, NH_3, SO_2, NMVOCs, BC, OC) as a function of 11 detailed emission source sectors (agriculture, energy generation, industry, on-road transportation, non-road and off-road transportation, residential energy combustion, commercial combustion, other combustion, solvent use, waste, and international shipping) and four fuel groups (emissions from the combustion of total coal, solid biofuel, liquid fuels and natural gas, plus all remaining process-level emissions) for the time period between 1970–2017. Similar to the prior CEDS inventory released for CMIP6 (Hoesly et al., 2018), $CEDS_{GBD\text{-}MAPS}$ provides surface-level emissions from all sectors, including fertilized soils, but does not include emissions from open burning. In the first two sections we provide an overview of the $CEDS_{GBD\text{-}MAPS}$ system and describe the updates that have allowed for the extension to the year 2017 and the added fuel type information. These include updates to the underlying activity data and input emission inventories used for default estimates and scaling procedures (including the use of two new inventories from Africa and India), the additional scaling of default BC and OC emissions, the use of updated spatial gridding proxies, and adjustments to the final gridding and aggregation steps that retain detailed sub-sector and fuel type information. The third section presents global $CEDS_{GBD\text{-}MAPS}$ emissions in 2017 and discusses historical trends as a function of compound, sector, fuel type, and world region. The final section provides a comparison of the global $CEDS_{GBD\text{-}MAPS}$ emissions with other global inventories as well as a discussion of the magnitude and sources of uncertainty associated with the $CEDS_{GBD\text{-}MAPS}$ products.

2 Methods

The 23 December 2019 full release of the Community Emissions Data System (Hoesly et al., 2019) provides the core system framework for the development of the contemporary $CEDS_{GBD\text{-}MAPS}$ inventory. The $CEDS_{GBD\text{-}MAPS}$ inventory is developed for the GBD-MAPS project and is not an updated release of the core CEDS emissions inventory. As detailed in Hoesly et al. (2018), the original version of the CEDS system was used to produce the first CEDS v2016-07-26 inventory (hereafter called $CEDS_{Hoesly}$) (CEDS, 2017a, b), which provides global gridded (0.5° × 0.5°) emissions of atmospheric reactive gases (NO_x (as NO_2), SO_2, NH_3, NMVOCs, CO), carbonaceous aerosol (BC, OC), and greenhouse gases (CO_2, CH_4) from eight anthropogenic sectors (agriculture – AGR; transportation – TRA; energy – ENE; industry – IND; residential, commercial, other – RCO; solvents – SLV; waste – WST; international shipping – SHP) over the time period from 1750–2014. Here we provide a brief overview of the Community Emissions Data System with detailed descriptions of the major updates that have been implemented to produce the new $CEDS_{GBD\text{-}MAPS}$ inventory. This inventory has been extended to provide emissions from 1970–2017 for reactive gases and carbonaceous aerosol (NO_x, SO_2, NMVOCs, NH_3, CO, BC, OC) with increased fuel and sectoral information relative to the $CEDS_{Hoesly}$ inventory (Sect. 2.2–2.3). Updates primarily include the use of updated input datasets (Sect. 2.1), new and updated global and regional scaling inventories (Sect. 2.2), added scaling of default BC and OC emissions (Sect. 2.3), and the disaggregation of emissions into contributions from additional source sectors and multiple fuel types (Sect. 2.4).

2.1 Overview of $CEDS_{GBD\text{-}MAPS}$ system

The CEDS system has five key procedural steps, illustrated in Fig. 1. After the collection of input data in Step 0, Step 1 calculates default global emission estimates (Em) for each chemical compound using a bottom-up approach shown in Eq. (1). In Eq. (1), emissions are calculated using relevant activity (A) and emission factor (EF) data for each country (c) and year (y) as a function of 52 detailed working sectors (s) (sub-sectors used for intermediate steps in the CEDS system) and nine working fuel types (f) (Table 2). CEDS conducts these calculations for two types of emission categories: (1) fuel combustion sources (e.g., electricity production, industrial machinery, on-road transportation, etc.) and (2) process sources (e.g., metal production, chemical industry, manure management, etc.). We note that the distinction between these source categories is reflective of both sector definition and CEDS methodology, as described further in Sect. S2.1 in the Supplement. This results in some working sectors that include emissions from combustion, such as waste incineration and fugitive petroleum and gas emissions, to be characterized in the CEDS system as process-level sources (further details in Sect. S2.1). In contrast to CEDS combustion source emissions, which are calculated in Eq. (1) as a function of eight fuel types, emissions from CEDS process-level sources are combined into a single "process" category, as described in Sect. 2.4. Table 2 provides a complete list of $\text{CEDS}_{\text{GBD-MAPS}}$ working sectors and fuel types as well as source category distinctions.

$$\text{Em}_{\text{species}}^{\text{country, sector, fuel, year}} = A^{\text{c,s,f,y}} \times \text{EF}_{\text{species}}^{\text{c,s,f,y}} \quad (1)$$

For emissions from CEDS combustion sources, annual activity drivers in Eq. (1) primarily include country-, fuel-, and sector-specific energy consumption data from the International Energy Agency (IEA, 2019). Sector- and compound-specific emission factors are typically derived from energy use and total emissions reported from other inventories, including from the GAINS model (Klimont et al., 2017; IIASA, 2014; Amann et al., 2015), Speciated Pollutant Emission Wizard (SPEW) (Bond et al., 2007), and the US National Emissions Inventory (NEI) (NEI, 2013). For international shipping, IEA activity data are supplemented with consumption data and EFs from the International Maritime Organization (IMO), as described in Hoesly et al. (2018) and its supplement. In contrast, default emissions (Em) for CEDS process sources are directly taken from other inventories, including from the EDGAR v4.3.2 global emission inventory (EC-JRC, 2018; Crippa et al., 2018). "Implied emission factors" are then calculated for these process sources in Eq. (1) using global population data (UN, 2019, 2018) or pulp and paper consumption (FAOSTAT, 2015) as the primary activity drivers. For years without available emissions, default estimates for CEDS process sources are calculated in Eq. (1) from a linear interpolation of the "implied emission factors" and available activity data (A) for that year. Supplement Sects. S2.1 and S2.2 provide additional details regarding the input datasets for activity drivers and emission factors used for both CEDS combustion and process source categories.

While CEDS Step 1 is designed to provide a complete set of historical emission estimates, CEDS Step 2 scales these total default emission estimates to existing, authoritative global-, regional-, and national-level inventories. As described in Hoesly et al. (2018), CEDS uses a "mosaic" scaling approach to retain detailed fuel- and sector-specific information across different inventories while maintaining consistent methodology over space and time. The development and use of mosaic inventories has been recently increasing as they provide a means to utilize detailed local emissions while harmonizing this information across large regional or global scales (C. Li et al., 2017; Janssens-Maenhout et al., 2015). The CEDS approach, however, differs from previous mosaic inventories (e.g., Janssens-Maenhout et al., 2015), in that local and regional inventories in $\text{CEDS}_{\text{GBD-MAPS}}$ are used to scale sectoral emissions at the national level rather than merge together spatially distributed gridded estimates.

The first step in the scaling procedure is to derive a time series of scaling factors (SFs) for each scaling inventory using Eq. (2), calculated as a function of chemical compound, country, sector, and fuel type (where available). Due to persistent differences and uncertainties in the underlying activity data and sectoral definitions in each scaling inventory, CEDS emissions are scaled to total emissions within aggregate scaling sectors (and fuels, where applicable). These aggregate scaling groups are defined for each scaling inventory and are chosen to be broad in order to improve the overlap between CEDS emission estimates and those reported in other inventories. For example, the sum of CEDS emissions from working sectors 1A4a_Commercial-institutional, 1A4b_Residential, and 1A4c_agriculture-forestry-fishing are scaled to the aggregate 1A4_energy-for-buildings sector in the EDGAR v4.3.2 inventory. Sections 2.2 and S2.3 provide further details about this scaling procedure and the scaling inventories used to develop the 1970–2017 $\text{CEDS}_{\text{GBD-MAPS}}$ inventory.

$$\text{SF}_{\text{species}}^{\text{c,s,f,y}} = \frac{\text{scaling inventory Em}_{\text{species}}^{\text{c,s,f,y}}}{\text{default CEDS Em}_{\text{species}}^{\text{c,s,f,y}}} \quad (2)$$

After SFs are calculated in Eq. (2), the second step in the scaling procedure is to extend these SFs forward and backward in time to fill years with missing data. For these time periods, the nearest available SF is applied. If a particular sector or compound is not present in a scaling inventory, default CEDS estimates are not scaled. For BC and OC emissions, the default procedure in the CEDS v2019-12-23 system was to retain all default BC and OC emission estimates due to limited availability of historical BC and OC emissions. In the $\text{CEDS}_{\text{GBD-MAPS}}$ inventory, these species are now scaled to available regional- and national-level inventories (further details in Sect. 2.2). For all other species, the $\text{CEDS}_{\text{GBD-MAPS}}$ system uses a sequential scaling methodology where total default emissions for each country are first scaled to available global inventories (primarily EDGAR v4.3.2) and then scaled to regional- and national-level inventories, many of which have been updated in this work (Sect. 2.2 and Table 3). This process results in final $\text{CEDS}_{\text{GBD-MAPS}}$ emissions that reflect the inventory last used to scale the emissions for that country (Fig. 2). Figure S2 in the Supplement provides a time series of implied emission factors after the scaling procedure for select sector and fuel combinations that dominate emis-

Table 2. CEDS sector and fuel type definitions. Aggregate sectors and fuel types in the $\text{CEDS}_{\text{Hoesly}}$ (bold) and $\text{CEDS}_{\text{GBD-MAPS}}$ (bold and italic) inventories as well as the system's intermediate gridding sectors (italic) and detailed working sectors and fuel types (consistent between $\text{CEDS}_{\text{Hoesly}}$ and $\text{CEDS}_{\text{GBD-MAPS}}$ inventories). CEDS working sectors are methodologically treated as two different categories: combustion sectors (c) and "process" sectors (p). As described in the text, combustion sector emissions are calculated as a function of CEDS working fuels, while process emissions are assigned to the single "process" fuel type.

CEDS emission sectors	
Energy production (ENE)	**Residential, commercial, other (RCO)**
Energy production (ENE)	***Residential (RCOR)***
Electricity and heat production	*Res., Comm., Other – Residential*
1A1a_Electricity-public (c)	1A4b_Residential (c)
1A1a_Electricity-autoproducer (c)	***Commercial (RCOC)***
1A1a_Heat-production (c)	*Res., Comm., Other – Commercial*
Fuel Production and Transformation	1A4a_Commercial-institutional (c)
1A1bc_Other-transformation (p)	***Other (RCOO)***
1B1_Fugitive-solid-fuels (p)	*Res., Comm., Other – Other*
Oil and Gas Fugitive/Flaring	1A4c_Agriculture-forestry-fishing (c)
1B2_Fugitive-petr-and-gas (p)	**Solvents (SLV)**
Fuel Production and Transformation	***Solvents (SLV)***
1B2d_Fugitive-other-energy (p)	*Solvents production and application*
Fossil Fuel Fires	2D_Degreasing-Cleaning (p)
7A_Fossil-fuel-fires (p)	2D3_Other-product-use (p)
Industry (IND)	2D_Paint-application (p)
Industry (IND)	2D3_ Chemical-products-manufacture-processing (p)
Industrial combustion	**Agriculture (AGR)**
1A2a_Ind-Comb-Iron-steel (c)	***Agriculture (AGR)***
1A2b_Ind-Comb-Non-ferrous-metals (c)	*Agriculture*
1A2c_Ind-Comb-Chemicals (c)	3B_Manure-management (p)
1A2d_Ind-Comb-Pulp-paper (c)	3D_Soil-emissions (p)
1A2e_Ind-Comb-Food-tobacco (c)	3I_Agriculture-other (p)
1A2f_Ind-Comb-Non-metallic-minerals (c)	3D_Rice-Cultivation (p)
1A2g_Ind-Comb-Construction (c)	3E_Enteric-fermentation (p)
1A2g_Ind-Comb-transpequip (c)	**Waste (WST)**
1A2g_Ind-Comb-machinery (c)	***Waste (WST)***
1A2g_Ind-Comb-mining-quarrying (c)	*Waste*
1A2g_Ind-Comb-wood-products (c)	5A_Solid-waste-disposal (p)
1A2g_Ind-Comb-textile-leather (c)	5E_Other-waste-handling (p)
1A2g_Ind-Comb-other (c)	5C_Waste-incineration (p)
1A5_Other-unspecified (c)	5D_Wastewater-handling (p)
Industrial process and product use	**Shipping (SHP)**
2A1_Cement-production (p)	***Shipping (SHP)***
2A2_Lime-production (p)	*International shipping*
2A6_Other-minerals (p)	1A3di_International-shipping (c)
2B_Chemical-industry (p)	*Tanker Loading*
2C_Metal-production (p)	1A3di_Oil_Tanker_Loading (p)
2H_Pulp-and-paper-food-beverage-wood (p)	
2L_Other-process-emissions (p)	
6A_Other-in-total (p)	
Transportation (TRA)	**Transportation Cont. (TRA)**
Road transportation (ROAD)	***Non-road transportation (NRTR)***
Road transportation	*Non-road Transport*ation
1A3b_Road (c)	1A3c_Rail (c)
	1A3dii_Domestic-navigation (c)
	1A3eii_Other-transp (c)
CEDS fuels	
Total	
Coal	***Liquid fuel and natural gas***
Brown coal	Heavy oil
Coal coke	Diesel oil
Hard coal	Light oil
Biofuel	Natural Gas
Biofuel	***Process***
	Process

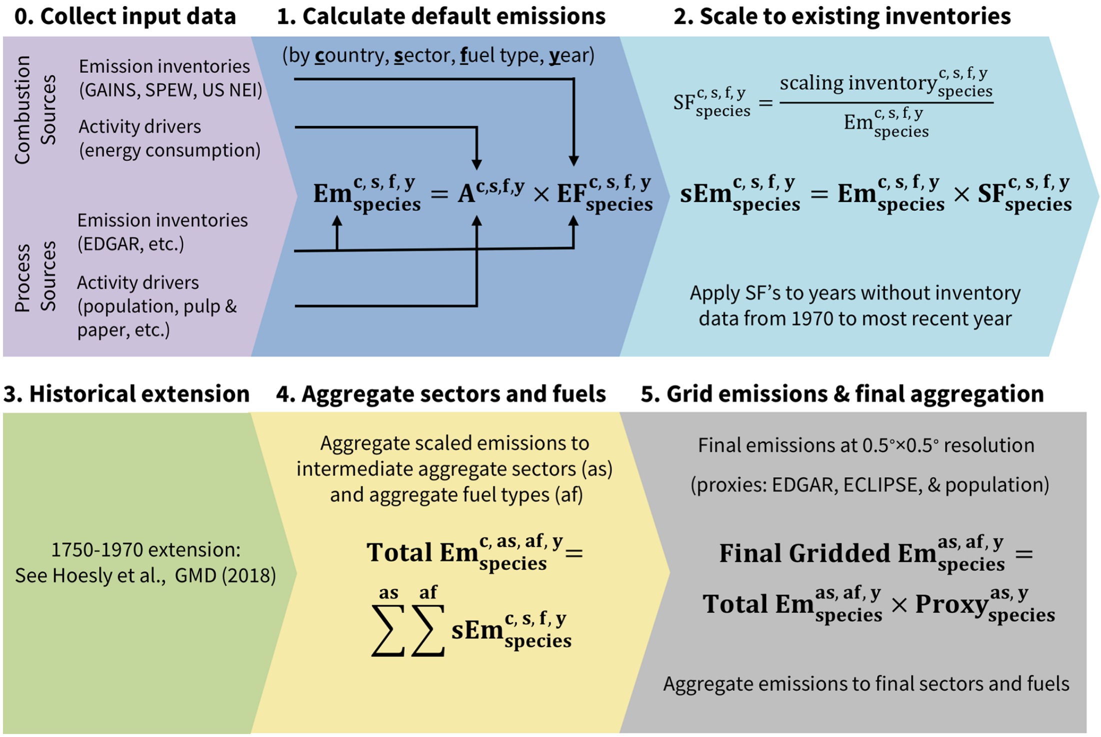

Figure 1. Default CEDS system summary, adapted from Fig. 1 in Hoesly et al. (2018). Key steps include (0) collecting activity driver (A) and emission factor (EF) input data for non-combustion and combustion emission sources; (1) calculating default emissions (Em) as a function of chemical species, country, emission sector, fuel type, and year; (2) calculating scaling factors (SFs) for overlapping years with existing inventories in order to scale default estimates (sEm) and extending SFs for non-overlapping years between 1970–2017 (for earlier emissions, see Hoesly et al., 2018); (4) aggregating scaled emissions to intermediate sectors and fuel types; and (5) using source- and compound-specific spatial proxies to calculate final gridded emissions and aggregate them to the final sectors and fuels. A list of intermediate and final sectors and fuels are in Table 2.

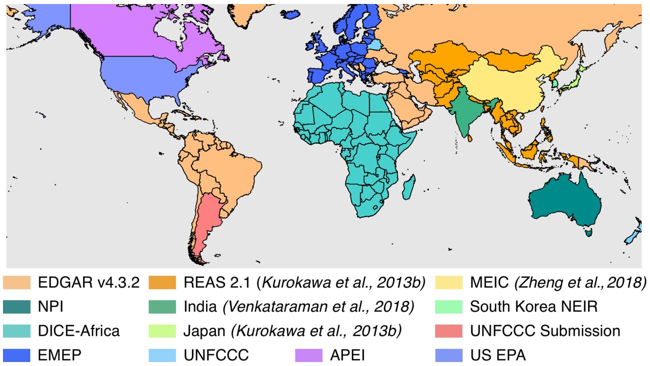

Figure 2. Final scaling inventories used for $\mathrm{CEDS_{GBD\text{-}MAPS}}$ NO_x emissions; inventory details in Table 3.

sions of each compound in the top 15 emitting countries. Sections 2.2 and S2.3 describe further details and updates to this scaling procedure.

CEDS Step 3 extends the scaled emission estimates from 1970 back in time to 1750. This process is necessary as reported emission estimates and energy data are not typically reported with the same level of sectoral and fuel type detail prior to 1970. Hoesly et al. (2018) provide a detailed description of this historical extension procedure, which is used to derive pre-1970 emissions in the $\mathrm{CEDS_{Hoesly}}$ inventory. The new $\mathrm{CEDS_{GBD\text{-}MAPS}}$ inventory only reports more contemporary emissions after 1970 and therefore does not utilize this historical extension.

CEDS Step 4 aggregates the scaled country-level $\mathrm{CEDS_{GBD\text{-}MAPS}}$ emissions into 17 intermediate gridding sectors (defined in Table 2). In the CEDS v2019-12-23 system, Step 4 additionally aggregated sectoral emissions from all fuel types. In contrast, the $\mathrm{CEDS_{GBD\text{-}MAPS}}$ system retains sectoral emissions from the combustion of total coal (hard coal + coal coke + brown coal), solid biofuel, the sum of liquid oil (light oil + heavy oil + diesel oil) and natural gas, and all CEDS process-level emissions (Table 2). Sections 2.4 and 4.2.4 describe the $\mathrm{CEDS_{GBD\text{-}MAPS}}$ fuel-specific emissions in further detail.

Lastly, CEDS Step 5 uses normalized spatial-distribution proxies to allocate annual country-level emission estimates onto a 0.5° × 0.5° global grid. Annual emissions from the 17 intermediate gridding sectors and four fuel groups are first distributed spatially using compound-, sector-, and year-specific spatial proxies, primarily from the gridded

Table 3. Scaling inventories.

Inventory name	Scaled inventory years	Scaled species	Reference
EDGAR v4.3.2	1992–2012	CO, NH_3, NMVOCs, NO_x	(EC-JRC, 2018)
EMEP NFR14	1990–2017	CO, NH_3, NMVOCs, NO_x, SO_2, BC	EMEP (2019)
UNFCCC	1990–2017	CO, NMVOCs, NO_x, SO_2	UNFCCC (2019)
REAS 2.1[a]	2000–2008	CO, NH_3, NMVOCs, NO_x, SO_2, BC	Kurokawa et al. (2013)
APEI (Canada)	1990–2017	CO, NH_3, NMVOCs, NO_x, SO_2	ECCC (2019)
US EPA	1970, 1975, 1980, 1985, 1990–2017	CO, NH_3, NMVOCs, NO_x, SO_2	US EPA (2019)
MEIC (China)	2008, 2010–2017	CO, NH_3, NMVOCs, NO_x, SO_2, BC, OC	Zheng et al. (2018), C. Li et al. (2017)
Argentina[a]	1990–1999, 2011–2009, 2011	CO, NMVOCs, NO_x, SO_2	Argentina UNFCCC Submission (2016)
Japan[a]	1960–2010	CO, NH_3, NMVOCs, NO_x, SO_2, BC, OC	preliminary update from Kurokawa et al. (2013)
NEIR (South Korea)[a]	1999–2012	CO, NMVOCs, NO_x, SO_2	South Korea National Institute of Environmental Research (2016)
Taiwan[a]	2003, 2006, 2010	CO, NMVOCs, NO_x, SO_2	TEPA (2016)
NPI (Australia)	2000–2017	CO, NMVOCs, NO_x, SO_2	ADE (2019)
DICE-Africa[b]	2006, 2013	CO, NMVOCs, NO_x, SO_2, BC, OC	Marais and Wiedinmyer (2016)
SMoG-India[b]	2015	CO, NMVOCs, NO_x, SO_2, BC, OC	Venkataraman et al. (2018)

[a] Not updated from CEDS v2019-12-23; details in Hoesly et al. (2018). [b] Emissions scaled as a function of sector and fuel type.

EDGAR v4.3.2 inventory. Supplement Table S7 provides a complete list of sector-specific gridding proxies. Details about the general CEDS gridding procedure are provided in Feng et al. (2020), with additional details specific to the $\text{CEDS}_{\text{GBD-MAPS}}$ system in Sect. S2.5. Second, gridded emission fluxes (units: $\text{kg}\,\text{m}^{-2}\,\text{s}^{-1}$) are aggregated into 11 final sectors (Table 2) and distributed over 12 months using sectoral and spatially explicit monthly fractions from the ECLIPSE project (IIASA, 2015) and EDGAR inventory (international shipping only). Relative to CEDS v2019-12-23, the new $\text{CEDS}_{\text{GBD-MAPS}}$ inventory retains detailed sub-sector emissions from the aggregate RCO (now RCO-residential, RCO-commercial, and RCO-other) and TRA (now on-road and non-road) sectors; separate sectoral emissions from process sources; and combustion sources that utilize coal, solid biofuel, and the sum of liquid fuels and natural gas. Table 2 contains a complete breakdown of the definitions of CEDS working, intermediate gridding, and final sectors. Gridded total NMVOCs are additionally disaggregated into 25 VOC classes following sector- and country-specific VOC speciation maps from the RETRO project (HTAP2, 2013), which are different from those used in the recent EDGAR v4.3.2 inventory (Huang et al., 2017). Similar to the gridding procedure, the same VOC speciation and monthly distributions are applied to sectoral emissions associated with each fuel category.

Final products from the $\text{CEDS}_{\text{GBD-MAPS}}$ system include total annual emissions from 1970–2017 for each country as well as monthly global gridded (0.5° × 0.5°) emission fluxes, both as a function of 11 final source sectors and four fuel categories (total coal, solid biofuel, liquid fuel + natural gas, and remaining process sources). Section 5 provides additional details on the dataset availability and file formats.

2.2 Default emission-scaling procedure – $\text{CEDS}_{\text{GBD-MAPS}}$ update details

As described above, default emission estimates for each compound are scaled in CEDS Step 2 to existing authoritative inventories as a function of emission sector and fuel type (where available). In the scaling procedure, annual emissions and EFs for each country are first scaled to available global inventories, then to available regional- and national-level inventories, assuming that the latter use local knowledge to derive more accurate regional estimates. Final $\text{CEDS}_{\text{GBD-MAPS}}$ emission totals for each country therefore reflect the inventory last used to scale each compound and sector. Many of these inventories are updated annually and, where available, have been updated in this work relative to the CEDS v2019-12-23 system (Table 3). For example, global $\text{CEDS}_{\text{GBD-MAPS}}$ combustion source emissions of NO_x, total NMVOCs, CO, and NH_3 are first scaled to EDGAR v4.3.2 country-level emissions as a means to incorporate additional country-specific information relative to default estimates derived using more regionally aggregate EFs from GAINS. $\text{CEDS}_{\text{GBD-MAPS}}$ emissions from European countries are then scaled to available EMEP (European Monitoring and Evaluation Programme) (EMEP, 2019) and UNFCCC (United Nations Framework Convention on Climate Change) (UNFCCC, 2019) inventories that extend to 2017, while CO, NMVOCs, NO_x and SO_2 emissions from the US, Canada, and Australia are scaled to emissions that extend to 2017 from the US NEI (US EPA, 2019), Canadian APEI (Air Pollutant Emissions Inventory) (ECCC, 2019), and Australian NPI (National Pollutant Inventory) (ADE, 2019), respectively. In addition, emissions of all seven compounds from China are scaled to emissions for 2008, 2010, and 2012 from C. Li et al. (2017), followed by subsequent scaling to emissions between 2010 and 2017 from Zheng et al. (2018). Relative to the CEDS v2019-12-23 system, regional inventories have also been added to scale $\text{CEDS}_{\text{GBD-MAPS}}$ emissions from India and Africa as described below. Updates to additional regional scaling inventories, including South Korea, Japan, and other European and Asian countries, are not available relative to those used in the CEDS v2019-12-23 system. Table 3 provides a complete list of the inventories used to scale $\mathrm{CEDS_{GBD\text{-}MAPS}}$ default emissions, with additional details in Sect. S2.3.

Relative to the CEDS v2019-12-23 system, the $\mathrm{CEDS_{GBD\text{-}MAPS}}$ system adds scaling inventories for two rapidly changing regions, Africa and India. First, $\mathrm{CEDS_{GBD\text{-}MAPS}}$ emissions from Africa for select sectors are now scaled to the Diffuse and Inefficient Combustion Emissions in Africa (DICE-Africa) inventory from Marais and Wiedinmyer (2016). This inventory provides gridded ($0.1° \times 0.1°$) emissions for NO_x ($= \mathrm{NO} + \mathrm{NO_2}$), $\mathrm{SO_2}$, 25 speciated VOCs, $\mathrm{NH_3}$, CO, BC, and OC for 2006 and 2013 for select anthropogenic sectors and fuels. In this work, default CEDS emissions are scaled to total DICE-Africa emissions from each country and later re-gridded in CEDS Step 5 using source-specific spatial proxies described in Sect. 2.1. Following the CEDS v2019-12-23 scaling procedure (Supplement Sect. S2.3), a set of aggregate scaling sectors and fuels are defined to ensure that $\mathrm{CEDS_{GBD\text{-}MAPS}}$ emissions are scaled to emissions from consistent sectors and fuel types within the DICE-Africa inventory (Table S3). Briefly, $\mathrm{CEDS_{GBD\text{-}MAPS}}$ 1A3b_Road and 1A4b_Residential emissions are scaled to DICE-Africa emissions from diesel- and gasoline-powered cars and motorcycles as well as biomass and oil combustion associated with residential charcoal, crop residue, fuelwood, and kerosene use. The DICE-Africa inventory also includes emission estimates from gas flares across Africa and ad hoc oil refining in the Niger Delta, fuelwood use for charcoal production and other commercial enterprises, and gas and diesel use in residential generators. Marais and Wiedinmyer (2016) state that these particular sources are missing or not adequately captured in existing global inventories. Therefore, depending on the source sector and inventory details, they recommend that these emissions be added to existing global inventories for formal industry and on-grid energy production in Africa (DICE-Africa, 2016). Due to uncertainties in the representation of these sectors in the default CEDS Africa emissions, these sources are not included in the scaling process here. Default $\mathrm{CEDS_{GBD\text{-}MAPS}}$ emissions from the 1B2_fugitive_pert_gas (gas flaring) sector (derived from the ECLIPSE and EDGAR inventories) are larger than DICE-Africa gas flaring emissions in 2013, suggesting that this source may be accurately represented in the default $\mathrm{CEDS_{GBD\text{-}MAPS}}$ estimates. As described in Sect. S2.3.2, however, residential generator and fuelwood use for charcoal production and other commercial activities are not explicitly represented in CEDS and will be accounted for only to the extent that these sources are included in the underlying IEA activity data and EDGAR process emission estimates. In the event that the DICE-Africa emissions from these sources are missing in the default CEDS estimates, total 2013 $\mathrm{CEDS_{GBD\text{-}MAPS}}$ emissions from Africa for each compound may be underestimated by up to 11 % (Sect. S2.3, Table S5). These values range from 0.7 % for $\mathrm{SO_2}$ to 11 % for CO (Table S5) and all fall within the range of uncertainties typically reported from regional bottom-up inventories ($> 20\,\%$; Sect. 4.2.3). Final emissions from additional sectors or species in CEDS that are not included in the DICE-Africa inventory are set to $\mathrm{CEDS_{GBD\text{-}MAPS}}$ default values.

Second, emissions from India for select sectors are now scaled to the Speciated Multi-pollutant Generator Inventory described by Venkataraman et al. (2018) (hereafter called SMoG-India). This inventory includes gridded emissions ($0.25° \times 0.25°$) of NO_x (as $\mathrm{NO_2}$), $\mathrm{SO_2}$, total NMVOCs, CO, BC, and OC for the year 2015 from select anthropogenic sectors and fuels (SMoG-India, 2019). Similar to DICE-Africa emissions, the final spatial distribution in the SMoG-India and $\mathrm{CEDS_{GBD\text{-}MAPS}}$ inventories will differ as country-level emissions are scaled to country totals and spatially reallocated using CEDS proxies in Step 5. SMoG-India emissions for each compound are available for 17 sectors and nine fuel types (coal, fuel oil, diesel, gasoline, kerosene, naphtha, gas, biomass, and fugitive or process). Similar to the DICE-Africa inventory, aggregate scaling groups have been defined to scale consistent sectors and fuels between inventories, as described in Sect. S2.3. Briefly, default $\mathrm{CEDS_{GBD\text{-}MAPS}}$ emissions for the 1A4c_Agriculture-forestry-fishing sector are scaled to the sum of SMoG-India emissions for agricultural pumps and tractors; 1A4b_Residential emissions are scaled to the sum of SMoG-India emissions from residential lighting, cooking, diesel generator use, and space and water heating; 1A1a electricity and heat generation sectors are scaled to SMoG-India thermal power plant emissions; 1A3b road and rail sectors are scaled to the respective SMoG-India road and rail emissions; and $\mathrm{CEDS_{GBD\text{-}MAPS}}$ industrial working sectors are allocated and scaled to four SMoG-India industrial sectors: light industry (e.g., mining and chemical production), heavy industry (e.g., iron and steel production), informal industry (e.g., food production), and brick production. Calculated scaling factors for these sectors are held constant before and after 2015. $\mathrm{CEDS_{GBD\text{-}MAPS}}$ emissions do not include contributions from open burning and are not scaled to SMoG-India open burning emissions. In cases where SMoG-India emissions are not reported (e.g., power generation from oil combustion), default $\mathrm{CEDS_{GBD\text{-}MAPS}}$ emissions are retained. Section S2.3.3 provides additional details.

To examine the changes in $\mathrm{CEDS_{GBD\text{-}MAPS}}$ emissions associated with the incorporation of the SMoG-India and DICE-Africa scaling inventories as well as the updated underlying input datasets, Fig. 3 compares the total and sectoral distribution of $\mathrm{CEDS_{GBD\text{-}MAPS}}$ and $\mathrm{CEDS_{Hoesly}}$ emissions for these two regions in 2014 (year with latest overlapping data). For the Africa comparison, panel a in Fig. 3 shows that total NO_x, BC, and OC emissions are generally

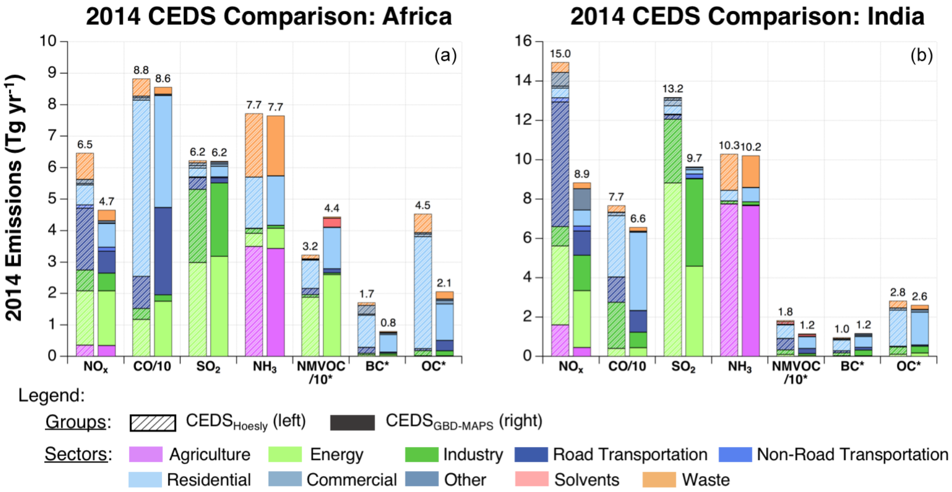

Figure 3. Sectoral contributions to total annual emissions for 2014 of CEDS$_{\text{Hoesly}}$ **(a)** and CEDS$_{\text{GBD-MAPS}}$ **(b)** emissions after scaling to DICE-Africa and SMoG-India regional inventories. The total annual emissions are given by the values above each bar; bar colors represent absolute sectoral contributions to emissions of each chemical compound. CO and NMVOC emissions are divided by 10 for clarity. Stars indicate that NMVOC, BC, and OC emissions are in units of Tg C yr^{-1}. NO_x is in units of Tg NO_2 yr^{-1}.

lower in the CEDS$_{\text{GBD-MAPS}}$ inventory than in CEDS$_{\text{Hoesly}}$. Lower NO_x and OC emissions are largely associated with smaller contributions from on-road transport and residential combustion, respectively, while lower BC emissions are associated with both lower residential and on-road transport contributions. Lower emissions of NO_x from the transport sector result from the lower EF used for diesel vehicles in the DICE-Africa inventory (Marais et al., 2019). Compared to GAINS (2010) and EDGAR v4.3.2 (2012), on-road emissions from African countries in CEDS$_{\text{GBD-MAPS}}$ are up to 2.5 Tg lower for NO_x but within 0.1 Tg for BC. In contrast to NO_x, larger EFs in the DICE-Africa inventory for on-road emissions of CO and OC result in CEDS$_{\text{GBD-MAPS}}$ emissions from this sector that are up to 14.8 and 0.3 Tg higher than previous estimates. Figure S2 shows that after scaling, the implied emission factors of CO from oil and gas combustion in the on-road transport sector for four African countries range from 0.19–0.28 g g^{-1}, slightly smaller than the range of 0.029–0.380 g g^{-1} used in the DICE-Africa inventory. Emissions from the residential and commercial sectors in Africa are generally lower in CEDS$_{\text{GBD-MAPS}}$ than in CEDS$_{\text{Hoesly}}$ due to both lower biofuel consumption and a lower assumed EF in the DICE-Africa inventory (Marais and Wiedinmyer, 2016). Residential BC and OC emission estimates are also lower than those from GAINS (Klimont et al., 2017). The difference in biofuel consumption is due to different data sources. The DICE-Africa inventory uses residential wood fuel consumption estimates from the UN, while CEDS$_{\text{Hoesly}}$ uses data from the IEA. Both of these sources consist largely of estimates for African countries because there is little country-reported biofuel consumption data available. The estimation methodologies for both the UN and IEA estimates are not well documented, which adds to the uncertainty in these values (Sect. 4.2). After scaling, the implied EFs for residential biofuel emissions of OC are ~ 0.001–0.002 g g^{-1} in three African countries (Fig. S2), within the range of EFs of 0.0007–0.003 g g^{-1} implemented in the DICE-Africa inventory. Total CEDS$_{\text{GBD-MAPS}}$ emissions of NMVOCs are larger, primarily due to increased contributions from solvent use in the energy sector associated with changes in the EDGAR v4.3.2 inventory, while total emissions of CO, SO_2, and NH_3 are relatively consistent between the two CEDS versions.

For the India comparison, panel b of Fig. 3 shows that total emissions of NO_x, CO, SO_2, NMVOCs, and OC are lower in CEDS$_{\text{GBD-MAPS}}$. Relative reductions in NO_x emissions are largely associated with on-road transport. Scaled CEDS$_{\text{GBD-MAPS}}$ transport emissions are 5 Tg smaller than NO_x emissions in CEDS$_{\text{Hoesly}}$, largely as a result of lower fuel consumption levels for gas, diesel, and compressed natural gas (CNG) on-road vehicles used to develop SMoG-India estimates (Sadavarte and Venkataraman, 2014). Figure S2 shows that the implied emission factor for NO_x emissions from oil and gas combustion in the on-road transport sector in India is ~ 0.015 g g^{-1} in 2015, which falls within the range of values of 0.0026–0.046 g g^{-1} used for various vehicles and fuel type in Venkataraman et al. (2018). Similarly, NO_x transport emissions are also lower in CEDS$_{\text{GBD-MAPS}}$ relative to the EDGAR and GAINS inventories. Causes of other reductions relative to the CEDS$_{\text{Hoesly}}$ are mixed. For example, lower emissions of SO_2 and NMVOCs are largely associated with the energy sector, while reductions in the industry sector contribute to reduced CO emissions. For SO_2, Fig. S2 shows that the implied EF for coal combustion in the energy sector is ~ 0.004 g g^{-1}, slightly lower than the range of 0.0049–0.0073 g g^{-1} used for the SMoG-India inventory.

To further examine the $\mathrm{CEDS_{GBD\text{-}MAPS}}$ inventory in these regions, Fig. 4 compares final $\mathrm{CEDS_{GBD\text{-}MAPS}}$ and $\mathrm{CEDS_{Hoesly}}$ emissions for India and Africa to total emissions from two widely used global inventories: GAINS (ECLIPSE v5a) and EDGAR (v4.3.2). First, Fig. 4 shows the percent difference between the $\mathrm{CEDS_{GBD\text{-}MAPS}}$ inventory and the GAINS and EDGAR inventories on the y axis against the percent difference between the $\mathrm{CEDS_{Hoesly}}$ inventory and GAINS and EDGAR emissions on the x axis. Percent differences are calculated from total emissions from Africa (left) and India (right) for the year 2012 for the comparison with EDGAR and for 2010 for the comparison to GAINS (most recent years with overlapping data). The green shaded areas indicate regions where the updated $\mathrm{CEDS_{GBD\text{-}MAPS}}$ inventory has improved agreement with EDGAR or GAINS relative to the $\mathrm{CEDS_{Hoesly}}$ inventory. This comparison shows that the additional scaling of $\mathrm{CEDS_{GBD\text{-}MAPS}}$ emissions to the SMoG-India inventory generally improves agreement with both the EDGAR and GAINS inventories relative to $\mathrm{CEDS_{Hoesly}}$ for all species except black carbon (BC). Scaling to the DICE-Africa inventory generally improves $\mathrm{CEDS_{GBD\text{-}MAPS}}$ agreement with the EDGAR inventory but not with GAINS (except for OC). Further comparisons to these two inventories are discussed in Sect. 4. While uncertainties in emissions from these inventories are expected to be at least 20 % for each compound (discussed in Sect. 3.3), this comparison provides an illustration of the changes between the two CEDS versions relative to two widely used global inventories.

2.3 Default BC- and OC-scaling procedure – $\mathrm{CEDS_{GBD\text{-}MAPS}}$ update details

Relative to the CEDS v2019-12-23 system, the second-largest change to the $\mathrm{CEDS_{GBD\text{-}MAPS}}$ system is the added scaling of BC and OC emissions in CEDS Step 2. In the v2019-12-23 system, OC and BC were not scaled due to a lack of historical BC and OC emission estimates in regional and global inventories. Due to the focus of the $\mathrm{CEDS_{GBD\text{-}MAPS}}$ inventory on more recent years, these two compounds are now scaled to available regional- and country-level estimates (Table 3) following the same scaling procedure described above for the reactive gases. Unlike the reactive gases, however, BC and OC emissions are not scaled to the global EDGAR v4.3.2 inventory due to the large reported uncertainties in this inventory (ranging from 46.8 % to 153.2 %; Crippa et al., 2018).

To examine the impact of the new BC and OC emissions scaling, in addition to the updated IEA energy consumption data, Figs. 5 and S3–S4 show time series of global BC and OC emissions from $\mathrm{CEDS_{GBD\text{-}MAPS}}$ compared to emissions from the $\mathrm{CEDS_{Hoesly}}$ inventory. In 2014, respective global annual emissions of BC and OC are 21 % and 28 % lower than the $\mathrm{CEDS_{Hoesly}}$ inventory and have total global annual emissions in 2017 of 6 and 13 $\mathrm{Tg\,C\,yr^{-1}}$ for BC and OC, respectively. These reductions in global emissions are largely due to the added scaling of emissions from China, Africa, Japan, and other countries in Asia included in the REAS inventory (Figs. S3–S4). Figures 5 and S3–S4 additionally compare $\mathrm{CEDS_{GBD\text{-}MAPS}}$ emissions to those from the GAINS (ECLIPSE v5a) and EDGAR (v4.3.2) inventories, which generally show improved agreement in BC and OC emissions with the GAINS inventory. $\mathrm{CEDS_{GBD\text{-}MAPS}}$ emissions between 1990 and 2015 are now 7 %–14 % lower than GAINS BC emissions, while $\mathrm{CEDS_{GBD\text{-}MAPS}}$ emissions of OC remain 12 %–25 % higher than GAINS estimates. Further discussion of $\mathrm{CEDS_{GBD\text{-}MAPS}}$ BC and OC emissions and comparisons to EDGAR and GAINS inventories are below in Sect. 4.1.2. As an additional point of comparison, Bond et al. (2013) report global BC and OC values for the year 2000, derived from averages of energy-related burning emissions from SPEW and GAINS. Reported global estimates of BC and OC are 5 and ∼ 11–14 Tg C (16 Tg organic aerosol reported; organic-mass-to-organic-carbon ratio = 1.1–1.4), respectively (Bond et al., 2013). These also have improved agreement with the $\mathrm{CEDS_{GBD\text{-}MAPS}}$ estimates of BC and OC in 2000 relative to those in the $\mathrm{CEDS_{Hoesly}}$ inventory. Lastly, we note plans for an upcoming update to the core CEDS system to improve historical trends in carbonaceous aerosol by incorporating reported inventory values for total $\mathrm{PM_{2.5}}$ and its ratio with BC and OC emissions.

2.4 Fuel-specific emissions – $\mathrm{CEDS_{GBD\text{-}MAPS}}$ update details

Prior to gridding, $\mathrm{CEDS_{GBD\text{-}MAPS}}$ Step 4 combines total country-level emissions for each of the 52 working sectors and nine fuel groups into 17 aggregate sectors and four fuel groups: total coal (hard coal + brown coal + coal coke), solid biofuel, the sum of liquid fuels (heavy oil + light oil + diesel oil) and natural gas, and all remaining “process” emissions (Table 2). In contrast, the CEDS v2019-12-23 system aggregates all fuel-specific emissions and reports inventory values as a function of sector only. In $\mathrm{CEDS_{GBD\text{-}MAPS}}$, country-total emissions from these aggregate sectors and fuel groups are distributed across a 0.5° × 0.5° global grid using spatial gridding proxies, as discussed in Sect. 2.1 (Table S7). During gridding, the same spatial proxies are applied to all fuel groups within each sector. In practice, this requires that the gridding procedure be repeated 4 times for each of the fuel groups. After gridding in CEDS Step 5, both annual country-total and gridded emission fluxes from each fuel group are aggregated to 11 final sectors. Figure S5 demonstrates the level of detail available in the new $\mathrm{CEDS_{GBD\text{-}MAPS}}$ gridded emission inventory by illustrating global BC emissions in 2017 from (1) all source sectors, (2) the residential sector only, (3) residential biofuel use only, and (4) residential coal use only. Additional uncertainties associated with the $\mathrm{CEDS_{GBD\text{-}MAPS}}$ fuel-specific emissions in both the country-

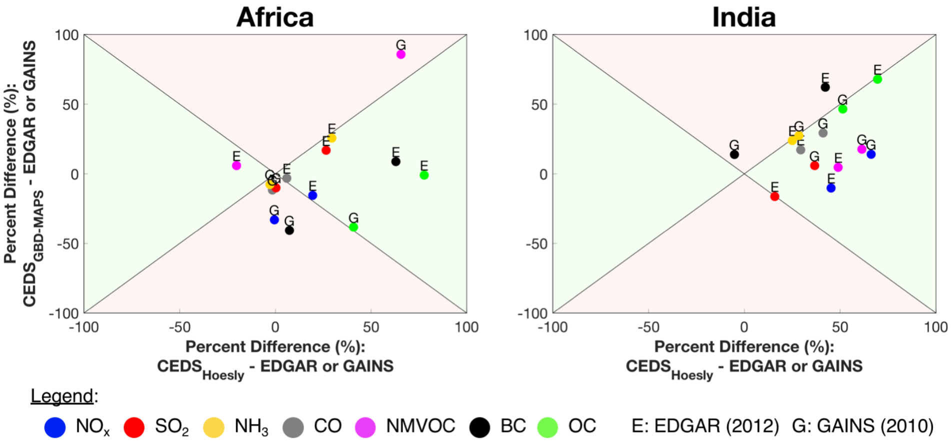

Figure 4. The x and y axes show the percent difference between CEDS emissions in India and Africa (y axis: CEDS$_{\mathrm{GBD\text{-}MAPS}}$; x axis: CEDS$_{\mathrm{Hoesly}}$) and those from the GAINS (ECLIPSE v5a) and EDGAR v4.3.2 inventories (i.e., $100 \times (\mathrm{CEDS} - \mathrm{EDGAR})/((\mathrm{CEDS} - \mathrm{EDGAR})/2)$). Comparisons are conducted with the most recent available year, 2010, for the comparison with GAINS and 2012 for the comparison with EDGAR. Green regions indicate where the CEDS$_{\mathrm{GBD\text{-}MAPS}}$ emissions have improved agreement with EDGAR and GAINS relative to the CEDS$_{\mathrm{Hoesly}}$ inventory. Red regions indicate where CEDS$_{\mathrm{GBD\text{-}MAPS}}$ emissions have worse agreement with EDGAR or GAINS relative to the CEDS$_{\mathrm{Hoesly}}$ inventory. The color of each point represents the chemical compound, and each point is labeled with an “E” or “G”, indicating that the percent difference was calculated using EDGAR or GAINS, respectively.

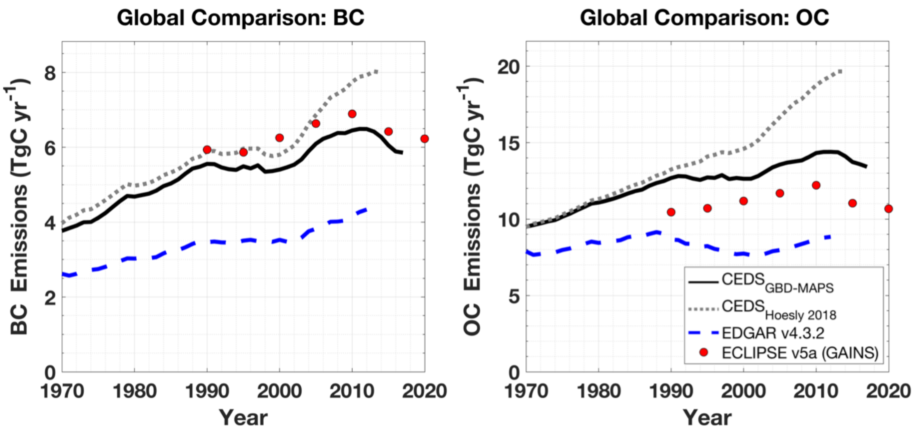

Figure 5. Comparison of global inventories of BC and OC emissions. Total EDGAR v4.3.2 and GAINS (ECLIPSE v5a) emission inventories shown without agricultural waste burning and aviation emissions. CEDS$_{\mathrm{GBD\text{-}MAPS}}$ emissions of BC and OC are not scaled to EDGAR or GAINS estimates.

total and annual gridded products are discussed further in Sect. 4.2.4

3 Results

The new CEDS$_{\mathrm{GBD\text{-}MAPS}}$ inventory provides global emissions of NO$_x$, SO$_2$, NMVOCs, NH$_3$, CO, OC, and BC for 11 anthropogenic sectors (agriculture, energy, industry, on-road, non-road transportation, residential, commercial, other, waste, solvents, international shipping) and four fuel groups (combustion of total coal, solid biofuel, liquid fuels and natural gas, and process sources) over the time period between 1970–2017. Final country-level emissions are provided as annual time series in units of metric kilotons per year ($\mathrm{kt\,yr^{-1}}$) for each sector and fuel type and include NO$_x$ as emissions of NO$_2$. Final global gridded ($0.5° \times 0.5°$) emissions for each compound, sector, and fuel group have been converted to emission fluxes ($\mathrm{kg\,m^{-2}\,s^{-2}}$), distributed over 12 months, and represent NO$_x$ as NO to facilitate use in earth system models. Total NMVOCs in gridded products are additionally separated into 25 sub-VOC classes. Using a combination of updated energy consumption data and scaling procedures, CEDS$_{\mathrm{GBD\text{-}MAPS}}$ provides the most contemporary bottom-up global emission inventory to date and is the first inventory to report global emissions of multiple atmospheric pollutants from multiple fuel groups and sectors using consistent methodology. The following results section presents an overview of the CEDS$_{\mathrm{GBD\text{-}MAPS}}$ emission inven-

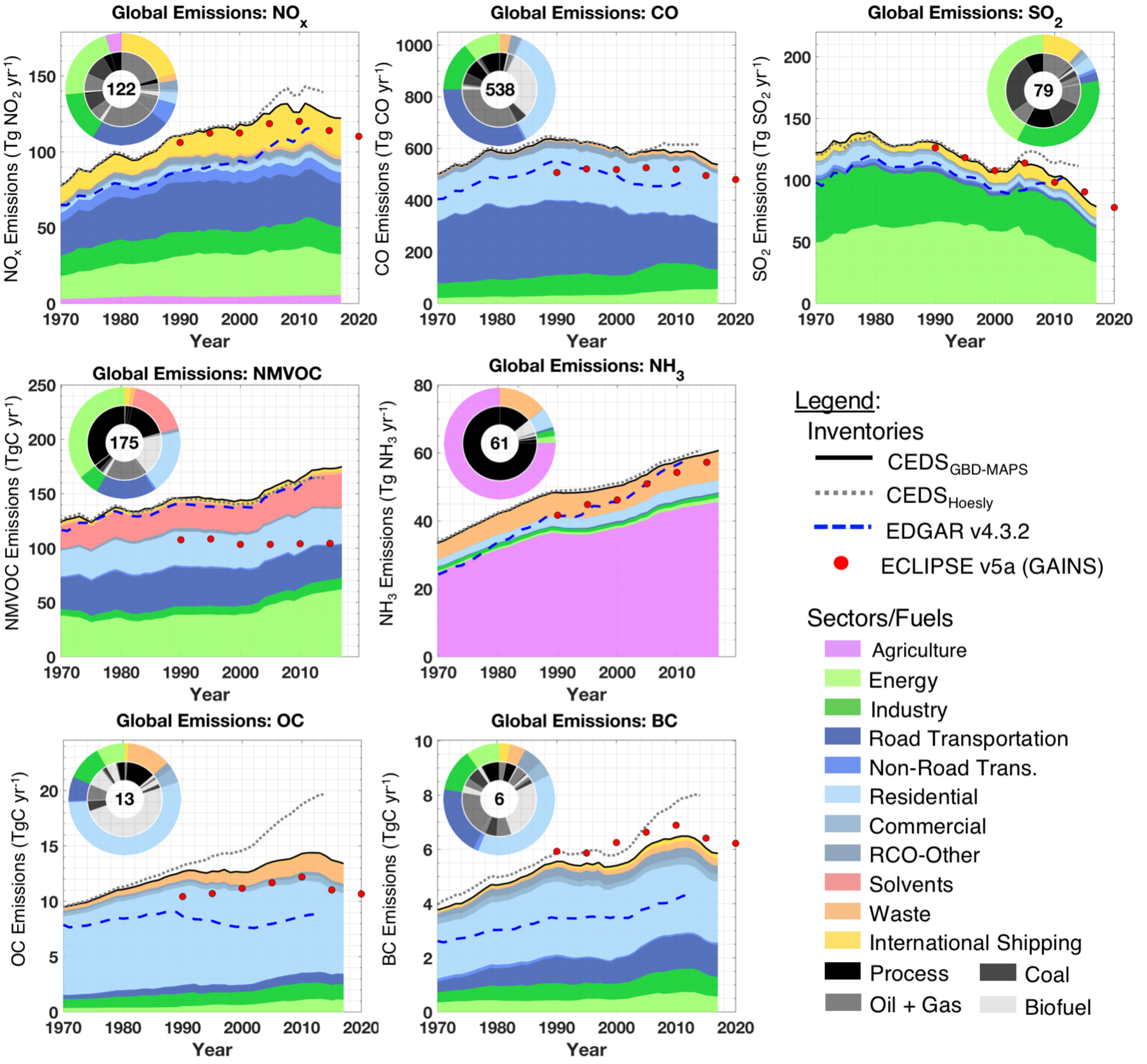

Figure 6. Time series of global annual emissions of NO_x (as NO_2), CO, SO_2, NMVOCs, NH_3, BC, and OC for all sectors and fuel types. Solid black lines are the $\text{CEDS}_{\text{GBD-MAPS}}$ inventory, with fractional sector contributions indicated by colors. Dashed gray lines are the $\text{CEDS}_{\text{Hoesly}}$ inventory. Dashed blue lines are the EDGAR v4.3.2 global inventory. Red markers are ECLIPSE v5a baseline "current legislation" (CLE) emissions (from the GAINS model) with data in 2015 and 2020 from GAINS CLE projections. All inventories include international shipping but exclude aircraft emissions. Pie chart inserts show fractional contributions of emission sectors to total 2017 emissions (outer) and fuel type contributions to each sector (inner). Emission totals for 2017 (units: $\text{Tg}\,\text{yr}^{-1}$; $\text{Tg}\,\text{C}\,\text{yr}^{-1}$ for NMVOCs, OC, BC) are given inside each pie chart.

tory, with particular focus on emissions in 2017 and historical trends as a function of compound, sector, fuel type, and world region. Section 4 compares these results to other global emission inventories and discusses the magnitudes and sources of inventory uncertainties. Known issues in the inventory data at the time of submission are detailed in Sect. S4.

3.1 Global annual total emissions in 2017

Figures 6 and 7 show time series from 1970–2017 of global annual $\text{CEDS}_{\text{GBD-MAPS}}$ emissions for each emitted compound. Global $\text{CEDS}_{\text{GBD-MAPS}}$ emissions for reactive gases in 2017 are 122 Tg for NO_x (as NO_2), 538 Tg for CO, 79 Tg for SO_2, 175 Tg C for total NMVOCs, and 61 Tg for NH_3. Global 2017 emissions of carbonaceous aerosol are 13 and

6 Tg C for OC and BC, respectively. The time series in Figs. 6 and 7 additionally show the contributions to global emissions from each of the 11 source sectors (Fig. 6) and four fuel groups (Fig. 7). Each panel in Fig. 6 additionally shows a pie chart with the fractional contribution of each sector to total global emissions in 2017 (outside), while the inner pie chart shows the fractional contributions from each of the fuel groups to each source sector. Numerical values for these fractional contributions are in Table S8. Global totals for 2017 are provided in the center of each pie chart. Global emissions from each compound are additionally split into contributions from 11 world regions (defined in Table S9) in Fig. 8 to aid in the interpretation of global trends below.

For global 2017 emissions of NO_x, Fig. 6 and Table S8 show that 60 % of NO_x emissions are associated with the energy generation (22 %), industry (15 %), and on-road transportation (23 %) sectors. These sectors have the largest contributions from emissions from coal combustion (>46 % for the energy and industry emissions) and the combined combustion of liquid fuels (oil) and natural gas (with these two fuels accounting for 100 % of NO_x on-road emissions). Time series of regional contributions to global emissions in Fig. 8 additionally show that 50 % of global 2017 NO_x emissions are from the combined Other Asia/Pacific region (Table S9) (13 Tg), China (24 Tg), and international shipping (25 Tg). For global 2017 emissions of remaining gas-phase pollutants, 67 % of CO emissions are from the on-road (100 %: oil + gas) and residential (86 %: biofuel) sectors; 78 % of SO_2 emissions are from the energy generation (63 %: coal) and industry (38 % coal, 36 % process, 25 % oil + gas) sectors; 89 % of NH_3 emissions are from the agriculture (100 %: process) and waste (100 %: process) sectors; and emissions of NMVOCs have the largest single contribution (36 %) from the energy sector, 99 % of which are associated with $\mathrm{CEDS_{GBD\text{-}MAPS}}$ process sources (Table 2). For carbonaceous aerosol in 2017, 58 % of global BC emissions are from the residential (70 %: biofuel) and on-road (100 %: oil + gas) sectors, while 67 % of global OC emissions are from the residential (92 %: biofuel) and waste (100 %: process) sectors. Figure 8 shows that in 2017, China is the dominant source of global CO (144 Tg, 27 % of global total), SO_2 (12 Tg, 15 % of global total), NH_3 (12 Tg, 20 % of global total), OC (2.7 Tg C, 20 % of global total), and BC (1.4 Tg C, 24 % of global total). In contrast, Africa is the dominant source of global NMVOCs in 2017 (48 Tg C, 27 % of global total), and international shipping is the dominant source of global NO_x emissions (25 Tg, 20 % of global total).

As discussed above in Sect. 2 and below in Sect. 4.2.4, the distinction between CEDS combustion- and process-level source categories for all species may result in the underrepresentation of emissions from combustion sources relative to those from CEDS process-level sectors. As shown in Table 2, for example, some combustion emissions from the energy, industry, and waste sectors, such as fossil fuel fires and waste incineration, are categorized as CEDS "process-level" source categories (Table 2). These emissions are allocated to the final CEDS process category rather than the CEDS total coal, biofuel, or oil and gas categories.

3.2 Historical trends in annual global emissions

Historical emission trends between 1970 and 2017 in Figs. 6 and 7 indicate that global emissions of each compound generally follow three patterns: (1) global CO and SO_2 emissions peak prior to 1990 and generally decrease until 2017; (2) global emissions of NO_x, BC, and OC peak much later, around 2010, and then decrease until 2017; and (3) global emissions of NH_3 and NMVOCs continuously increase throughout the entire time period. These trends generally reflect the sector-specific regulations implemented in dominant source regions around the world. For example, global emissions of CO generally decrease after the incorporation of catalytic converters in North America and Europe around 1990 (Figs. S7 and S8). Despite, however, continued reductions in these regions, global emissions of CO slightly increase between 2002 and 2012 due to simultaneous increases among the energy, industry, and residential sectors in China, India, Africa, and the Other Asia/Pacific region (Figs. S9–S12). Global CO emissions then decrease by 9 % between 2012 and 2017, largely due to reductions in industrial coal, residential biofuel, and process energy sector emissions in China (Figs. S9, S17–S18, S20), associated with the implementation of emission control strategies (reviewed in Zheng et al., 2018) as well as continued reductions in on-road transport emissions in North America and Europe (Figs. S7–S8). Similarly, global SO_2 emissions decrease after peaking in 1979, largely due to emission control policies in the energy and industry sectors in North America and Europe (Figs. S7–S8). While simultaneous increases in emissions from coal use in the energy and industry sectors in China result in a brief increase in global SO_2 emissions between 1999 and 2004 (Figs. 6, S9), global SO_2 emissions decline by 32 % between 2004 and 2017 due to the implementation of stricter emission standards for the energy and industry sectors after 2010 in China (Zheng et al., 2018) as well as continued reductions in North America and Europe (Figs. S7–S8). Regional SO_2 emission trends are particularly large with a factor of 9.5 decrease in total SO_2 emissions in North America between 1973 and 2017, a factor of 6.9 decrease in Europe between 1979 and 2017, and a factor of 5.9 increase in China between 1970 and 2004, followed by a factor of 2.6 decrease after 2011 (Fig. 8). While China is the largest global contributor to SO_2 emissions between 1994 and 2017, these large regional reductions, coupled with increasing SO_2 emissions in the Other Asia/Pacific region, African countries, and India (Fig. 8), indicate that future global SO_2 emissions will increasingly reflect activities in these other rapidly growing regions.

In contrast to historical emissions of SO_2 and CO, global emissions of NO_x, BC, and OC peak later, between 2011

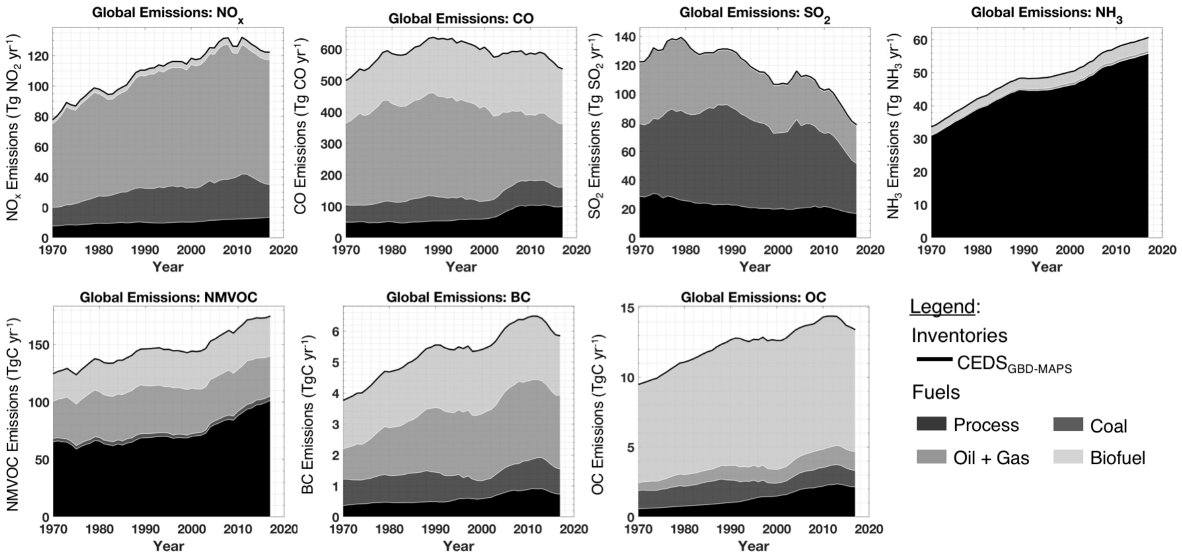

Figure 7. Time series of global annual emissions of NO_x, CO, SO_2, NH_3, NMVOCs, BC, and OC for all sectors, colored by fuel group.

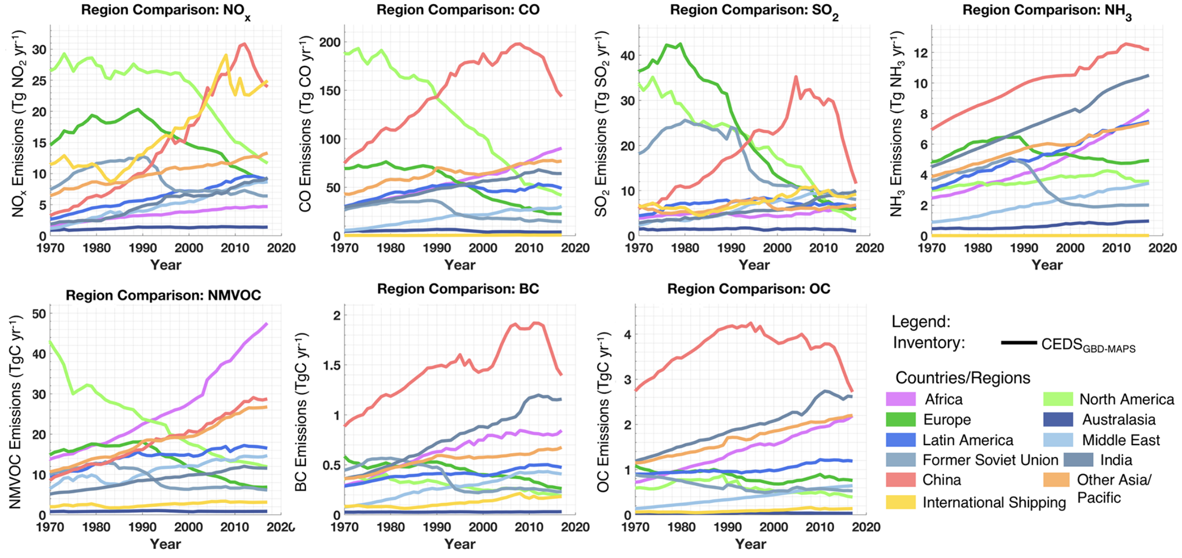

Figure 8. Time series of global annual CEDS$_{GBD-MAPS}$ emissions of NO_x, CO, SO_2, NH_3, NMVOCs, BC, and OC for all sectors and fuel types, split into 11 regions and countries (defined in Table S9).

and 2013. Global emissions then decrease by 7 %, 9 %, and 7 %, respectively, by 2017 (Fig. 6). These trends also reflect the sector-specific regulations implemented in dominant source regions. For NO_x for example, global emissions between 1970 and 2017 are dominated by the combustion of coal, oil, and gas in the on-road transportation, energy generation, industry, and international shipping sectors (Figs. 6, 8). Global on-road transportation emissions are generally flat between 1988 and 2013 due to competing trends across world regions. While more stringent vehicle emission standards result in more than a factor of 2 decrease in on-road transportation NO_x emissions in North America and Europe between 1992 and 2017 (Figs. S7–S8), on-road transport emissions in China, India, and the Other Asia/Pacific region simultaneously experience between a factor of 1.3 and 2.8 increase (Figs. S9–S11). Subsequent reductions between 2013 and 2017 in global on-road emissions correspond to a 12 % reduction in on-road transportation emissions in China due to the phase-in of stricter emission standards (Zheng et al., 2018), coupled with a continued decrease in emissions from North America and Europe. Global NO_x emissions from the energy and industry sectors increase by up to a factor of 6 between 1970 and 2011 due to regional increases in China, India, the Other Asia/Pacific region, and African countries, with reductions between 2011 and 2017, again largely from reductions in China from stricter emissions control policies for coal-fired power plants and coal use in industrial processes (Zheng et al., 2018; Liu et al., 2015). Global emissions of NO_x from waste combustion and agricultural activities also increased by 2 % and 65 %, respectively, between 1970 and 2017, also contributing to the offset of recent reductions in emissions from regulated combustion sources (Fig. 6). Similar to global NO_x emissions, trends in historical BC and OC emissions reflect a balance between emission trends in North America, Europe, and other world regions, with reduction between 2010 and 2017 largely driven by reductions in emissions from China (Figs. 8, S9). In contrast to NO_x emissions, however, BC and OC emissions are dominated by contributions from biofuel combustion in the residential sector as well as on-road transportation, industry, and energy sectors for BC and the waste sector for global OC (Fig. 6). Though emissions of BC and OC have a higher level of uncertainty relative to other compounds (Sect. 4), emissions from African countries and the Other Asia/Pacific region experience growth in BC and OC emissions from these sectors. The exceptions are in China and India, both of which experience a plateau or reduction in BC and OC emissions from the residential, energy (China only), industry, and on-road transportation sectors between 2010 and 2017. In India, reductions in BC and OC emissions from the residential and informal industry sectors are expected to continue under policies to switch to cleaner residential fuels and energy sources, while BC emissions from on-road transport may increase due to increased transport demand (Venkataraman et al., 2018). Similar to trends in SO_2 emissions, increasing trends in total OC and BC emissions from Africa, India, Latin America, the Middle East, and the Other Asia/Pacific region, coupled with large decreases in emissions from China, North America, and Europe (Fig. 8), indicate that global emissions will increasingly reflect activities in these rapidly growing regions.

Trends in historical emissions of NMVOCs and NH_3 differ from other pollutants in that they continuously increase between 1970 and 2017. Global emissions of NH_3 increase by 81 % between 1970 and 2017 and are largely associated with emissions from agricultural practices (75 % in 2017) and waste disposal and handling (14 % in 2017) (Fig. 6, Table S8). Unlike emissions from combustion sources, there are no large-scale regulations outside of Europe targeting NH_3 emissions from agricultural activities, such as livestock manure management. As a result, global agricultural emissions of NH_3 increase between 1970 and 2017 by 82 %, driven by increases in all regions other than Europe (Figs. 6, S6–S12). Similarly, global NH_3 emissions from the waste sector increase by 77 % between 1970 and 2017, driven by increases in Latin America, the Other Asia/Pacific region, Africa, and India (Figs. S10–S12). Global emissions of NMVOCs increase by 40 % between 1970 and 2017 and are largely associated with emissions from the on-road transport, residential, energy, industry, and solvent use sectors (Fig. 6). In contrast to other emitted pollutants, Africa is the largest global source of NMVOC emissions between 2010 and 2017, largely due to large contributions and continued increases in emissions from the residential (factor of 2.7) and energy (factor of 4) sectors (Fig. S12). Increases in energy sector emissions after 2003 are largely driven by increases in fugitive emissions from select African countries, including Nigeria, Kenya, Angola, and Mozambique. Emissions from China are the second-largest global NMVOC source between 1996 and 2017 (Fig. 8), while the Other Asia/Pacific region is the third-largest source between 1999 and 2017. Total NMVOCs in China increase by a factor of 3.4 between 1970 and 2017 due to activity increases in the solvent, energy, and industry sectors (Zheng et al., 2018), while targeted emission controls for the residential and on-road transport sectors result in their reduced contributions to NMVOC emissions between 2012 and 2017 (Fig. S9). Total emissions of NMVOCs in Europe and North America decrease by up to a factor of 2.4 between 1970 and 2017 due to reductions in all source sectors, except for energy emissions in North America, which increase between 2007 and 2011 and remain flat through 2017 (Fig. S7).

To provide a fuel-centric perspective of global historical emissions trends, Fig. 7 illustrates the contributions from the combustion of coal, solid biofuel, the sum of liquid fuel and natural gas, and all remaining CEDS "process-level" sources (Table 2) to total global emissions between 1970 and 2017. Reductions discussed above between 2010 and 2017 for global emissions of NO_x, CO, SO_2, BC, and OC are largely associated with reductions in coal combustion from the energy, industry, and residential sectors associated with emission control policies and residential fuel replacement in China as well as coal-fired power plant reductions in North America and Europe (Figs. 7, S13, S17–S18). Despite large reductions in emissions, China is still the single largest source of global emissions from coal combustion in 2017 (23 %–64 % for each compound except NH_3). Figure S17, however, also shows that emissions from coal combustion are simultaneously increasing in India, the Other Asia/Pacific region, and Africa. Specifically, SO_2 emissions from coal combustion in India are set to surpass those from China by 2018 if recent $\mathrm{CEDS_{GBD\text{-}MAPS}}$ trends hold. For solid biofuel combustion, global emissions of all compounds are primarily associated with the residential sector (Fig. S14), with recent reductions in biofuel CO, SO_2, BC, and OC emissions largely from reductions in China (Fig. S18). In contrast, biofuel emissions from all other regions remain relatively flat or increase between 1970 and 2017, though biofuel emissions of NMVOCs, CO, SO_2, and OC in India as well as SO_2 emissions in North America both decrease between 2010 and 2017 (Fig. S18). In 2017, biofuel emissions of all compounds are dominated by emissions from either Africa (NO_x, SO_2, NH_3, NMVOC, BC) or India (OC). For oil and gas combustion, global emissions of all compounds are primarily associated with on-road transportation, international shipping, and energy and industry (SO_2 only) sectors, with general decreases in associated emissions in North America and Europe between 1970 and 2017 and increases in other regions (Fig. S19). In contrast to other combustion sectors and fuels, emissions of NO_x, CO, NMVOCs, BC, and OC from the combustion of liquid fuels and natural gas in China remain relatively flat or slightly decrease between 2010 and 2017. Dominant global regions vary by compound (Fig. S19) and include international shipping (NO_x, SO_2), Africa (OC), India (BC), North America (CO, NH_3), and the Other Asia/Pacific region (NMVOCs). Global CEDS process source emissions, which include contributions from some fuel combustion processes (Table 2), decrease between 2010 and 2017 for CO, SO_2, BC, and OC. These trends are primarily associated with reductions in emissions from the energy and industry sectors. In contrast, process source contributions to NO_x, NH_3, and NMVOCs increase over this same time period due to increases in non-combustion agricultural and solvent use emissions as well as emissions from waste disposal and energy generation and transformation (Fig. S16). Increases in emissions from these sectors between 1970–2017 drive the continuous increases in global NH_3 and NMVOCs, discussed above. Dominant source regions in 2017 of these process-level emissions include China (NO_x, CO, NH_3, BC, OC), India (SO_2), and African countries (NMVOCs) (Fig. S20).

4 Discussion

4.1 Comparison to global inventories

4.1.1 Comparison to $\mathrm{CEDS_{Hoesly}}$ inventory

As a result of the similar methodologies, Fig. 6 shows that $\mathrm{CEDS_{GBD\text{-}MAPS}}$ and $\mathrm{CEDS_{Hoesly}}$ emission inventories predict similar magnitudes and historical trends in global emissions of each compound between 1970 and 2014. The two inventories, however, diverge in recent years due to the incorporation of updated activity data and both updated and new scaling emission inventories included in the $\mathrm{CEDS_{GBD\text{-}MAPS}}$ system. For global emissions of NO_x, CO, and SO_2, the $\mathrm{CEDS_{GBD\text{-}MAPS}}$ emissions are smaller than the $\mathrm{CEDS_{Hoesly}}$ emissions after 2006 and show a faster decreasing trend. By 2014, global emissions of these compounds are between 7 % and 21 % lower than previous $\mathrm{CEDS_{Hoesly}}$ estimates. These differences are largely associated with large emission reductions in China as a result of the updated national-level scaling inventory from Zheng et al. (2018), along with the added DICE-Africa (Marais and Wiedinmyer, 2016) and SMoG-India (Venkataraman et al., 2018) scaling inventories. Differences in emissions from India and Africa in the two CEDS inventories are discussed in Sect. 2 (Fig. 3) and, combined, account for ∼ 60 % of the reduction in global NO_x emissions, 23 % of the reduction in global CO, and 14 % of the reduction in global SO_2. The largest differences between these two inventories in India and Africa are the reduced NO_x emissions from the transport sector as well as reduced energy emissions of SO_2 in India. Remaining differences between NO_x and SO_2 emissions in the two CEDS inventories are largely associated with the updated China emission inventory from Zheng et al. (2018), which reports lower emissions in 2010 and 2012 than a previous version of the MEIC inventory that was used to scale China emissions in the $\mathrm{CEDS_{Hoesly}}$ inventory (C. Li et al., 2017). These emission reductions are largely associated with the industrial and residential sectors in China and are partially offset by a simultaneous increase in transportation emissions of all compounds relative to $\mathrm{CEDS_{Hoesly}}$.

For global emissions of NH_3 and NMVOCs, these species remain relatively unchanged between the $\mathrm{CEDS_{Hoesly}}$ and $\mathrm{CEDS_{GBD\text{-}MAPS}}$ inventories. In 2014 $\mathrm{CEDS_{GBD\text{-}MAPS}}$ emissions are 5 % higher than $\mathrm{CEDS_{Hoesly}}$ emissions for NMVOCs and 2 % lower than $\mathrm{CEDS_{Hoesly}}$ global NH_3 emissions. Emissions of NH_3 remain relatively unchanged (within $< 2\,\%$) from dominant source regions, including India, Africa (Fig. 3), and China. In contrast, emissions of NMVOCs from Africa and China in the DICE-Africa and Zheng et al. (2018) scaling inventories are larger than those in the $\mathrm{CEDS_{Hoesly}}$ inventory. Global emissions of NMVOCs are also higher in the EDGAR v4.3.2 inventory relative to the previous version used in the $\mathrm{CEDS_{Hoesly}}$ inventory. NMVOCs are particularly large from the process energy sector emissions in Africa (Fig. S12), which primarily include fugitive emissions from oil and gas operations (Table 2). Default energy sector emissions from "non-combustion" processes are taken from the EDGAR inventory and are not scaled to the DICE-Africa inventory. Therefore, the large increase in these emissions in Africa relative to $\mathrm{CEDS_{Hoesly}}$ is largely driven by changes in the EDGAR v4.3.2 inventory, with emissions from the 1B2_Fugitive_Fossil fuels sector increasing for example by a factor of 5 in Nigeria between 2003 and 2017.

Global emissions of OC and BC have the largest differences between the two CEDS inventories, with $\mathrm{CEDS_{GBD\text{-}MAPS}}$ emissions consistently smaller than $\mathrm{CEDS_{Hoesly}}$ emissions between 1970 and 2014. By 2014, $\mathrm{CEDS_{GBD\text{-}MAPS}}$ emissions of BC and OC are 24 % and 33 % smaller than corresponding $\mathrm{CEDS_{Hoesly}}$ emissions. In the $\mathrm{CEDS_{Hoesly}}$ inventory, default emissions of BC and OC are not scaled, and therefore these differences are largely associated with the added scaling inventories, discussed in Sect. 2 and shown in Table 3. As shown in Figs. S3–S4, the added scaling of BC and OC emissions leads to a reduction in global $\mathrm{CEDS_{GBD\text{-}MAPS}}$ emissions of OC in all scaled regions and a reduction in BC emissions in all regions other than India. In India, increases in industry and residential BC emissions from the SMoG-India scaling inventory result in a slight increase in BC emissions relative to the $\mathrm{CEDS_{Hoesly}}$ inventory (Fig. 3). Waste emissions of OC and BC are also reduced in the $\mathrm{CEDS_{GBD\text{-}MAPS}}$ inventory due to updated assumptions for the fraction of waste burned (Sect. S1.1).

As discussed in Hoesly et al. (2018) and further below, BC and OC emissions typically have the largest uncertainties of all the emitted species, and their recent changes in the residential and waste sectors are particularly uncertain.

The relative contributions of each source sector to emissions in the two CEDS versions are additionally shown in Fig. S21. This comparison shows that the fractional sectoral contributions to global emissions in 2014 are the same to within 10 % in the two CEDS inventories. The largest differences are a 9 % increase in the relative contribution of on-road transportation emissions of CO and reductions in the relative contribution of waste emissions across all compounds. These trends reflect the large update to default waste emissions described above as well as changes associated with the DICE-Africa and national China scaling inventories.

Similar to the total global emissions, changes between the two CEDS versions for the national-level and 0.5° × 0.5° gridded products will also result from updates to the energy consumption data, scaling inventories (Sects. 2.2–2.3), and spatial distribution proxies from EDGAR v4.3.2 (Sect. 2.1). Time series of differences between the $\mathrm{CEDS_{Hoesly}}$ and $\mathrm{CEDS_{GBD\text{-}MAPS}}$ inventories for 11 world regions are shown for each compound in Fig. S22. Fig. S22 shows that $\mathrm{CEDS_{GBD\text{-}MAPS}}$ emissions are, in recent years, generally lower in each region, with the greatest differences in Africa, India, and China. The relative changes in Africa and India are discussed in Sect. 2. For China, the $\mathrm{CEDS_{GBD\text{-}MAPS}}$ emissions are generally lower than the $\mathrm{CEDS_{Hoesly}}$ estimates after the year 2010 as a result of the updated scaling inventory. Regional differences between inventories are also greater for OC and BC emissions relative to other compounds due to the added scaling procedure discussed in Sect. 2. Differences in spatial distributions are not discussed here as changes represent differences in the spatial proxies, which are largely from updates to the EDGAR inventory.

4.1.2 Comparison to other global inventories (EDGAR and GAINS)

Figure 6 additionally provides a comparison of the $\mathrm{CEDS_{GBD\text{-}MAPS}}$ global emissions to those from two widely used inventories: EDGAR v4.3.2 (Crippa et al., 2018; EC-JRC, 2018) and ECLIPSE v5a (GAINS) (IIASA, 2015; Klimont et al., 2017). For a comparison of global emissions across similar emission sectors, the EDGAR v4.3.2 inventory in Fig. 6 includes emissions from all reported sectors (including international shipping), except for those from agricultural waste burning and domestic and international aviation. Similarly, the GAINS ECLIPSE v5a baseline scenario inventory in Fig. 6 includes all reported emissions other than those from agricultural waste burning. These include contributions from aggregate residential and commercial combustion sources (“dom”), energy generation (“ene”), industrial combustion processes (“ind”), road and non-road transportation (“tra”), agricultural practices (“agr”), and waste disposal (“wst”). GAINS ECLIPSE v5a baseline estimates for international shipping emissions are also included in Fig. 6. A table with sectoral mappings of the $\mathrm{CEDS_{GBD\text{-}MAPS}}$, EDGAR v4.3.2, and GAINS inventories is provided in Table S10.

The comparison in Fig. 6 shows that global emissions of all compounds in the $\mathrm{CEDS_{GBD\text{-}MAPS}}$ inventory are consistently larger than in the EDGAR v4.3.2 inventory (Crippa et al., 2018). Global $\mathrm{CEDS_{GBD\text{-}MAPS}}$ emissions of NO_x, $\mathrm{SO_2}$, CO, and NMVOCs are at least 27 % larger, while global emissions of $\mathrm{NH_3}$, BC, and OC are within 52 %. Figure S23 indicates that differences in global BC and OC emissions are largely due to higher waste and residential and commercial emissions in the $\mathrm{CEDS_{GBD\text{-}MAPS}}$ inventory. Figure 6, however, also shows that the trends in global emissions are similar between EDGAR v4.3.2 and $\mathrm{CEDS_{GBD\text{-}MAPS}}$ for most compounds. For example, between 1970 and 2012, global emissions of $\mathrm{SO_2}$, $\mathrm{NH_3}$, NMVOCs, and BC peak in the same years. Global CO and NO_x emissions both peak 1 year earlier in the $\mathrm{CEDS_{GBD\text{-}MAPS}}$ inventory but otherwise follow similar historical trends. Trends in OC emissions are the most different between the two inventories, with a peak in emissions in 1988 in the EDGAR inventory compared to 2012 in the $\mathrm{CEDS_{GBD\text{-}MAPS}}$ inventory. A comparison of relative sectoral contributions in Fig. S23 shows that these differences in OC emissions are largely due to the residential and commercial sectors, which may be underestimated in the EDGAR v4.3.2 inventory relative to GAINS (Crippa et al., 2018) and $\mathrm{CEDS_{GBD\text{-}MAPS}}$. Both inventories also show a net increase in global emissions of all compounds other than $\mathrm{SO_2}$ between 1970 and 2012. Global $\mathrm{SO_2}$ emissions follow a similar trend until 2007, after which the emissions in $\mathrm{CEDS_{GBD\text{-}MAPS}}$ decrease at a faster rate than in EDGAR v4.3.2. These differences are largely due to the energy sector, which increases between 2006 and 2012 in EDGAR and decreases as a result of emission reductions in China in the $\mathrm{CEDS_{GBD\text{-}MAPS}}$ inventory (Fig. S23). For all other compounds, the rate of increase in emissions between 1970 and 2012 is also slightly different between the two inventories. For example, $\mathrm{NH_3}$ emissions in the $\mathrm{CEDS_{GBD\text{-}MAPS}}$ inventory increase by 74 % compared to a 139 % increase in EDGAR. In contrast, BC and OC emissions increase at a faster rate in the $\mathrm{CEDS_{GBD\text{-}MAPS}}$ inventory. Due to similar sources of uncertainty and the additional scaling of $\mathrm{CEDS_{GBD\text{-}MAPS}}$ emissions to EDGAR (except for BC and OC), levels of uncertainty between the two inventories are expected to be similar, as discussed further in Sect. 4.2.

Similar to the comparison with EDGAR emissions, Fig. 6 also shows that global emissions in the $\mathrm{CEDS_{GBD\text{-}MAPS}}$ inventory are generally larger than emission estimates from the GAINS model, published as part of the ECLIPSE v5a inventory (referred to here as GAINS) (Klimont et al., 2017). Two exceptions are for $\mathrm{SO_2}$ emissions, which are up to 6 % lower than GAINS in select years, and BC emissions, which are consistently 5 %–15 % lower than GAINS for all years. While the sectoral definitions may slightly differ between these inventories, Fig. S24 shows that these differences are largely due to different trends in energy and industry SO_2 emissions between 2005 and 2015 and consistently lower BC emissions from the residential and commercial sector in the $\text{CEDS}_{\text{GBD-MAPS}}$ inventory. For all years with overlapping data between 1990 and 2015, the absolute magnitude of global emissions is within ±15 % for NO_x, SO_2, NH_3, and BC; within 22 % for CO and OC; and within 50 % for NMVOCs. Historical trends in each inventory are also similar for all compounds other than CO and NMVOCs (Fig. 6). Peak global emissions occur between 2010 and 2012 for NO_x, BC, and OC, while both inventories show a net decrease in emissions in SO_2 and a net increase in emissions of NH_3. In contrast, GAINS emissions of CO peak in 2010, while $\text{CEDS}_{\text{GBD-MAPS}}$ emissions peak in 1990. The largest differences in historical trends are for global NMVOC emissions, with GAINS showing a 3 % decrease between 1990 and 2010, while $\text{CEDS}_{\text{GBD-MAPS}}$ NMVOC emissions increase by 13 % over this same time period (Fig. 6). Sectoral contributions between the two inventories in Fig. S24 indicate that these differences are largely due differences in the energy, industry, and on-road transport emissions of NMVOCs. Uncertainties in the GAINS model have been previously estimated to fall between 10 % and 30 % in Europe for gas-phase species (Schöpp et al., 2005) and within the uncertainty estimates for BC and OC of other global bottom-up inventories (Klimont et al., 2017; Bond et al., 2004), as discussed in the following section.

4.2 Uncertainties

The level and sources of uncertainty in the $\text{CEDS}_{\text{GBD-MAPS}}$ inventory are similar to those in the $\text{CEDS}_{\text{Hoesly}}$ inventory, which are largely a function of uncertainty in the activity data, emission factors, and country-level inventories. As these uncertainties have been previously discussed in Hoesly et al. (2018), we have not performed a formal uncertainty analysis here but rather provide a brief summary of the sources of uncertainty associated with this work. We note plans for a robust uncertainty analysis in an upcoming release of the CEDS core system. While this section highlights many of the challenges associated with estimating comprehensive and accurate global bottom-up emission inventories, such inventories remain vital for their use in chemistry and climate models and for the development and evaluation of future control and mitigation strategies.

4.2.1 Uncertainties in activity data

As discussed in Sect. 2.1, CEDS default emissions from combustion sources are largely informed by fuel consumption data from the IEA 2019 World Energy Statistics Product (IEA, 2019). While this database provides energy consumption data as a function of detailed source sector and fuel type for most countries, the IEA data are uncertain and include breaks in time series data that can lead to abrupt changes in the $\text{CEDS}_{\text{GBD-MAPS}}$ emissions for select sectors, fuels, and countries. For example, Fig. S7 shows an order of magnitude decrease (0.1 Tg C) in OC industrial emissions from North America between 1992 and 1993, which is driven by a break in IEA biofuel consumption data for the non-specified manufacturing industry sector (CEDS sector: 1A2g_Ind-Comb-other) in the United States. While the magnitude of this particular change is negligible on the global scale, this is not the case for all sectors. For example, as noted in Sect. S4, a known issue in the IEA data in China in the energy sector causes peaks in the associated NO_x and SO_2 $\text{CEDS}_{\text{GBD-MAPS}}$ emissions in 2004. These peak emissions may be overestimated by up to 4 and 10 Tg, respectively, which is large enough to impact historical trends in both regional (Fig. 8: NO_x and SO_2) and global (Figs. 6–7: SO_2) emissions. These point to areas where improvements could be made to the underlying driver data in future work.

4.2.2 Uncertainties in global bottom-up inventories

Uncertainties in bottom-up emission inventories vary as a function of space, time, and compound, making total uncertainties difficult to quantify. Default emission estimates in the CEDS system are subject to uncertainties in underlying activity data, such as IEA energy consumption data, as well as activity drivers for process-level emissions. Knowledge of accurate emission factors also drives inventory uncertainty as EFs are not often available for all sectors in countries with emerging economies and are heavily dependent on the use, performance, and enforcement of control technologies within each sector and country (e.g., Zhang et al., 2009; Wang et al., 2015). While improvements in data collection and reporting standards may decrease the uncertainty in some underlying sources over time, the most recent years of $\text{CEDS}_{\text{GBD-MAPS}}$ emissions are still subject to considerable uncertainty. For instance, the degree of local and national compliance with control measures is often variable or unknown (e.g., Wang et al., 2015; Zheng et al., 2018); recent activity and regional emissions data are often updated as new information becomes available; and emissions in generally more uncertain regions, including India and Africa, are becoming an increasingly large fraction of global totals. Additionally, from a methodological standpoint, default CEDS emissions after 2010 also currently rely on the projection of emission factors from the GAINS EMF30 data release for sectors and countries where contemporary regional scaling inventories are not available.

As the CEDS system uses a "mosaic" approach and incorporates information from other global- and national-level inventories, the final $\text{CEDS}_{\text{GBD-MAPS}}$ emissions will also be subject to the same sources and levels of uncertainty as these external inventories. For example, as discussed in Sect. 2.1, default process-level emissions in $\text{CEDS}_{\text{GBD-MAPS}}$ are derived using emissions from the EDGAR v4.3.2 inventory, with many countries additionally scaled to this inventory during Step 2. As reported and discussed in Crippa et al. (2018), EDGAR v4.3.2 emissions for 2012 at the regional level are estimated to have the smallest uncertainties for SO_2, between 14.4 % and 47.6 %, with uncertainties in NO_x between 17.2 % and 69.4 % (up to 124 % for Brazil), CO between 25.9 % and 123 % (lower for industrialized countries), and NMVOCs between 32.7 % and 148 % (lower for industrialized countries). Emissions of NH_3 are highly uncertain in all inventories (186 % to 294 % in EDGAR) due to uncertainties in the reporting of agricultural statistics and emission factors that will depend on individual farming practices, biological processes, and environmental conditions (e.g., Paulot et al., 2014). As noted in Crippa et al. (2018) and Klimont et al. (2017), EDGAR v4.3.2 and GAINS uncertainty estimates for BC and OC fall within the factor of 2 range that has been previously estimated by the seminal work of Bond et al. (2004). While $\mathrm{CEDS_{GBD\text{-}MAPS}}$ emissions are not scaled to EDGAR v4.3.2 BC and OC emissions, estimates are derived from similar sources and are therefore expected to be consistent with uncertainties in both EDGAR and other global bottom-up inventories. It should also be noted that these reported uncertainty estimates from EDGAR only reflect the uncertainties associated with the emission estimation process and do not account for the potential of missing emissions sources or super-emitters within a given sector (Crippa et al., 2018).

To evaluate and improve the accuracy of these bottom-up emission estimates, inventories are increasingly using information from high-resolution satellite retrievals, particularly for major cities, large-area sources, natural sources, and large point sources (e.g., M. Li et al., 2017a; McLinden et al., 2016; Streets et al., 2013; van der Werf et al., 2017; Beirle et al., 2011; McLinden et al., 2012; Lamsal et al., 2011; Zheng et al., 2019; Elguindi et al., 2020). For example, both the $\mathrm{CEDS_{Hoesly}}$ and $\mathrm{CEDS_{GBD\text{-}MAPS}}$ inventories incorporate SO_2 emission estimates derived using satellite retrievals in McLinden et al. (2016) to account for previously missing SO_2 point sources in the CEDS 1B2_Fugitive-petr-and-gas sector (described further in the supplement of Hoesly et al., 2018), with additional use of satellite data planned for a future CEDS core release. With the continued advancement of satellite retrievals, the development of source- and sector-specific inventories, such as $\mathrm{CEDS_{GBD\text{-}MAPS}}$, will continue to provide new opportunities for the application of new satellite-based inventories, which will aid in the quantification of spatial and temporal emissions from distinct sources associated with specific sectors and fuel types that may not be accurately estimated using conventional bottom-up approaches.

4.2.3 Uncertainties in regional-level scaling inventories

Similar to the $\mathrm{CEDS_{Hoesly}}$ inventory, the $\mathrm{CEDS_{GBD\text{-}MAPS}}$ emissions will also reflect the uncertainties associated with the inventories used for the scaling procedure. The inventories with the largest impact on the $\mathrm{CEDS_{GBD\text{-}MAPS}}$ emission uncertainties relative to the $\mathrm{CEDS_{Hoesly}}$ inventory will be those from China from Zheng et al. (2018), the DICE-Africa emission inventory from Marais and Wiedinmyer (2016), and the SMoG-India inventory from Venkataraman et al. (2018). While formal uncertainty analyses were not performed for all of these inventories, similar bottom-up methods used in these studies will result in similar sources of uncertainties (activity and emission factors) as the global inventories. For example, Zheng et al. (2018) state that the largest sources of uncertainty are the accuracy and availability of underlying data (reviewed in M. Li et al., 2017b) and that the levels of uncertainty for China emissions between 2010 and 2017 are expected to be similar to previous national-level bottom-up inventories derived using similar data sources and methodology, such as Zhao et al. (2011), Lu et al. (2011), and Zhang et al. (2009). Similar to global inventories, these previous regional studies estimate much lower levels of uncertainty for SO_2 and NO_x (±16 % and −13 % to +37 %, respectively) than for CO (70 %) and OC and BC emissions (−43 % to +258 % and −43 % to +208 %, respectively). Some sectors in China and other regions are particularly uncertain, as discussed further below.

Regional and national inventories, however, have the added benefit of using local knowledge to reduce potential uncertainties in emission factors and missing emission sources. For example, Marais and Wiedinmyer (2016) note that the DICE-Africa emissions are uncertain due to gaps in fuel consumption data. This inventory, however, also includes sources frequently missing in global inventories such as widespread diesel and petrol generator use, kerosene use, and ad hoc oil refining and have used emission factors for on-road car and natural-gas flaring that are more representative of the inefficient fuel combustion conditions in Africa (Marais and Wiedinmyer, 2016; Marais et al., 2019). As discussed in Sect. 2, the $\mathrm{CEDS_{GBD\text{-}MAPS}}$ inventory may still underestimate total emissions from some of these sources (up to 11 % in 2013; Sect. 2.2.3) but otherwise will have uncertainties for total Africa emissions similar to the DICE-Africa inventory. For emissions in India, uncertainties also arise from missing fuel consumption data and the application of non-local or uncertain emission factors. Venkataraman et al. (2018), however, is one of the few studies to present a detailed uncertainty analysis of their inventory and use the propagation of source-specific activity data and emission factors to estimate that total emission uncertainties are smaller for SO_2 (−20 % to 24 %) than for NO_x (−65 % to 125 %) and NMVOCs (−44 % to +66 %). While uncertainties are not explicitly reported for OC and BC emissions, Fig. 1 in Venkataraman et al. (2018) indicates that uncertainties in these emissions are between −60 % and +95 %, consistent with BC and OC uncertainties reported in other bottom-up inventories. We also note the ongoing work to improve the accuracy of highly uncertain emission sectors in a future release of the SMoG-India inventory through the CarbOnaceous AerosoL Emissions, Source apportionment and ClimatE impacts (COALESCE) project (Venkataraman et al., 2020).

In addition to uncertainties in the scaling inventory emissions, uncertainties are also introduced by the $\mathrm{CEDS}_{\text{GBD-MAPS}}$ scaling procedure. Uncertainties arise when mapping sectoral- and fuel-specific (when available) emissions between inventories (as discussed previously) as well as in the application of the calculated scaling factors outside the range of available scaling inventory years. For example, the implied CO EFs in Fig. S2 highlight one case in China where the EFs for oil and gas combustion in the on-road transport sector peak in 1999 at a value over 3 times larger than EFs in all other top-emitting countries. For China specifically, the calculated scaling factors for the year 2010 (earliest scaling inventory year) are applied to emissions from all years prior, which was calculated as a value of ~ 1.58 for the on-road transport sector. The implied EF of $\sim 1.8\,\mathrm{g\,g^{-1}}$ for this sector in 2003 (Fig. S2) suggests that the SF from 2010 may not be representative of emissions during this earlier time period. We do note, however, that the 1999 peak in total CO emissions in China (Fig. S9) is driven by the IEA energy data and is consistent with the $\mathrm{CEDS}_{\text{Hoesly}}$ inventory (Hoesly et al., 2018). In contrast, EFs from this sector in China after the year 2010 agree with the magnitude and trends found in other countries, further indicating that the scaling factors are most appropriate for years with overlapping inventory data. Other similar examples include coal energy emissions of SO_2 in Thailand (Fig. S2). In this case, the REAS scaling inventory spans the years 2000–2008. The default EFs for the energy sector, however, independently decrease between 1997 and 2001. As a result, when the implied EF of 3.3 for the year 2000 is applied to all historical energy emissions, the implied EFs prior to 1997 become an order of magnitude larger than those in nearly all other top-emitting countries (Fig. S2). Overall, the applicability of the scaling factors to emissions in years outside the available scaling inventory years remains uncertain due to real historical changes in activity, fuel-use, and emissions mitigation strategies. These uncertainties, however, vary by compound and sector as, for example, there are no similar peaks in on-road emissions for compounds other than CO in China.

Though the inclusion of these regional inventories can improve the accuracy of the global CEDS system (particularly during years with overlapping data), Hoesly et al. (2018) note that large uncertainties may still persist, even in developed countries with stringent reporting standards. In the US for example, it has been suggested that compared to the US National Emissions Inventory (US NEI), total NO_x emissions from on-road and industrial sources in some regions may be overestimated by up to a factor of 2 (e.g., Travis et al., 2016). In addition, NH_3 emissions in agricultural regions in winter may be underestimated by a factor of 1.6 to 4.4 (Moravek et al., 2019), and national and regional emissions of NMVOCs from oil and gas extraction regions, solvents, and the use of personal care products may also be underestimated by up to a factor of 2 (McDonald et al., 2018; Ahmadov et al., 2015).

4.2.4 Uncertainties in sectoral and fuel contributions

Emissions reported as a function of individual source sectors are typically considered to have higher levels of uncertainty than those reported as country totals due to the cancelation of compounding errors (Schöpp et al., 2005). Source sectors with the largest levels of uncertainty in $\mathrm{CEDS}_{\text{GBD-MAPS}}$ estimates are generally consistent with other inventories, which include waste burning, residential emissions, and agricultural processes (Hoesly et al., 2018). This higher level of sectoral uncertainty is reflected in the relatively larger uncertainties discussed above in global emissions of OC, BC, and NH_3 relative to other gas-phase species. In general, uncertainties from these sources are larger due to the difficulty in accurately tracking energy consumption statistics and uncertainties in the variability in source-specific emission factors, which will depend on local operational and environmental conditions. For example, residential emission factors from heating and cooking vary depending on technology used and operational conditions (e.g., Venkataraman et al., 2018; Carter et al., 2014; Jayarathne et al., 2018), while soil NO_x emissions and NH_3 from wastewater and agriculture result from biological processes that depend on local practices and environmental conditions (e.g., Chen et al., 2012; Paulot et al., 2014). While uncertainties are not always reported at the sectoral level, Venkataraman et al. (2018) do report that industry emissions of NO_x and NMVOCs in the SMoG-India inventory actually have larger uncertainties than those from the transportation, agriculture, and residential (NMVOCs only) sectors, while the relative uncertainties for SO_2 emissions follow the opposite trend. For emissions of total fine particulate matter, Venkataraman et al. (2018) estimate that the sectors with the largest uncertainties are the residential and industry emissions. Similarly, Lei et al. (2011) estimate that BC and OC emissions from the residential sector in China have the largest inventory uncertainties, while Zhang et al. (2009) and Zheng et al. (2018) also report relatively smaller uncertainties from power plants and heavy industry in China due to known activity data, local emission factors, pollution control technologies, and direct emissions monitoring. Overall, the mosaic scaling procedure in the CEDS system will result in similar levels of uncertainties as these regional scaling inventories.

With the release of fuel-specific information in the $\mathrm{CEDS}_{\text{GBD-MAPS}}$ inventory, additional uncertainty in the allocation of fuel types is expected. In this work, activity data at the detailed sector and fuel level are taken from the IEA World Energy statistics (IEA, 2019) and are subject to the same sources of uncertainty. Emission factors for CEDS working sectors and fuels (Table S2) are derived from GAINS. In general, emissions from solid biofuel combustion are considered to be less certain than fossil fuel consumption due to large uncertainties in both fuel consumption and EFs, particularly in the residential and commercial sectors. For example, by combining information from EDGAR v4.3.2 (Crippa et al., 2018) and a recent TNO-RWC (Netherland Organization for Applied Scientific Research, Residential Wood Combustion) inventory from Denier van der Gon et al. (2015), Crippa et al. (2019) estimated that uncertainties in emissions from wood combustion in the residential sector in Europe are between 200 % and 300 % for OC, BC, and NH_3. Crippa et al. (2019) also report that these uncertainties are largely driven by uncertainties in regional emission factors as uncertainties in biofuel consumption are estimated to be between 38.9 % and 59.5 %. These uncertainties, however, are still larger than those estimated for fossil fuel consumption in many countries. As noted in Hoesly et al. (2018), increased levels of uncertainty in fossil fuel emissions are also expected in some countries, including the consumption and emission factors related to coal combustion in China (e.g., Liu et al., 2015; Guan et al., 2012; Hong et al., 2017), which will have the largest impacts on $\text{CEDS}_{\text{GBD-MAPS}}$ emissions of NO_x, SO_2, and BC. Specific to the $\text{CEDS}_{\text{GBD-MAPS}}$ fuel inventory, additional uncertainties may arise from the potential underestimation of total coal, oil and gas, and biofuel emissions associated with fugitive emissions and gas flaring in the energy sector as well as waste incineration in the waste sector. As discussed above and in Hoesly et al. (2018), fugitive emissions are highly uncertain. The degree of underestimation in combustion fuel contributions will be dependent on the fractional contribution of process-level emissions in these sectors relative to those from coal, biofuel, and oil and gas combustion (Table S8). Additional uncertainties in the gridded fuel-specific products are discussed in the following section.

4.2.5 Uncertainties and limitations in gridded emission fluxes

As noted in Sect. 2.1, global gridded $\text{CEDS}_{\text{GBD-MAPS}}$ emission fluxes are provided to facilitate their use in earth system models. Relative to the reported country-total emission files, additional uncertainties are introduced in the $0.5^\circ \times 0.5^\circ$ global gridded $\text{CEDS}_{\text{GBD-MAPS}}$ emission fluxes through the use of source-specific spatial gridding proxies in CEDS Step 5. Historical spatial distributions within each country are largely based on normalized gridded emissions from the EDGAR v4.3.2 inventory. These spatial proxies are held constant after 2012, which serves to increase the uncertainties in spatial allocation in large countries in recent years. The magnitude of this uncertainty will depend on the specific compound and sector. For example, gridded emissions from the energy sector will not reflect the closure or fuel-switching of individual coal-fired power stations after 2012. Changes in total country-level emissions from this sector and fuel type, however, will be accurately reflected in the total country-level emission files. This source of uncertainty is also present in the $\text{CEDS}_{\text{Hoesly}}$ inventory. An additional source of uncertainty in the gridded emissions is that the same spatial allocations are applied uniformly across emissions of all fuel types within each source sector. This may lead to additional uncertainties if, for example, emissions from the use of coal, biofuel, oil and gas, and remaining sources within each sector are spatially distinct. These uncertainties, however, do not impact the final country-level $\text{CEDS}_{\text{GBD-MAPS}}$ products because they are not gridded.

Lastly, while $\text{CEDS}_{\text{GBD-MAPS}}$ emissions provide a global inventory of key atmospheric pollutants, this inventory does not include a complete set of sources or species required for GCM or CTM simulations of atmospheric chemical processes. As noted in Sect. 2, neither $\text{CEDS}_{\text{Hoesly}}$ nor $\text{CEDS}_{\text{GBD-MAPS}}$ estimates include emissions from large or small open fires, which must be supplemented with additional open-burning inventories, such as the Global Fire Emissions Database (GFED, 2019; van der Werf et al., 2017) or Fire INventory from NCAR (FINN, 2018; Wiedinmyer et al., 2011). In addition, simulations of atmospheric chemistry require emissions from biogenic sources, typically supplied from inventories, such as the Model of Emissions of Gases and Aerosols from Nature (MEGAN, 2019; Guenther et al., 2012). Other sources to consider in atmospheric simulations include volcanic emissions, sea spray, and windblown dust. In addition, the CEDS system does not include dust emissions from windblown and anthropogenic sources such as roads, combustion, or industrial process. Anthropogenic dust sources may contribute up to $\sim 10\,\%$ of total fine-dust emissions in recent years and are important to consider when simulating concentrations of total atmospheric particulate matter (Philip et al., 2017). Lastly, the $\text{CEDS}_{\text{GBD-MAPS}}$ inventory also excludes emissions of greenhouse gases such as methane and carbon dioxide (CH_4, CO_2). These compounds were previously included through 2014 in the $\text{CEDS}_{\text{Hoesly}}$ inventory.

5 Data availability

The source code for the $\text{CEDS}_{\text{GBD-MAPS}}$ system is available on GitHub (https://github.com/emcduffie/CEDS/tree/CEDS_GBD-MAPS, last access: 1 December 2020, and https://doi.org/10.5281/zenodo.3865670; McDuffie et al., 2020a). To run the CEDS system, users are required to first purchase the proprietary energy consumption data from the IEA (World Energy Statistics; https://www.iea.org/subscribe-to-data-services/world-energy-balances-and-statistics, last access: 1 December 2020). The IEA is updated annually and provides the most comprehensive global energy statistics available to date. All additional input data are available in the CEDS GitHub repository.

Final products from the $\text{CEDS}_{\text{GBD-MAPS}}$ system include total annual emissions for each country as well as monthly global gridded ($0.5^\circ \times 0.5^\circ$) emission fluxes for the years 1970–2017. Both products are available on Zenodo (https://doi.org/10.5281/zenodo.3754964; McDuffie et al., 2020c) and report total emissions and gridded fluxes as a function of 11 final source sectors and four fuel categories (total coal, solid biofuel, oil + gas, process). Time series of annual country-total emissions from 1970–2017 are provided in units of $\mathrm{kt\,yr^{-1}}$ and provide NO_x emissions as NO_2. These data do not speciate total NMVOCs into sub-VOC classes. In these .csv files, total anthropogenic emissions for each country are calculated as the sum of all sectors and fuel types within each country. For the global gridded products, emission fluxes of each compound as a function of 11 sectors and four fuel types are available for each year in individual netCDF files. These data are in units of $\mathrm{kg\,m^{-2}\,s^{-1}}$ and provide NO_x emissions as NO. Total NMVOCs are speciated into 25 sub-VOC classes as described in Sect. 2. For consistency with the CEDS data released for CMIP6 (CEDS, 2017a, b), gridded anthropogenic fluxes for 1970–2017 are additionally available in the CMIP6 format. Note that NO_x is in units of NO_2 in this format. Additional file format details are in the README.txt file in the Zenodo repository (https://doi.org/10.5281/zenodo.3754964, McDuffie et al., 2020c).

To provide an example of the products and file formats available for download from the full $\mathrm{CEDS_{GBD\text{-}MAPS}}$ repository, we have also prepared an additional data "snapshot" inventory that provides emissions in all three file formats described above for the 2014–2015 time period (McDuffie et al., 2020b). The gridded data are provided as monthly averages for the December 2014–February 2015 time period, while the annual data include total emissions from both 2014 and 2015. These data can be downloaded from https://doi.org/10.5281/zenodo.3833935 (McDuffie et al., 2020b) and are further described in the associated README.txt file.

6 Summary and conclusions

We described the new $\mathrm{CEDS_{GBD\text{-}MAPS}}$ global emission inventory for key atmospheric reactive gases and carbonaceous aerosol from 11 anthropogenic emission sectors and four fuel types (total coal, solid biofuel, liquid-fuel and natural-gas combustion, and remaining process-level emissions) over the time period from 1970–2017. The $\mathrm{CEDS_{GBD\text{-}MAPS}}$ inventory was derived from an updated version of the Community Emissions Data System, which incorporates updated activity data for combustion- and process-level emission sources, updated scaling inventories, the added scaling of BC and OC emissions, and adjustments to the aggregation and gridding procedures to enable the extension of emission estimates to 2017 while retaining sectoral and fuel type information. We incorporated new regional scaling inventories for India and Africa; as a result default $\mathrm{CEDS_{GBD\text{-}MAPS}}$ emissions are now lower than previous $\mathrm{CEDS_{Hoesly}}$ estimates for all compounds in these regions other than NMVOCs in Africa and BC in India. These updates improve the agreement of $\mathrm{CEDS_{GBD\text{-}MAPS}}$ Africa emissions with those from EDGAR v4.3.2 as well as the agreement of all India emissions other than BC with both the EDGAR (2012) and GAINS (2010) inventories. Scaling default BC and OC estimates reduces these global emissions by up to 21 % and 28 %, respectively, relative to the $\mathrm{CEDS_{Hoesly}}$ inventory. This reduction improves $\mathrm{CEDS_{GBD\text{-}MAPS}}$ agreement with both GAINS and EDGAR global estimates of BC and OC, particularly in recent years. The resulting $\mathrm{CEDS_{GBD\text{-}MAPS}}$ inventory provides the most contemporary global emission inventory to date for these key atmospheric pollutants and is the first to provide their global emissions as a function of both detailed source sector and fuel type.

Global 2017 emissions from the $\mathrm{CEDS_{GBD\text{-}MAPS}}$ inventory suggest that coal and oil and gas combustion in both the energy and industry sectors are the largest global sources of SO_2 emissions, while CO emissions are primarily from on-road transportation and biofuel combustion in the residential sector. Global emissions of both compounds peak by 1990 and decrease until 2017 as a result of continuous reductions in on-road transport emissions in Europe and North America as well as reductions in coal combustion emissions from the energy and industry sectors across these regions and in China. In contrast, global NO_x, BC, and OC emissions peak later, between 2010 and 2012, but also decrease until 2017 due to reductions in North America, Africa, and China. Dominant sources of NO_x in 2017 are from international shipping, energy, industry, and on-road transportation sectors. Major sources of BC emissions are from residential biofuel combustion and on-road transportation, while dominant OC sources are from the residential biofuel and the waste sector. Outside of international shipping, China is the largest regional source of global emissions of all compounds other than NMVOCs. As emissions in North America, Europe, and China continue to decrease, global emissions of NO_x, CO, SO_2, BC, and OC will increasingly reflect emissions in rapidly growing regions such as Africa, India, and countries throughout Asia, Latin America, and the Middle East. Lastly, in contrast to other compounds, global emissions of NMVOCs and NH_3 continuously increase over the entire time period. These increases are predominantly due to increases in agricultural NH_3 emissions in nearly all world regions as well as NMVOCs from increased waste, energy sector, and solvent use emissions. In 2017, global emissions of these compounds had the largest regional contributions from India, China, and countries throughout Africa, Asia, and the Pacific.

Historical global emission trends in the $\mathrm{CEDS_{GBD\text{-}MAPS}}$ inventory are generally similar to those in three other global inventories: $\mathrm{CEDS_{Hoesly}}$, EDGAR v4.3.2, and ECLIPSE v5a (GAINS). Relative to the $\mathrm{CEDS_{Hoesly}}$ inventory, however, $\mathrm{CEDS_{GBD\text{-}MAPS}}$ emissions diverge in recent years, particularly for NO_x, CO, SO_2, BC, and OC emissions. In addition to the use of updated underlying activity data in the $CEDS_{GBD\text{-}MAPS}$ inventory, emissions of these compounds were most impacted by the updated CEDS scaling inventories, including those for China, India, and Africa. These same updates also contribute to the different trends in global NO_x, CO, and SO_2 emissions after 2010 between $CEDS_{GBD\text{-}MAPS}$ and the GAINS and EDGAR inventories. Global emissions between 1970 and 2017 from the $CEDS_{GBD\text{-}MAPS}$ inventory are generally smaller than the $CEDS_{Hoesly}$ emissions for all compounds other than NMVOCs and are consistently higher than all emissions from EDGAR v4.3.2. Global $CEDS_{GBD\text{-}MAPS}$ emissions are also larger than GAINS emissions, except for BC and select years of SO_2 emissions.

Due to similar bottom-up methodologies and the use of EDGAR v4.3.2 data in the CEDS system, country-level $CEDS_{GBD\text{-}MAPS}$ emissions are expected to have similar sources and magnitudes of uncertainty as those in the $CEDS_{Hoesly}$, EDGAR v4.3.2, GAINS, and scaling emission inventories. These inventories consistently predict the smallest uncertainties in emissions of SO_2 and the largest for emissions of NH_3, OC, and BC. The latter three compounds largely depend on accurate knowledge of activity data and emission factors for small scattered sources that vary by location, combustion technologies used, and environmental conditions. Uncertainties in the sectoral and fuel allocations in $CEDS_{GBD\text{-}MAPS}$ emissions will also generally follow the uncertainties in the CEDS v2019-12-23 system and will largely depend on the accuracy of the fuel allocations for combustion sources in the underlying IEA activity data. Gridded $CEDS_{GBD\text{-}MAPS}$ emissions also have uncertainties associated with the accuracy of the normalized spatial emission distributions from EDGAR v4.3.2, which are equally applied to all four fuel categories and are held constant after 2012.

Contemporary global emission estimates with detailed sector- and fuel-specific information are vital for quantifying the anthropogenic sources of air pollution and mitigating the resulting impacts on human health, the environment, and society. While bottom-up methods can provide sector-specific emission estimates, previous global inventories of multiple compounds and sources have lagged in time and do not provide fuel-specific emissions for multiple compounds at the global scale. To address this community need, the $CEDS_{GBD\text{-}MAPS}$ inventory utilizes the CEDS system (v2019-12-23) to provide emissions of seven key atmospheric pollutants with detailed sectoral and fuel type information, extended to the year 2017. Due to the direct and secondary contribution of these reactive gases and carbonaceous aerosol to ambient air pollution, contemporary gridded and country-level emissions with both sector and fuel type information can provide new insights necessary to motivate and develop effective strategies for emission reductions and air pollution mitigation around the world. The $CEDS_{GBD\text{-}MAPS}$ source code is publicly available (https://github.com/emcduffie/CEDS/tree/CEDS_GBD-MAPS and https://doi.org/10.5281/zenodo.3865670, McDuffie et al., 2020a), and both country-total and global gridded emissions from the 2020_v1 version of this dataset are publicly available at Zenodo with the following DOI: https://doi.org/10.5281/zenodo.3754964 (McDuffie et al., 2020c).

Supplement. The supplement for this article describes a list of known inventory issues at the time of submission as well as a number of additional $CEDS_{GBD\text{-}MAPS}$ details, tables and figures, and data sources, including the following: Boden et al. (2016, 2017), BP (2015), Doxsey-Whitfield et al. (2015), EC-JRC/PBL (2012, 2016), EIA (2019), IEA (2015), Klein Goldewijk et al. (2011), Sharma et al. (2019), Stohl et al. (2015), The World Bank (2016), UN (2014, 2015), Wiedinmyer et al. (2014), Commoner et al. (2000), Reyna-Bensusan et al. (2018), Nagpure et al. (2015), Meidiana and Gamse (2010), and US EPA, (2006). The supplement related to this article is available online at: https://doi.org/10.5194/essd-12-3413-2020-supplement.

Author contributions. EEM prepared the manuscript with contributions from all co-authors. RVM, MB, and SJS supervised the scientific content of this publication. EEM led the development of the $CEDS_{GBD\text{-}MAPS}$ source code and $CEDS_{GBD\text{-}MAPS}$ dataset, with significant contributions from SJS and PO as well as supplemental data from KT, CV, and EAM.

Competing interests. The authors declare that they have no conflict of interest.

Acknowledgements. We thank Christine Wiedinmyer and Qiang Zhang for their respective contributions to the DICE-Africa and updated China nation-level inventories, used here for scaling $CEDS_{GBD\text{-}MAPS}$ emissions. CEDS utilizes many sources of input data, and we are grateful for these contributions from a large number of research teams.

Financial support. This research has been supported by the Health Effects Institute (grant no. 4965/19-1).

Review statement. This paper was edited by David Carlson and reviewed by Hugo Denier van der Gon and one anonymous referee.

References

ADE: Australian Department of the Environment: National Pollution Inventory, 2017/2018, http://www.npi.gov.au/npidata/action/load/advance-search (lastaccess: 15 August 2019), 2019.

Ahmadov, R., McKeen, S., Trainer, M., Banta, R., Brewer, A., Brown, S., Edwards, P. M., de Gouw, J. A., Frost, G. J., Gilman, J., Helmig, D., Johnson, B., Karion, A., Koss, A., Langford, A., Lerner, B., Olson, J., Oltmans, S., Peischl, J., Pétron, G., Pichugina, Y., Roberts, J. M., Ryerson, T., Schnell, R., Senff, C., Sweeney, C., Thompson, C., Veres, P. R., Warneke, C., Wild, R., Williams, E. J., Yuan, B., and Zamora, R.: Understanding high wintertime ozone pollution events in an oil- and natural gas-producing region of the western US, Atmos. Chem. Phys., 15, 411–429, https://doi.org/10.5194/acp-15-411-2015, 2015.

Ainsworth, E. A.: Understanding and improving global crop response to ozone pollution, Plant J., 90, 886–897, https://doi.org/10.1111/tpj.13298, 2017.

Amann, M., Bertok, I., Borken-Kleefeld, J., Cofala, J., Heyes, C., Höglund-Isaksson, L., Klimont, Z., Nguyen, B., Posch, M., Rafaj, P., Sandler, R., Schöpp, W., Wagner, F., and Winiwarter, W.: Cost-effective control of air quality and greenhouse gases in Europe: Modeling and policy applications, Environ. Modell. Softw., 26, 1489–1501, https://doi.org/10.1016/j.envsoft.2011.07.012, 2011.

Amann, M., Bertok, I., Borken-Kleefeld, J., Cofala, J., Heyes, C., Hoglund-Isaksson, L., Kiesewetter, G., Klimont, Z., Schopp, W., Vellinga, N., and Winiwarter, W.: Adjusted historic emission data, projections, and optimized emission reduction targets for 2030 – a comparison with COM data 2013, IIASA, Laxenburg, Austria, available at: http://ec.europa.eu/environment/air/pdf/review/TSAP_16a.pdf (last access: 15 January 2018), 2015.

Argentina UNFCCC Submission: Argentinian Inventory 1990–2012, submitted to UNFCCC, 2016.

Avnery, S., Mauzerall, D. L., Liu, J., and Horowitz, L. W.: Global crop yield reductions due to surface ozone exposure: 1. Year 2000 crop production losses and economic damage, Atmos. Environ., 45, 2284–2296, https://doi.org/10.1016/j.atmosenv.2010.11.045, 2011.

Behera, S. N., Sharma, M., Aneja, V. P., and Balasubramanian, R.: Ammonia in the atmosphere: a review on emission sources, atmospheric chemistry and deposition on terrestrial bodies, Environ. Sci. Pollut. R., 20, 8092–8131, https://doi.org/10.1007/s11356-013-2051-9, 2013.

Beirle, S., Boersma, K. F., Platt, U., Lawrence, M. G., and Wagner, T.: Megacity Emissions and Lifetimes of Nitrogen Oxides Probed from Space, Science, 333, 1737, https://doi.org/10.1126/science.1207824, 2011.

Boden, T. A., Marland, G., and Andres, R. J.: Global, Regional, and National Fossil-Fuel CO_2 Emissions, Carbon Dioxide Information Analysis Center, US Department of Energy, Oak Ridge, USA, 2016.

Boden, T. A., Marland, G., and Andres, R. J.: Global, Regional, and National Fossil-Fuel CO_2 Emissions, Carbon Dioxide Information Analysis Center, US Department of Energy, Oak Ridge, USA, https://doi.org/10.3334/CDIAC/00001_V2017, 2017.

Bond, T. C., Streets, D. G., Yarber, K. F., Nelson, S. M., Woo, J.-H., and Klimont, Z.: A technology-based global inventory of black and organic carbon emissions from combustion, J. Geophys. Res., 109, D14203, https://doi.org/10.1029/2003JD003697, 2004.

Dong, R., Jogani, R., Jung, S., Roden, C., Streets, D. G., and Trautmann, N. M.: Historical emissions of black and organic carbon aerosol from energy-related combustion, 1850–2000, Global Biogeochem. Cycles, 21, GB2018, https://doi.org/10.1029/2006GB002840, 2007.

Bond, T. C., Doherty, S. J., Fahey, D. W., Forster, P. M., Berntsen, T., DeAngelo, B. J., Flanner, M. G., Ghan, S., Kärcher, B., Koch, D., Kinne, S., Kondo, Y., Quinn, P. K., Sarofim, M. C., Schultz, M. G., Schulz, M., Venkataraman, C., Zhang, H., Zhang, S., Bellouin, N., Guttikunda, S. K., Hopke, P. K., Jacobson, M. Z., Kaiser, J. W., Klimont, Z., Lohmann, U., Schwarz, J. P., Shindell, D., Storelvmo, T., Warren, S. G., and Zender, C. S.: Bounding the role of black carbon in the climate system: A scientific assessment, J. Geophys. Res.-Atmos., 118, 5380–5552, https://doi.org/10.1002/jgrd.50171, 2013.

BP: BP Statistical Review of World Energy, available at: https://www.bp.com/statisticalreview (last access: 15 January 2018), 2015.

BP: Statistical Review of World Energy: 2019, available at: https://www.bp.com/content/dam/bp/business-sites/en/global/corporate/pdfs/energy-economics/statistical-review/bp-stats-review-2019-full-report.pdf (last access: 23 January 2020), 2019.

Brock, C. A., Washenfelder, R. A., Trainer, M., Ryerson, T. B., Wilson, J. C., Reeves, J. M., Huey, L. G., Holloway, J. S., Parrish, D. D., Hübler, G., and Fehsenfeld, F. C.: Particle growth in the plumes of coal-fired power plants, J. Geophys. Res.-Atmos., 107, D124155, https://doi.org/10.1029/2001JD001062, 2002.

Carter, E. M., Shan, M., Yang, X., Li, J., and Baumgartner, J.: Pollutant Emissions and Energy Efficiency of Chinese Gasifier Cooking Stoves and Implications for Future Intervention Studies, Environ. Sci. Technol., 48, 6461–6467, https://doi.org/10.1021/es405723w, 2014.

Castellanos, P. and Boersma, K. F.: Reductions in nitrogen oxides over Europe driven by environmental policy and economic recession, Sci. Rep.-UK, 2, 265, https://doi.org/10.1038/srep00265, 2012.

CEDS: v2017_08_30, available at: https://esgf-node.llnl.gov/search/input4mips/ (last access: 7 January 2020), 2017a.

CEDS: v2017_10_05, available at: https://esgf-node.llnl.gov/search/input4mips/ (last access: 7 January 2020), 2017b.

Chameides, W. L.: The photochemical role of tropospheric nitrogen oxides, Geophys. Res. Lett., 5, 17–20, https://doi.org/10.1029/GL005i001p00017, 1978.

Chen, Y., Roden, C. A., and Bond, T. C.: Characterizing Biofuel Combustion with Patterns of Real-Time Emission Data (PaRTED), Environ. Sci. Technol., 46, 6110–6117, https://doi.org/10.1021/es3003348, 2012.

Commoner, B., Bartlett, P. W., Eisl, H., and Couchot, K.: Air Transport of Dioxin from North American Sources to Ecologically Vulnerable Receptors in Nunavut, Arctic Canada: Final Report to the North American Commission for Environmental Cooperation, available at: http://www3.cec.org/islandora/en/item/1596-long-range-air-transport-dioxin-from-north-american-sources-ecologically-vulnerable-en.pdf (last access: 25 April 2020), 2000.

Crippa, M., Guizzardi, D., Muntean, M., Schaaf, E., Dentener, F., van Aardenne, J. A., Monni, S., Doering, U., Olivier, J. G. J., Pagliari, V., and Janssens-Maenhout, G.: Gridded emissions of air pollutants for the period 1970–2012 within EDGAR v4.3.2, Earth Syst. Sci. Data, 10, 1987–2013, https://doi.org/10.5194/essd-10-1987-2018, 2018.

Crippa, M., Janssens-Maenhout, G., Guizzardi, D., Van Dingenen, R., and Dentener, F.: Contribution and uncertainty of sectorial and regional emissions to regional and global $PM_{2.5}$ health impacts, Atmos. Chem. Phys., 19, 5165–5186, https://doi.org/10.5194/acp-19-5165-2019, 2019.

Crutzen, P. J.: The influence of nitrogen oxides on the atmospheric ozone content, Q. J. Roy. Meteor. Soc., 96, 320–325, https://doi.org/10.1002/qj.49709640815, 1970.

de Gouw, J. A., Parrish, D. D., Frost, G. J., and Trainer, M.: Reduced emissions of CO_2, NO_x, and SO_2 from US power plants owing to switch from coal to natural gas with combined cycle technology, Earths Future, 2, 75–82, https://doi.org/10.1002/2013EF000196, 2014.

Denier van der Gon, H. A. C., Bergström, R., Fountoukis, C., Johansson, C., Pandis, S. N., Simpson, D., and Visschedijk, A. J. H.: Particulate emissions from residential wood combustion in Europe – revised estimates and an evaluation, Atmos. Chem. Phys., 15, 6503–6519, https://doi.org/10.5194/acp-15-6503-2015, 2015.

DICE-Africa: DICE-Africa User Manual, available at: https://www2.acom.ucar.edu/modeling/dice-africa (last access: 9 January 2020), 2016.

Doxsey-Whitfield, E., MacManus, K., Adamo, S. B., Pistolesi, L., Squires, J., Borkovska, O., and Baptista, S. R.: Taking Advantage of the Improved Availability of Census Data: A First Look at the Gridded Population of the World, Version 4, Papers in Applied Geography, 1, 226–234, https://doi.org/10.1080/23754931.2015.1014272, 2015.

Duncan, B. N., Yoshida, Y., de Foy, B., Lamsal, L. N., Streets, D. G., Lu, Z., Pickering, K. E., and Krotkov, N. A.: The observed response of Ozone Monitoring Instrument (OMI) NO_2 columns to NO_x emission controls on power plants in the United States: 2005–2011, Atmos. Environ., 81, 102–111, https://doi.org/10.1016/j.atmosenv.2013.08.068, 2013.

ECCC: Environment and Climate Change Canada, EN_APEI-Canada, Canada's 2019 Air Pollutant Emissions Inventory, available at: http://data.ec.gc.ca/data/substances/monitor/canada-s-air-pollutant-emissions-inventory/APEI_Tables_Canada_Provinces_Territories/?lang, last access: 13 August 2019.

EC-JRC: Emissions Database for Global Atmospheric Research (EDGAR), release EDGARv4.3.2, available at: https://edgar.jrc.ec.europa.eu/overview.php?v (last access: 12 August 2019), 2018.

EC-JRC/PBL: Emission Database for Global Atmospheric Research (EDGAR), release EDGAR v4.2 FT2012, available at: http://edgar.jrc.ec.europa.eu (last access: 15 January 2018), 2012.

EC-JRC/PBL: Emission Database for Global Atmospheric Research (EDGAR), release version 4.3.1, available at: http://edgar.jrc.ec.europa.eu/overview.php?v (last access: 15 January 2018), 2016.

EIA: US Energy Information Administration: Table 10.2a: Renewable Energy Cnsumption, Residential and Commercial Sectors, available at: https://www.eia.gov/totalenergy/data/monthly/#renewable (last access: 26 August 2019), 2019.

EIA: US Energy Information Administration: Drilling Productivity Report, available at: https://www.eia.gov/petroleum/drilling/, last access: 7 April 2020.

Elguindi, N., Granier, C., Stavrakou, T., Darras, S., Bauwens, M., Cao, H., Chen, C., Denier van der Gon, H. A. C., Dubovik, O., Fu, T. M., Henze, D. K., Jiang, Z., Keita, S., Kuenen, J. J. P., Kurokawa, J., Liousse, C., Miyazaki, K., Müller, J. F., Qu, Z., Solmon, F., and Zheng, B.: Intercomparison of Magnitudes and Trends in Anthropogenic Surface Emissions From Bottom-Up Inventories, Top-Down Estimates, and Emission Scenarios, Earths Future, 8, e2020EF001520, https://doi.org/10.1029/2020EF001520, 2020.

EMEP: Officially reported emission data to the European Monitoring and Evaluation Programme: EMEP_NFR14_LEVEL1 data, available at: https://www.ceip.at/ms/ceip_home1/ceip_home/webdab_emepdatabase/reported_emissiondata/, last access: 19 December 2019.

FAOSTAT: FAOSTAT-Forestry database, available at: http://www.fao.org/forestry/statistics/84922/en/ (last access: 15 January 2018), 2015.

Feng, L., Smith, S. J., Braun, C., Crippa, M., Gidden, M. J., Hoesly, R., Klimont, Z., van Marle, M., van den Berg, M., and van der Werf, G. R.: The generation of gridded emissions data for CMIP6, Geosci. Model Dev., 13, 461–482, https://doi.org/10.5194/gmd-13-461-2020, 2020.

FINN: Fire INventory from NCAR, Version 1.5, available at: http://bai.acom.ucar.edu/Data/fire/ (last access: 4 March 2020), 2018.

GBD 2017 Risk Factor Collaborators: Global, regional, and national comparative risk assessment of 84 behavioural, environmental and occupational, and metabolic risks or clusters of risks for 195 countries and territories, 1990–2017: a systematic analysis for the Global Burden of Disease Study 2017, The Lancet, 392, 1923–1994, https://doi.org/10.1016/S0140-6736(18)32225-6, 2018.

GBD MAPS Working Group: Burden of Disease Attributable to Coal-Burning and Other Major Sources of Air Pollution in China, Special Report 20, Health Effects Institute, available at: https://www.healtheffects.org/publication/burden-disease-attributable-coal-burning-and-other-air-pollution-sources-china (last access: 1 December 2020), 2016.

GBD MAPS Working Group: Burden of Disease Attributable to Major Air Pollution Sources in India, Special Report 21, Health Effects Institute available at: https://www.healtheffects.org/publication/gbd-air-pollution-india, (last access: 1 December 2020) 2018.

GFED: Global Fire Emissions Database, available at: http://globalfiredata.org/index.html (last access: 15 March 2020), 2019.

Gidden, M. J., Riahi, K., Smith, S. J., Fujimori, S., Luderer, G., Kriegler, E., van Vuuren, D. P., van den Berg, M., Feng, L., Klein, D., Calvin, K., Doelman, J. C., Frank, S., Fricko, O., Harmsen, M., Hasegawa, T., Havlik, P., Hilaire, J., Hoesly, R., Horing, J., Popp, A., Stehfest, E., and Takahashi, K.: Global emissions pathways under different socioeconomic scenarios for use in CMIP6: a dataset of harmonized emissions trajectories through the end of the century, Geosci. Model Dev., 12, 1443–1475, https://doi.org/10.5194/gmd-12-1443-2019, 2019.

Guan, D., Liu, Z., Geng, Y., Lindner, S., and Hubacek, K.: The gigatonne gap in China's carbon dioxide inventories, Nat. Clim. Change, 2, 672–675, https://doi.org/10.1038/nclimate1560, 2012.

Guenther, A. B., Jiang, X., Heald, C. L., Sakulyanontvittaya, T., Duhl, T., Emmons, L. K., and Wang, X.: The Model of Emissions of Gases and Aerosols from Nature version 2.1

(MEGAN2.1): an extended and updated framework for modeling biogenic emissions, Geosci. Model Dev., 5, 1471–1492, https://doi.org/10.5194/gmd-5-1471-2012, 2012.

Haywood, J. and Boucher, O.: Estimates of the direct and indirect radiative forcing due to tropospheric aerosols: A review, Rev. Geophys., 38, 513–543, https://doi.org/10.1029/1999RG000078, 2000.

Hoesly, R. M., Smith, S. J., Feng, L., Klimont, Z., Janssens-Maenhout, G., Pitkanen, T., Seibert, J. J., Vu, L., Andres, R. J., Bolt, R. M., Bond, T. C., Dawidowski, L., Kholod, N., Kurokawa, J.-I., Li, M., Liu, L., Lu, Z., Moura, M. C. P., O'Rourke, P. R., and Zhang, Q.: Historical (1750–2014) anthropogenic emissions of reactive gases and aerosols from the Community Emissions Data System (CEDS), Geosci. Model Dev., 11, 369–408, https://doi.org/10.5194/gmd-11-369-2018, 2018.

Hoesly, R., O'Rourke, P., Braun, C., Feng, L., Smith, S. J., Pitkanen, T., Siebert, J., Vu, L., Presley, M., Bolt, R., Goldstein, B., and Kholod, N.: CEDS: Community Emissions Data System (Version Dec-23-2019), Zenodo, https://doi.org/10.5281/zenodo.3592073, 2019.

Hong, C., Zhang, Q., He, K., Guan, D., Li, M., Liu, F., and Zheng, B.: Variations of China's emission estimates: response to uncertainties in energy statistics, Atmos. Chem. Phys., 17, 1227–1239, https://doi.org/10.5194/acp-17-1227-2017, 2017.

HTAP2: RETRO NMVOC Ratio, available at: http://iek8wikis.iek.fz-juelich.de/HTAPWiki/WP1.1?action (last access: 7 January 2020), 2013.

Huang, G., Brook, R., Crippa, M., Janssens-Maenhout, G., Schieberle, C., Dore, C., Guizzardi, D., Muntean, M., Schaaf, E., and Friedrich, R.: Speciation of anthropogenic emissions of non-methane volatile organic compounds: a global gridded data set for 1970–2012, Atmos. Chem. Phys., 17, 7683–7701, https://doi.org/10.5194/acp-17-7683-2017, 2017.

IEA: World Energy Statistics, available at: http://www.iea.org/statistics/ (last access: 15 January 2018), 2015.

IEA: World Energy Statistics 2019 Edition, Database Documentation, available at: http://wds.iea.org/wds/pdf/WORLDBES_Documentation.pdf, last access: 17 September 2019.

IIASA: GAINS – Sulfur content of fuels, available at: http://gains.iiasa.ac.at/models/index.html (last access: 15 January 2018), 2014.

IIASA: ECLIPSE v5a, available at: https://www.iiasa.ac.at/web/home/research/researchPrograms/air/ECLIPSEv5a.html (last access: 7 January 2020), 2015.

IPCC: Summary for Policy Makers, in: Climate Change 2013: The Physical Science Basis, Contribution of Working Group I to the Fifth Assessment Report of the Intergovernmental Panel on Climate Change, edited by: Stocker, T. F., Qin, D., Plattner, G.-K., Tignor, M., Allen, S. K., Boschung, J., Nauels, Y., Xia, Y., Bex, V., and Midgley, P. M., Cambridge University Press, Cambridge, United Kingdom and New York, USA, 1–29, 2013.

Janssens-Maenhout, G., Crippa, M., Guizzardi, D., Dentener, F., Muntean, M., Pouliot, G., Keating, T., Zhang, Q., Kurokawa, J., Wankmüller, R., Denier van der Gon, H., Kuenen, J. J. P., Klimont, Z., Frost, G., Darras, S., Koffi, B., and Li, M.: HTAP_v2.2: a mosaic of regional and global emission grid maps for 2008 and 2010 to study hemispheric transport of air pollution, Atmos. Chem. Phys., 15, 11411–11432, https://doi.org/10.5194/acp-15-11411-2015, 2015.

Jayarathne, T., Stockwell, C. E., Bhave, P. V., Praveen, P. S., Rathnayake, C. M., Islam, Md. R., Panday, A. K., Adhikari, S., Maharjan, R., Goetz, J. D., DeCarlo, P. F., Saikawa, E., Yokelson, R. J., and Stone, E. A.: Nepal Ambient Monitoring and Source Testing Experiment (NAMaSTE): emissions of particulate matter from wood- and dung-fueled cooking fires, garbage and crop residue burning, brick kilns, and other sources, Atmos. Chem. Phys., 18, 2259–2286, https://doi.org/10.5194/acp-18-2259-2018, 2018.

Jimenez, J. L., Canagaratna, M. R., Donahue, N. M., Prevot, A. S. H., Zhang, Q., Kroll, J. H., DeCarlo, P. F., Allan, J. D., Coe, H., Ng, N. L., Aiken, A. C., Docherty, K. S., Ulbrich, I. M., Grieshop, A. P., Robinson, A. L., Duplissy, J., Smith, J. D., Wilson, K. R., Lanz, V. A., Hueglin, C., Sun, Y. L., Tian, J., Laaksonen, A., Raatikainen, T., Rautiainen, J., Vaattovaara, P., Ehn, M., Kulmala, M., Tomlinson, J. M., Collins, D. R., Cubison, M. J., Dunlea, J., Huffman, J. A., Onasch, T. B., Alfarra, M. R., Williams, P. I., Bower, K., Kondo, Y., Schneider, J., Drewnick, F., Borrmann, S., Weimer, S., Demerjian, K., Salcedo, D., Cottrell, L., Griffin, R., Takami, A., Miyoshi, T., Hatakeyama, S., Shimono, A., Sun, J. Y., Zhang, Y. M., Dzepina, K., Kimmel, J. R., Sueper, D., Jayne, J. T., Herndon, S. C., Trimborn, A. M., Williams, L. R., Wood, E. C., Middlebrook, A. M., Kolb, C. E., Baltensperger, U., and Worsnop, D. R.: Evolution of Organic Aerosols in the Atmosphere, Science, 326, 1525, https://doi.org/10.1126/science.1180353, 2009.

Klein Goldewijk, K., Beusen, A., van Drecht, G., and de Vos, M.: The HYDE 3.1 spatially explicit database of human-induced global land-use change over the past 12,000 years, Global Ecol. Biogeogr., 20, 73–86, https://doi.org/10.1111/j.1466-8238.2010.00587.x, 2011.

Klimont, Z., Kupiainen, K., Heyes, C., Purohit, P., Cofala, J., Rafaj, P., Borken-Kleefeld, J., and Schöpp, W.: Global anthropogenic emissions of particulate matter including black carbon, Atmos. Chem. Phys., 17, 8681–8723, https://doi.org/10.5194/acp-17-8681-2017, 2017.

Krotkov, N. A., McLinden, C. A., Li, C., Lamsal, L. N., Celarier, E. A., Marchenko, S. V., Swartz, W. H., Bucsela, E. J., Joiner, J., Duncan, B. N., Boersma, K. F., Veefkind, J. P., Levelt, P. F., Fioletov, V. E., Dickerson, R. R., He, H., Lu, Z., and Streets, D. G.: Aura OMI observations of regional SO_2 and NO_2 pollution changes from 2005 to 2015, Atmos. Chem. Phys., 16, 4605–4629, https://doi.org/10.5194/acp-16-4605-2016, 2016.

Kurokawa, J., Ohara, T., Morikawa, T., Hanayama, S., Janssens-Maenhout, G., Fukui, T., Kawashima, K., and Akimoto, H.: Emissions of air pollutants and greenhouse gases over Asian regions during 2000–2008: Regional Emission inventory in ASia (REAS) version 2, Atmos. Chem. Phys., 13, 11019–11058, https://doi.org/10.5194/acp-13-11019-2013, 2013.

Lacey, F. and Henze, D.: Global climate impacts of country-level primary carbonaceous aerosol from solid-fuel cookstove emissions, Environ. Res. Lett., 10, 114003, https://doi.org/10.1088/1748-9326/10/11/114003, 2015.

Lacey, F. G., Marais, E. A., Henze, D. K., Lee, C. J., van Donkelaar, A., Martin, R. V., Hannigan, M. P., and Wiedinmyer, C.: Improving present day and future estimates of anthropogenic sectoral emissions and the resulting air quality impacts in Africa, Faraday Discuss., 200, 397–412, https://doi.org/10.1039/C7FD00011A, 2017.

Lamsal, L. N., Martin, R. V., Padmanabhan, A., van Donkelaar, A., Zhang, Q., Sioris, C. E., Chance, K., Kurosu, T. P., and Newchurch, M. J.: Application of satellite observations for timely updates to global anthropogenic NO_x emission inventories, Geophys. Res. Lett., 38, L05810, https://doi.org/10.1029/2010GL046476, 2011.

Lei, Y., Zhang, Q., He, K. B., and Streets, D. G.: Primary anthropogenic aerosol emission trends for China, 1990–2005, Atmos. Chem. Phys., 11, 931–954, https://doi.org/10.5194/acp-11-931-2011, 2011.

Lelieveld, J., Klingmüller, K., Pozzer, A., Burnett, R. T., Haines, A., and Ramanathan, V.: Effects of fossil fuel and total anthropogenic emission removal on public health and climate, P. Natl. Acad. Sci. USA, 116, 7192, https://doi.org/10.1073/pnas.1819989116, 2019.

Li, C., McLinden, C., Fioletov, V., Krotkov, N., Carn, S., Joiner, J., Streets, D., He, H., Ren, X., Li, Z., and Dickerson, R. R.: India Is Overtaking China as the World's Largest Emitter of Anthropogenic Sulfur Dioxide, Sci. Rep.-UK, 7, 14304, https://doi.org/10.1038/s41598-017-14639-8, 2017.

Li, M., Liu, H., Geng, G., Hong, C., Liu, F., Song, Y., Tong, D., Zheng, B., Cui, H., Man, H., Zhang, Q., and He, K.: Anthropogenic emission inventories in China: a review, Natl. Sci. Rev., 4, 834–866, https://doi.org/10.1093/nsr/nwx150, 2017a.

Li, M., Zhang, Q., Kurokawa, J.-I., Woo, J.-H., He, K., Lu, Z., Ohara, T., Song, Y., Streets, D. G., Carmichael, G. R., Cheng, Y., Hong, C., Huo, H., Jiang, X., Kang, S., Liu, F., Su, H., and Zheng, B.: MIX: a mosaic Asian anthropogenic emission inventory under the international collaboration framework of the MICS-Asia and HTAP, Atmos. Chem. Phys., 17, 935–963, https://doi.org/10.5194/acp-17-935-2017, 2017b.

Liang, C.-K., West, J. J., Silva, R. A., Bian, H., Chin, M., Davila, Y., Dentener, F. J., Emmons, L., Flemming, J., Folberth, G., Henze, D., Im, U., Jonson, J. E., Keating, T. J., Kucsera, T., Lenzen, A., Lin, M., Lund, M. T., Pan, X., Park, R. J., Pierce, R. B., Sekiya, T., Sudo, K., and Takemura, T.: HTAP2 multi-model estimates of premature human mortality due to intercontinental transport of air pollution and emission sectors, Atmos. Chem. Phys., 18, 10497–10520, https://doi.org/10.5194/acp-18-10497-2018, 2018.

Liu, Z., Guan, D., Wei, W., Davis, S. J., Ciais, P., Bai, J., Peng, S., Zhang, Q., Hubacek, K., Marland, G., Andres, R. J., Crawford-Brown, D., Lin, J., Zhao, H., Hong, C., Boden, T. A., Feng, K., Peters, G. P., Xi, F., Liu, J., Li, Y., Zhao, Y., Zeng, N., and He, K.: Reduced carbon emission estimates from fossil fuel combustion and cement production in China, Nature, 524, 335–338, https://doi.org/10.1038/nature14677, 2015.

Lu, Z., Zhang, Q., and Streets, D. G.: Sulfur dioxide and primary carbonaceous aerosol emissions in China and India, 1996–2010, Atmos. Chem. Phys., 11, 9839–9864, https://doi.org/10.5194/acp-11-9839-2011, 2011.

Marais, E. A. and Wiedinmyer, C.: Air Quality Impact of Diffuse and Inefficient Combustion Emissions in Africa (DICE-Africa), Environ. Sci. Technol., 50, 10739–10745, https://doi.org/10.1021/acs.est.6b02602, 2016.

Marais, E. A., Silvern, R. F., Vodonos, A., Dupin, E., Bockarie, A. S., Mickley, L. J., and Schwartz, J.: Air Quality and Health Impact of Future Fossil Fuel Use for Electricity Generation and Transport in Africa, Environ. Sci. Technol., 53, 13524–13534, https://doi.org/10.1021/acs.est.9b04958, 2019.

Mauzerall, D. L., Sultan, B., Kim, N., and Bradford, D. F.: NO_x emissions from large point sources: variability in ozone production, resulting health damages and economic costs, Atmos. Environ., 39, 2851–2866, https://doi.org/10.1016/j.atmosenv.2004.12.041, 2005.

McDonald, B. C., de Gouw, J. A., Gilman, J. B., Jathar, S. H., Akherati, A., Cappa, C. D., Jimenez, J. L., Lee-Taylor, J., Hayes, P. L., McKeen, S. A., Cui, Y. Y., Kim, S.-W., Gentner, D. R., Isaacman-VanWertz, G., Goldstein, A. H., Harley, R. A., Frost, G. J., Roberts, J. M., Ryerson, T. B., and Trainer, M.: Volatile chemical products emerging as largest petrochemical source of urban organic emissions, Science, 359, 760, https://doi.org/10.1126/science.aaq0524, 2018.

McDuffie, E. E., Hoesly, R., O'Rourke, P., Braun, C., Feng, L., Smith, S. J., Pitkanen, T., Seibert, J. J., Vu, L., Presley, M., Bolt, R., Goldstein, B., and Kholod, N.: CEDS_GBD-MAPS_SourceCode_2020_v1.0, Zenodo, https://doi.org/10.5281/zenodo.3865670, 2020a.

McDuffie, E. E., Smith, S. J., O'Rourke, P., Tibrewal, K., Venkataraman, C., Marais, E. A., Zheng, B., Crippa, M., Brauer, M., and Martin, R. V.: CEDS_GBD-MAPS: Data Snapshot (2014–2015), Zenodo, https://doi.org/10.5281/zenodo.3833935, 2020b.

McDuffie, E. E., Smith, S. J., O'Rourke, P., Tibrewal, K., Venkataraman, C., Marais, E. A., Zheng, B., Crippa, M., Brauer, M., and Martin, R. V.: CEDS_GBD-MAPS: Global Anthropogenic Emission Inventory of NO_x, SO_2, CO, NH_3, NMVOCs, BC, and OC from 1970–2017 (Version 2020_v1.0), Zenodo, https://doi.org/10.5281/zenodo.3754964, 2020c.

McLinden, C. A., Fioletov, V., Boersma, K. F., Krotkov, N., Sioris, C. E., Veefkind, J. P., and Yang, K.: Air quality over the Canadian oil sands: A first assessment using satellite observations, Geophys. Res. Lett., 39, L04804, https://doi.org/10.1029/2011GL050273, 2012.

McLinden, C. A., Fioletov, V., Shephard, M. W., Krotkov, N., Li, C., Martin, R. V., Moran, M. D., and Joiner, J.: Space-based detection of missing sulfur dioxide sources of global air pollution, Nat. Geosci., 9, 496, https://doi.org/10.1038/ngeo2724, 2016.

MEGAN: The Model of Emissions of Gases and Aerosols from Nature, Version 3.1, available at: https://sites.google.com/uci.edu/bai/megan/data-and-code (last access: 4 March 2020), 2019.

Meidiana, C. and Gamse, T.: Development of Waste Management Practices in Indonesia, European Journal of Scientific Research, 40, 199–210, 2010.

Mickley, L. J., Jacob, D. J., Field, B. D., and Rind, D.: Effects of future climate change on regional air pollution episodes in the United States, Geophys. Res. Lett., 31, L24103, https://doi.org/10.1029/2004GL021216, 2004.

Moravek, A., Murphy, J. G., Hrdina, A., Lin, J. C., Pennell, C., Franchin, A., Middlebrook, A. M., Fibiger, D. L., Womack, C. C., McDuffie, E. E., Martin, R., Moore, K., Baasandorj, M., and Brown, S. S.: Wintertime spatial distribution of ammonia and its emission sources in the Great Salt Lake region, Atmos. Chem. Phys., 19, 15691–15709, https://doi.org/10.5194/acp-19-15691-2019, 2019.

Mozurkewich, M.: The dissociation constant of ammonium nitrate and its dependence on temperature, relative humidity and particle size, Atmos. Environ., 27, 261–270, https://doi.org/10.1016/0960-1686(93)90356-4, 1993.

Nagpure, A. S., Ramaswami, A., and Russell, A.: Characterizing the Spatial and Temporal Patterns of Open Burning of Municipal Solid Waste (MSW) in Indian Cities, Environ. Sci. Technol., 49, 12904–12912, https://doi.org/10.1021/acs.est.5b03243, 2015.

NEI: 2011 National Emissions Inventory (NEI) Data, available at: https://www.epa.gov/air-emissions-inventories/2011-national-emissions-inventory-nei-data (last access: 12 December 2020), 2013.

Paulot, F., Jacob, D. J., Pinder, R. W., Bash, J. O., Travis, K., and Henze, D. K.: Ammonia emissions in the United States, European Union, and China derived by high-resolution inversion of ammonium wet deposition data: Interpretation with a new agricultural emissions inventory (MASAGE_NH3), J. Geophys. Res.-Atmos., 119, 4343–4364, https://doi.org/10.1002/2013JD021130, 2014.

Philip, S., Martin, R. V., Snider, G., Weagle, C. L., van Donkelaar, A., Brauer, M., Henze, D. K., Klimont, Z., Venkataraman, C., Guttikunda, S. K., and Zhang, Q.: Anthropogenic fugitive, combustion and industrial dust is a significant, underrepresented fine particulate matter source in global atmospheric models, Environ. Res. Lett., 12, 044018, https://doi.org/10.1088/1748-9326/aa65a4, 2017.

RAQC: Regional Air Quality Council: Summary of State Implementation Plans, available at: https://raqc.egnyte.com/dl/KZXQmQtFaQ/2019_SIP_Summaries_Update.pdf (last access: 23 January 2020), 2019.

Reyna-Bensusan, N., Wilson, D. C., and Smith, S. R.: Uncontrolled burning of solid waste by households in Mexico is a significant contributor to climate change in the country, Environ. Res., 163, 280–288, https://doi.org/10.1016/j.envres.2018.01.042, 2018.

Sadavarte, P. and Venkataraman, C.: Trends in multi-pollutant emissions from a technology-linked inventory for India: I. Industry and transport sectors, Atmos. Environ., 99, 353–364, https://doi.org/10.1016/j.atmosenv.2014.09.081, 2014.

Saxena, P. and Seigneur, C.: On the oxidation of SO_2 to sulfate in atmospheric aerosols, Atmos. Environ., 21, 807–812, https://doi.org/10.1016/0004-6981(87)90077-1, 1987.

Schöpp, W., Klimont, Z., Suutari, R., and Cofala, J.: Uncertainty analysis of emission estimates in the RAINS integrated assessment model, Environ. Sci. Policy, 8, 601–613, https://doi.org/10.1016/j.envsci.2005.06.008, 2005.

Sharma, G., Sinha, B., Pallavi, Hakkim, H., Chandra, B. P., Kumar, A., and Sinha, V.: Gridded Emissions of CO, NO_x, SO_2, CO_2, NH_3, HC_l, CH_4, $PM_{2.5}$, PM_{10}, BC, and NMVOC from Open Municipal Waste Burning in India, Environ. Sci. Technol., 53, 4765–4774, https://doi.org/10.1021/acs.est.8b07076, 2019.

Shindell, D. and Smith, C. J.: Climate and air-quality benefits of a realistic phase-out of fossil fuels, Nature, 573, 408–411, https://doi.org/10.1038/s41586-019-1554-z, 2019.

SMoG-India: Speciated Multi-pollutant Generator, available at: https://sites.google.com/view/smogindia (last access: 28 February 2020), 2019.

South Korea National Institute of Environmental Research: National air pollutants emission service, available at: http://airemiss.nier.go.kr/ (last access: 15 Janurary 2018), 2016.

Stevens, C. J., Dise, N. B., Mountford, J. O., and Gowing, D. J.: Impact of Nitrogen Deposition on the Species Richness of Grasslands, Science, 303, 1876, https://doi.org/10.1126/science.1094678, 2004.

Stohl, A., Aamaas, B., Amann, M., Baker, L. H., Bellouin, N., Berntsen, T. K., Boucher, O., Cherian, R., Collins, W., Daskalakis, N., Dusinska, M., Eckhardt, S., Fuglestvedt, J. S., Harju, M., Heyes, C., Hodnebrog, Ø., Hao, J., Im, U., Kanakidou, M., Klimont, Z., Kupiainen, K., Law, K. S., Lund, M. T., Maas, R., MacIntosh, C. R., Myhre, G., Myriokefalitakis, S., Olivié, D., Quaas, J., Quennehen, B., Raut, J.-C., Rumbold, S. T., Samset, B. H., Schulz, M., Seland, Ø., Shine, K. P., Skeie, R. B., Wang, S., Yttri, K. E., and Zhu, T.: Evaluating the climate and air quality impacts of short-lived pollutants, Atmos. Chem. Phys., 15, 10529–10566, https://doi.org/10.5194/acp-15-10529-2015, 2015.

Streets, D. G., Canty, T., Carmichael, G. R., de Foy, B., Dickerson, R. R., Duncan, B. N., Edwards, D. P., Haynes, J. A., Henze, D. K., Houyoux, M. R., Jacob, D. J., Krotkov, N. A., Lamsal, L. N., Liu, Y., Lu, Z., Martin, R. V., Pfister, G. G., Pinder, R. W., Salawitch, R. J., and Wecht, K. J.: Emissions estimation from satellite retrievals: A review of current capability, Atmos. Environ., 77, 1011–1042, https://doi.org/10.1016/j.atmosenv.2013.05.051, 2013.

TEPA: Taiwan Emission Data System, available at: https://erdb.epa.gov.tw/eng/DataRepository/EnvMonitor/ReportInspectAirTEDS.aspx?topic1 (last access: 15 January 2018), 2016.

The World Bank: World Development Indicators, available at: http://databank.worldbank.org/data/download/WDI_excel.zip (last access: 15 January 2018), 2016.

Travis, K. R., Jacob, D. J., Fisher, J. A., Kim, P. S., Marais, E. A., Zhu, L., Yu, K., Miller, C. C., Yantosca, R. M., Sulprizio, M. P., Thompson, A. M., Wennberg, P. O., Crounse, J. D., St. Clair, J. M., Cohen, R. C., Laughner, J. L., Dibb, J. E., Hall, S. R., Ullmann, K., Wolfe, G. M., Pollack, I. B., Peischl, J., Neuman, J. A., and Zhou, X.: Why do models overestimate surface ozone in the Southeast United States?, Atmos. Chem. Phys., 16, 13561–13577, https://doi.org/10.5194/acp-16-13561-2016, 2016.

UN: World Urbanization Prospects: The 2014 Revision, available at: https://esa.un.org/unpd/wup/CD-ROM/WUP2014_XLS_CD_FILES/WUP2014-F01-Total_Urban_Rural.xls (last access: 15 January 2018), 2014.

UN: UN World Population Prospects: The 2015 Revision, available at: http://esa.un.org/unpd/wpp/DVD/ (last access: 15 January 2018), 2015.

UN: World urbanization prospects: The 2018 revision, annual percentage of population at mid-year residing in urban areas by region, subregion, country and area, 1950–2050, available at: https://population.un.org/wup/Download/ (last access: 24 July 2019), 2018.

UN: World Population Prospects 2019: Total population (both sexes combined) by region, subregion and country, annually for 1950 to 2100, available at: https://esa.un.org/unpd/wpp/Download/Standard/Population/ (last access: 24 July 2019), 2019.

UNFCCC: National Inventory Submissions of Annex I Parties to the UNFCCC, available at: https://di.unfccc.int/ (last access: 12 August 2019), 2019.

US EPA: An inventory of sources and environmental releases of dioxin-like compounds in the US for the years 1987, 1995, and

2000, US Environmental Protection Agency, Washington DC, USA, EPA/600/P-03/002F, 667 pp., 2006.

US EPA: Criteria Air Pollutants, available at: https://www.epa.gov/criteria-air-pollutants (last access: 23 January 2020), 2018.

US EPA: National Annual Emissions Trend: 1970–2018, available at: https://www.epa.gov/air-emissions-inventories/air-pollutant-emissions-trends-data, last access: 26 August 2019.

van der Werf, G. R., Randerson, J. T., Giglio, L., van Leeuwen, T. T., Chen, Y., Rogers, B. M., Mu, M., van Marle, M. J. E., Morton, D. C., Collatz, G. J., Yokelson, R. J., and Kasibhatla, P. S.: Global fire emissions estimates during 1997–2016, Earth Syst. Sci. Data, 9, 697–720, https://doi.org/10.5194/essd-9-697-2017, 2017.

Venkataraman, C., Brauer, M., Tibrewal, K., Sadavarte, P., Ma, Q., Cohen, A., Chaliyakunnel, S., Frostad, J., Klimont, Z., Martin, R. V., Millet, D. B., Philip, S., Walker, K., and Wang, S.: Source influence on emission pathways and ambient $PM_{2.5}$ pollution over India (2015–2050), Atmos. Chem. Phys., 18, 8017–8039, https://doi.org/10.5194/acp-18-8017-2018, 2018.

Venkataraman, C., Bhushan, M., Dey, S., Ganguly, D., Gupta, T., Habib, G., Kesarkar, A., Phuleria, H., and Raman, R. S.: Indian Network Project on Carbonaceous Aerosol Emissions, Source Apportionment and Climate Impacts (COALESCE), B. Am. Meteorol. Soc., 101, E1052–E1068, 2020.

Wang, S., Zhang, Q., Martin, R. V., Philip, S., Liu, F., Li, M., Jiang, X., and He, K.: Satellite measurements oversee China's sulfur dioxide emission reductions from coal-fired power plants, Environ. Res. Lett., 10, 114015, https://doi.org/10.1088/1748-9326/10/11/114015, 2015.

Wiedinmyer, C., Akagi, S. K., Yokelson, R. J., Emmons, L. K., Al-Saadi, J. A., Orlando, J. J., and Soja, A. J.: The Fire INventory from NCAR (FINN): a high resolution global model to estimate the emissions from open burning, Geosci. Model Dev., 4, 625–641, https://doi.org/10.5194/gmd-4-625-2011, 2011.

Wiedinmyer, C., Yokelson, R. J., and Gullett, B. K.: Global Emissions of Trace Gases, Particulate Matter, and Hazardous Air Pollutants from Open Burning of Domestic Waste, Environ. Sci. Technol., 48, 9523–9530, https://doi.org/10.1021/es502250z, 2014.

Zhang, Q., Streets, D. G., Carmichael, G. R., He, K. B., Huo, H., Kannari, A., Klimont, Z., Park, I. S., Reddy, S., Fu, J. S., Chen, D., Duan, L., Lei, Y., Wang, L. T., and Yao, Z. L.: Asian emissions in 2006 for the NASA INTEX-B mission, Atmos. Chem. Phys., 9, 5131–5153, https://doi.org/10.5194/acp-9-5131-2009, 2009.

Zhao, Y., Nielsen, C. P., Lei, Y., McElroy, M. B., and Hao, J.: Quantifying the uncertainties of a bottom-up emission inventory of anthropogenic atmospheric pollutants in China, Atmos. Chem. Phys., 11, 2295–2308, https://doi.org/10.5194/acp-11-2295-2011, 2011.

Zheng, B., Tong, D., Li, M., Liu, F., Hong, C., Geng, G., Li, H., Li, X., Peng, L., Qi, J., Yan, L., Zhang, Y., Zhao, H., Zheng, Y., He, K., and Zhang, Q.: Trends in China's anthropogenic emissions since 2010 as the consequence of clean air actions, Atmos. Chem. Phys., 18, 14095–14111, https://doi.org/10.5194/acp-18-14095-2018, 2018.

Zheng, B., Chevallier, F., Yin, Y., Ciais, P., Fortems-Cheiney, A., Deeter, M. N., Parker, R. J., Wang, Y., Worden, H. M., and Zhao, Y.: Global atmospheric carbon monoxide budget 2000–2017 inferred from multi-species atmospheric inversions, Earth Syst. Sci. Data, 11, 1411–1436, https://doi.org/10.5194/essd-11-1411-2019, 2019.

Supplement of Earth Syst. Sci. Data, 12, 3413–3442, 2020
https://doi.org/10.5194/essd-12-3413-2020-supplement

Supplement of

A global anthropogenic emission inventory of atmospheric pollutants from sector- and fuel-specific sources (1970–2017): an application of the Community Emissions Data System (CEDS)

Erin E. McDuffie et al.

Correspondence to: Erin E. McDuffie (erin.mcduffie@wustl.edu)

Section S1. CEDS Update Details: CEDSv2019-12-23 relative to CEDSv2016-07-26

CEDSv2019-12-23 (Hoesly et al., 2019) was the first full public CEDS release (https://github.com/JGCRI/CEDS) and is used as the core system version in this work. An earlier version, CEDSv2016-07-26 was used to produce the $\text{CEDS}_{\text{Hoesly}}$ inventory, as described in detail in Hoesly et al. (2018) and its supplement. Changes to the CEDS code between versions v2016-07-26 and v2019-12-23 are described in the CEDS System Release Notes on GitHub (https://github.com/JGCRI/CEDS/wiki/ Release-Notes). These updates include structural changes as well as improvements in the emissions data. The most significant improvements, which are also carried through to the $\text{CEDS}_{\text{GBD-MAPS}}$ inventory include:

- Updated residential waste burning estimates
- Fixed an error in 1960s USA SO_2 emissions and several other issues.

These updates are described in further detail in the following sections. A graphical summary of the differences between versions v2016-07-26 ($\text{CEDS}_{\text{Hoesly}}$) and v2019-12-23 is available at the CEDS repository (https://github.com/JGCRI/CEDS/ at the link "Graphs of emission differences"). Additional updates are described in the CEDS System Release Notes (https://github.com/JGCRI/CEDS/wiki/Release-Notes) and the git log of the $\text{CEDS}_{\text{GBD-MAPS}}$ system, available for download at https://github.com/emcduffie/CEDS/tree/CEDS_GBD-MAPS.

S1.1 Residential waste burning

Updates to emissions from residential open waste burning reduces emissions of all air pollutant species, particularly BC and OC emissions in lower income countries. The major change is a reduction in the assumed amount of uncollected waste that is burnt. The previous CEDS estimate was based on the 2010 value from Wiedinmyer et al. (2014) who assumed that 60% of uncollected solid waste was combusted. We conducted a literature survey, summarized below, to provide more insight into this value. We note that, for the purpose of emission estimation, the parameter we wish to know is the fraction of waste by weight that is combusted. This will be smaller than the fraction of waste that is disposed of through burning, since a significant portion of waste can be inert (e.g., ash, glass, and metals).

Reyna-Bensusan et al. (2018) examined waste disposal by surveying a "representative community" in Mexico about waste generation rates and disposal practices (Huejutla de Reyes Municipality). The Municipality has areas ranging from rural to urban and peri-urban in character. They found that in rural areas with limited access to municipal waste collection (69% had access only to a once-a-month service), 36% of household waste by weight was combusted. Commoner et al. (2000) additionally found in a survey in the Mexico state of Morelos that 14% of household waste was combusted in backyard burning, which corresponded to 52% of uncollected household waste, although only waste practices were surveyed, and waste generation rates were taken from national statistics. This is likely to overestimate the total amount of waste burnt since rural households generate half the waste per capita as compared to urban households (Reyna-Bensusan et al., 2018).

Nagpure et al. (2015) examined waste disposal using a more direct field methodology in three neighborhoods in Delhi India. The neighborhood with the lowest socio-economic status, where "field observation showed very sparse waste management facilities" had the highest rate of waste burning of ∼24% of the total generated.

For Indonesia, Meidiana and Gamse (2010) report on government statistics that imply that only 15% of uncollected waste was burnt in 2006, while 70% was burnt in 2001. It is not clear if this difference is a true difference in burning rate, or different statistical methodologies.

Data is not necessary more available in higher income countries. In the United States residential waste has long been disposed by burning in barrels ("barrel burning"), particularly in rural areas. However, "The amount of refuse that is combusted annually in the United States in residential backyard burn barrels is largely unknown (US EPA, 2006)." This same report identified seven literature sources of survey data largely developed "to estimate the barrel-burning activity in a specific state, county, or region." The "prevalence of barrel burning within the rural population [was found] to range from 12 to 40%". The EPA ultimately assumed that from 40% (1995 and 1987) to 28% (2000) of the rural population burned household refuse, the decrease reflecting a larger number of jurisdictions banning refuse burning in 2000 as compared to earlier years. EPA further assumed that 63% of the household refuse (not including yard waste) was combusted. The confidence of these estimates is rated as low. Multiplying burning prevalence by the fraction of waste burnt results in overall waste burnt fractions of 25% (1995 and 1987) and 18% (2000) for rural populations.

Overall, the fraction of residential waste that is combusted is uncertain and is likely to vary spatially and over time. For the current estimate, informed by the literature discussed above, we assume that 30% of uncollected waste is bunt, which is half the value assumed by Wiedinmyer et al. (2014), with a correspondingly lower emissions level.

With one exception the per-capita waste generation rates from Wiedinmyer et al. (2014) have been retained. For India, however, we use the value from Sharma et al. (2019), which is twice the value in Wiedinmyer et al. (2014), leaving estimates from India largely unchanged.

S1.2 Other Changes

An error in US SO_2 emissions over the 1960s caused an incorrect step-increase in emissions in 1960 in CEDSv2016-07-26. This update will not be carried through to $\text{CEDS}_{\text{GBD-MAPS}}$ as these emissions are reported from 1970 onward. An error that caused a spike in BC emissions in the Netherlands was also corrected and the consistency of Korea BC and OC emissions with the Korea national inventory was improved. These issues and their fixes are further described in the *issues* section of the CEDS GitHub repository. There are also small differences in the CEDSv2016-07-26 and CEDSv2019-12-23 emissions in the US after 2011, particularly NH_3, due to scaling to more recent EPA Trends data. Note also that the monthly seasonality profile for the gridded industrial sector emissions was removed in CEDSv2019-12-23. While there is likely some seasonality in emissions in this sector, seasonality in the CEDSv2016-07-26 data was judged to be too large.

Section S2. CEDS Update Details: $\text{CEDS}_{\text{GBD-MAPS}}$ relative to CEDSv2019-12-23

Section 2 in the Main Text describes updates to the CEDSv2019-12-23 code that are used to derive the new 1970 – 2017 $\text{CEDS}_{\text{GBD-MAPS}}$ inventory. Sections S2.1 – S2.5 below provide additional details regarding these updates. The $\text{CEDS}_{\text{GBD-MAPS}}$ source code is available at: https://github.com/emcduffie/CEDS/tree/CEDS_GBD-MAPS.

S2.1 Activity Data Updates – Additional Details

For the $\text{CEDS}_{\text{GBD-MAPS}}$ system, we have updated the inputs for activity data for both types of CEDS source categories (combustion and process) in order to enable the extension of the $\text{CEDS}_{\text{GBD-MAPS}}$ inventory out to the year 2017. We note that the distinction between CEDS combustion and process category sources is reflective of both the emission sector definition and CEDS methodology. For example, the 1A1bc_Other_transformation sector includes emissions from fuel combustion, but is treated as a process sector in CEDS due to the complexity of its processes, which include emissions from coal coke production, oil refining, and charcoal production (Hoesly et al., 2018). Other similar process sectors include emissions from the 5C_waste-incineration and 1B1_Fugitive-petr-and-gas sectors. Unlike CEDS combustion source categories, emissions from all process sectors are assigned to a single 'process' fuel-type, which may misallocate total emissions from biofuel, coal, and liquid oil and gas combustion to the process source category in the final fuel-specific $\text{CEDS}_{\text{GBD-MAPS}}$ products, as discussed in Sect. 4.2.

S2.1.1 Combustion Sources

For $\text{CEDS}_{\text{GBD-MAPS}}$ combustion category sources, activity data are primarily from energy consumption data, which have been updated to use the 2019 release of the World Energy Statistics from the International Energy Agency (IEA, 2019) for 40 OECD and 114 non-OECD countries and regions. For a small number of countries in Africa, Asia, and the Americas, data are only reported by the IEA at an aggregate region-level and are further disaggregated into their individual countries using historical CO_2 emissions data, as described in Hoesly et al. (2018). Historical national-level CO_2 emissions have been updated here to the most recent release from the Carbon Dioxide Information Analysis Center (CDIAC), which includes data from 1750 to 2014 (Boden et al., 2017). As IEA energy consumption data are provided at finer sectoral and fuel-type resolution than CEDS working sectors and fuels, CEDS Step 1 maps the IEA data to 52 working CEDS sectors and nine working fuel-types. Table S1 provides an example of the mapping between IEA fuels and CEDS working fuel types. Following the CEDSv2019-12-23 procedures, IEA data for residential biofuel consumption from the U.S. are replaced with renewable energy consumption data from the U.S. Energy Information Administration (EIA, 2019), which have been updated here to include the period from 1970 – 2017. In addition, $\text{CEDS}_{\text{GBD-MAPS}}$ no longer applies corrections to the IEA data for coal consumption from China, which were previously used in the CEDSv2019-12-23 system. There is, however, a known issue in the updated IEA data from China that is listed in Sect. S4 below. As described in Hoesly et al. (2018), the CEDSv2019-12-23 system additionally used coal, oil, and gas consumption data from the BP Energy Statistics product (BP, 2015) to extend available IEA data (IEA, 2015) out to the year 2014. Complete IEA data for the year 2017 are available in this work (IEA, 2019), therefore BP energy statistics are no longer used to extend emission estimates, but have been updated (BP, 2019) here as they are also used to estimate emissions from fossil fuel flaring.

Table S1. CEDS fuel-type definitions. CEDS$_{\text{GBD-MAPS}}$ fuel types, *CEDS working fuel-type definitions*, **and** IEA fuel-types

CEDS Fuels

- **Coal**
  - *Brown coal*
    - Brown coal (if no detail)
    - Lignite
    - Peat
    - Peat products
  - *Coal Coke*
    - Coke oven coke
  - *Hard coal*
    - Hard coal (if no detail)
    - Anthracite
    - Coking coal
    - Other bituminous coal
    - Sub-bituminous coal
    - Patent fuel
    - Gas coke
    - Coal tar
    - BKB
- **Biofuel**
  - *Biofuel*
    - Industrial waste
    - Municipal waste (renewable)
    - Municipal waste (non-renewable)
    - Primary solid biofuels
    - Non-specified primary biofuels/waste
    - Charcoal
- **Process**
  - *Process*
- **Liquid Fuel + Natural Gas**
  - *Heavy Oil*
    - Oil shale and oil sands
    - Crude/NGL/feedstocks
    - Crude oil
    - Fuel oil
    - Bitumen
    - Paraffin waxes
    - Petroleum coke
    - Other oil products
  - *Diesel Oil*
    - Gas/diesel oil excl. biofuels
    - Lubricants
    - Biodiesels
  - *Light Oil*
    - Refinery stocks
    - Additives/blending components
    - Other hydrocarbons
    - Ethane
    - Liquefied petroleum gases (LPG)
    - Motor gasoline excl. biofuels
    - Aviation gasoline
    - Gasoline type jet fuel
    - Kerosene type jet fuel excl. biofuels
    - Other kerosene
    - Naptha
    - White spirit & SBP
    - Biogasoline
    - Other liquid biofuels
    - Bio jet kerosene
  - *Natural Gas*
    - Natural gas liquids
    - Gas works gas
    - Coke oven gas
    - Blast furnace gas
    - Other recovered gases
    - Natural gas
    - Refinery gas
    - Biogases

S2.1.2 Process Sources

For $\text{CEDS}_{\text{GBD-MAPS}}$ process category sources, activity drivers are primarily from the UN World Population and World Urbanization Prospects, which are updated here to extend to 2017 (UN, 2019, 2018). These data are used as activity drivers for all CEDS process sources except for 5C_waste-incineration, 1B2_Fugitive-pert-and-gas, and 1B2d_Fugitive-other-energy. As described in Hoesly et al. (2018), pulp and paper consumption data (FAOSTAT, 2015) are used for default emission estimates of waste incineration (held constant here after 2014), while the latter two sectors now use a composite product that is derived from updated 2019 IEA energy statistics. World Bank data were not updated in this work (last year 2014) relative to CEDSv2019-12-23 since these data are only used to supplement population data for Kosovo. Table S2 summarizes the activity driver dataset updates that are used in $\text{CEDS}_{\text{GBD-MAPS}}$ relative to CEDSv2019-12-23. The Supplemental Information of Hoesly et al. (2018) provides a complete list of all additional CEDS input datasets, which have not been updated in this work.

Table S2. Comparison of activity driver datasets that are updated between CEDSv2019-12-23 and $\text{CEDS}_{\text{GBD-MAPS}}$ systems. For a complete list of CEDS activity drivers, see Hoesly et al. (2018).

CEDS Emission Source Category	Hoesly et al. (2018)	$\text{CEDS}_{\text{GBD-MAPS}}$
Fuel combustion	(IEA, 2015) (BP, 2015) EIA, 2(The World Bank, 2016;UN, 2014, 2015;Wiedinmyer et al., 2014)015 (biofuel from US) (Boden et al., 2016)	(IEA, 2019) (BP, 2019) (flaring estimates only) (EIA, 2019) (biofuel from US) (Boden et al., 2017)
Process	(UN, 2014, 2015) (The World Bank, 2016) (FAOSTAT, 2015)	(UN, 2019, 2018) (The World Bank, 2016) (FAOSTAT, 2015)

S2.2. Emission Factors & Inventory Input Updates – Additional Details

S2.2.1 Combustion Sources

The datasets used to calculate default emission factors (EF) for combustion sources in the $\text{CEDS}_{\text{GBD-MAPS}}$ system are largely unchanged relative to those in CEDSv2019-12-23 (see Table 2 in Hoesly et al. (2018) for a complete list). For reactive gases, combustion EFs are primarily estimated using information from the GAINS model (as released for the Energy Modeling Forum 30 (EMF30) project (Klimont et al., 2017;Stohl et al., 2015)), SPEW for BC and OC (Bond et al., 2007), and the U.S. 2011 NEI for NH_3. As described in Hoesly et al. (2018), EF calculations take into account historical changes in emission abatement strategies, while some EFs for SO_2 are also calculated explicitly using fuel sulfur content, ash retention, and country-specific percent controls (NEI, 2013). EF and emission calculations do not include information about the vertical distribution of emissions. For countries with missing contemporary sectoral or fuel-type information, EFs are extended forward to 2017 using trends from GAINS projections. The minimum allowable EFs for road transportation have also been extended to 2017, which ensures the use of realistic EFs from this sector in recent years for countries with missing data.

S2.2.2 Process Sources

For non-combustion sectors, EFs in CEDS$_{\text{GBD-MAPS}}$ Step 1 are estimated using existing emission inventories and calculated activity drivers, as described previously in Sect. 2.1. These emission estimates are primarily from the global EDGAR inventory, which has been updated in this work to use a more recent release of EDGAR (v4.3.2; EC-JRC, 2018;Crippa et al., 2018). For emissions of waste combustion, all versions of the CEDS system use country-specific EFs for 2010 from Wiedinmyer et al. (2014), along with estimates of the total mass. As described in Sect. S1.1 above, relative to CEDSv2016-07-26, assumptions for the fraction of waste burnt have been updated in both CEDSv2019-12-23 and CEDS$_{\text{GBD-MAPS}}$, along with estimates for the amount of waste generated per-capita in India (Sharma et al., 2019). Additional details on these updates can be found in the core CEDS system release notes (https://github.com/JGCRI/CEDS/wiki/Release-Notes). Similar to combustion sources, missing EFs are also extended forward and backwards in time to produce a complete time series for 1970 - 2017. Table 2 in Hoesly et al. (2018) provides a complete list of all input datasets used to estimate default process source emissions. Other than those described here, all remaining datasets are unchanged in this work relative to CEDSv2019-12-23. Despite uncertainties in contemporary EFs and default emission estimates for both source categories, many of these values are later scaled to match contemporary regional and national-level inventories (see Sect. 2.2).

S2.3 Default CEDS Emissions Scaling Procedure Updates – Additional Details

S2.3.1 Scaling Mapping Files & Misc. Details

The first step of the scaling procedure is to aggregate emissions from common sectors and fuel-types into "scaling sectors" and "scaling fuel" groups (when fuel-specific emissions are available) for each scaling inventory. This is necessary as there are often differences in the availability and definitions of emission from source sectors and fuel-types between CEDS and the scaling inventories. Total default CEDS emissions within these aggregate groups are then scaled to the corresponding emissions in each scaling inventory, using the scaling factors calculated from Eq. (2) in the main text. All mapping files can be found at: https://github.com/emcduffie/CEDS/tree/CEDS_GBD-MAPS/input/mappings/scaling, with specific examples described below.

The first column in each mapping file provides the sectoral names from the scaling inventory. When emissions are reported as a function of fuel type, the second column lists the fuel-types reported for each emission sector in the scaling inventory. When applicable, column three defines the aggregate scaling fuel groups. Column four defines the aggregate scaling sector groups. Columns five and six list the CEDS working sectors and working fuels that correspond to these aggregate scaling groups. Table S3 provides an example scaling mapping file for the DICE-Africa scaling inventory. Table S3 shows that the DICE-Africa inventory reports combined emissions from gas (petrol) and diesel use in cars and motorcycles. The CEDS system does not differentiate between different types of on-road sources and therefore, DICE-Africa emissions from both cars and motorcycles are mapped to the common 'road_transport' scaling sector, which corresponds to the CEDS 1A3b_Road sector. Similarly, the DICE-Africa inventory does not distinguish between emissions from gas and diesel fuel, therefore total CEDS road emissions from light_oil and diesel_oil combustion in the road sector are scaled to the total DICE-Africa emissions reported for cars and motorcycles. Example scaling factors for select years and countries in Africa, as a function of scaling sector are provided in Table S4. Data are included for illustrative purposes only. Following original CEDS protocols, scaling factors are limited to values between 0.01 and 100, with select inventories and sectors expanded to a range of 0.001 and 1000, as described below in Section S2.3.2. As discussed in Hoesly et al. (2018), particularly small or large scaling factors may result for multiple reasons, including default CEDS estimates that are drastically different than regional emissions or imprecise mapping between CEDS and regional emission sectors.

Table S3. Example scaling mapping file for DICE-Africa in $\text{CEDS}_{\text{GBD-MAPS}}$ system.

DICE-Africa sector	DICE-Africa fuel	Scaling Fuel	Scaling Sector	CEDS Sector	CEDS Fuel
cars	gas_diesel	gas_diesel	road_transport	1A3b_Road	light_oil
		gas_diesel	road_transport	1A3b_Road	diesel_oil
motorcycles	gas_diesel	gas_diesel	road_transport		
charcoal-use	biomass	biomass	residential	1A4b_Residential	biomass
household-crop-residue-use	biomass	biomass	residential		
household-fuelwood-use	biomass	biomass	residential		
kerosene-use	light_oil	light_oil	residential	1A4b_Residential	light_oil
other-fuelwood-use[a]	biomass	n/a	n/a	n/a	n/a
adhoc-oil-refining[a]	process	n/a	n/a	n/a	n/a
generator-use[a]	gas_diesel	n/a	n/a	n/a	n/a
charcoal-production[a]	biomass	n/a	n/a	n/a	n/a
gas-flares[a]	process	n/a	n/a	n/a	n/a

[a] Suggested additions, not replacements, see Sect. S2.3.2

Table S4. Example BC scaling factors for select DICE-Africa countries and years.

Country (ISO)	Scaling Sector	Scaling Fuel	2006	2007	2008	2009	2010	2011	2012	2013	2014	2015
ago	residential	biomass	0.332	0.338	0.344	0.350	0.355	0.361	0.367	0.373	0.373	0.373
ago	residential	light oil	0.340	0.311	0.282	0.252	0.223	0.194	0.165	0.136	0.136	0.136
ago	road_transport	gas_diesel	0.307	0.293	0.278	0.264	0.250	0.235	0.221	0.207	0.207	0.207
nam	residential	biomass	0.297	0.320	0.342	0.364	0.386	0.409	0.431	0.453	0.453	0.453
nam	residential	light oil	44.71	44.72	44.72	44.72	44.73	44.73	44.73	44.74	44.74	44.74
nam	road_transport	gas_diesel	0.274	0.260	0.247	0.234	0.220	0.207	0.194	0.180	0.180	0.180

Relative to CEDS v2019-12-23, minor adjustments have been made to other inventory scaling mapping files in order to better reflect the overlap between $\text{CEDS}_{\text{GBD-MAPS}}$ working sectors and the updated scaling inventories. One example is the adjustment of scaling factors for agricultural NO_x emissions for the U.S. NEI and Canadian APEI inventories. In these national inventories, NO_x emissions from soils are not reported (report NH_3 emissions only). In CEDSv2019-12-23, NO_x emissions from the sum of all agricultural working sectors (3B+3D+3E+3I; including soil emissions) are scaled to the total agricultural NO_x emissions reported in these scaling inventories, resulting in scaled CEDS agricultural NO_x emissions that are erroneously low. In this work, $\text{CEDS}_{\text{GBD-MAPS}}$ 3D_Soil-emissions from the US and Canada are no longer scaled to these inventories and default emission estimates are used for this working sector. These updated scaling mapping files can be found at: https://github.com/emcduffie/CEDS/tree/CEDS_GBD-MAPS/input/mappings/scaling.

After the scaling procedure, $\text{CEDS}_{\text{GBD-MAPS}}$ emissions are then disaggregated back into the original 52 CEDS working sectors and 9 working fuel-types (Table 2, combustion source only) using the initial fractional contributions from each sector and fuel-type. This method allows CEDS to maintain detailed fuel and sectoral information while simultaneously scaling total country-level emissions to authoritative inventories. This process, however, often results in total $\text{CEDS}_{\text{GBD-MAPS}}$ emissions that are higher than the individual scaling inventories, depending on the amount of overlap with each inventory. For example, Fig. (S1) shows that in China, total CEDS$_{\text{GBD-MAPS}}$ emissions for OC after 2010 are larger than those in the national scaling inventory, reported by Zheng et al. (2018). This difference is largely due to the inclusion of the waste sector in CEDS$_{\text{GBD-MAPS}}$, which is not reported in the Zheng et al. (2018) inventory. In contrast, other inventories report emissions from sources that are not included in CEDS, such as open burning on agricultural fields or road dust emissions. In these cases, these sectors are not included in the CEDS scaling procedure and are not included in the final CEDS$_{\text{GBD-MAPS}}$ inventory. In addition, sectors such as domestic shipping are not scaled and are always set to default CEDS estimates due to large uncertainties and differences in the definitions of these sectors in individual scaling inventories. To illustrate the outcome of the scaling procedure, implied emission factors for the top 15 emitting countries are additionally shown in Figure S2 for the select fuel-types and sectors that dominantly contribute to global emission of each compound. Various anomalies in the implied EFs can arise from multiple sources of uncertainty, including the underlying activity data or application of scaling factors outside the available scaling inventory years, as is the case with the on-road CO emission factor for China in 1999. These uncertainties are discussed further in Section 4.2 in the main text.

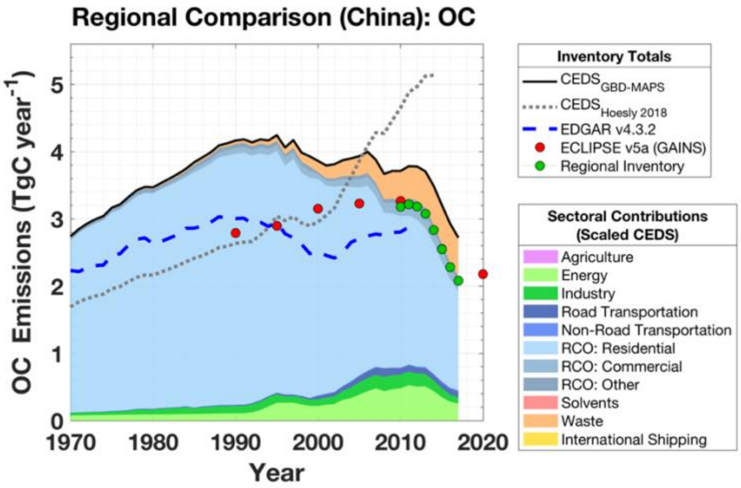

Figure S1. Inventory comparison of annual OC emissions from China. Black line) total CEDS$_{\text{GBD-MAPS}}$ emissions, colored by sectoral contributions, dashed gray line) CEDS$_{\text{Hoesly}}$ emissions, dashed blue line) EDGAR v4.3.2 emissions, red dots) ECLIPSE v5a (GAINS) inventory with 2015 and 2020 projections, green dots) scaling inventory from Zheng et al. (2018). This comparison does not include contributions from agricultural waste burning, shipping, or aviation emissions.

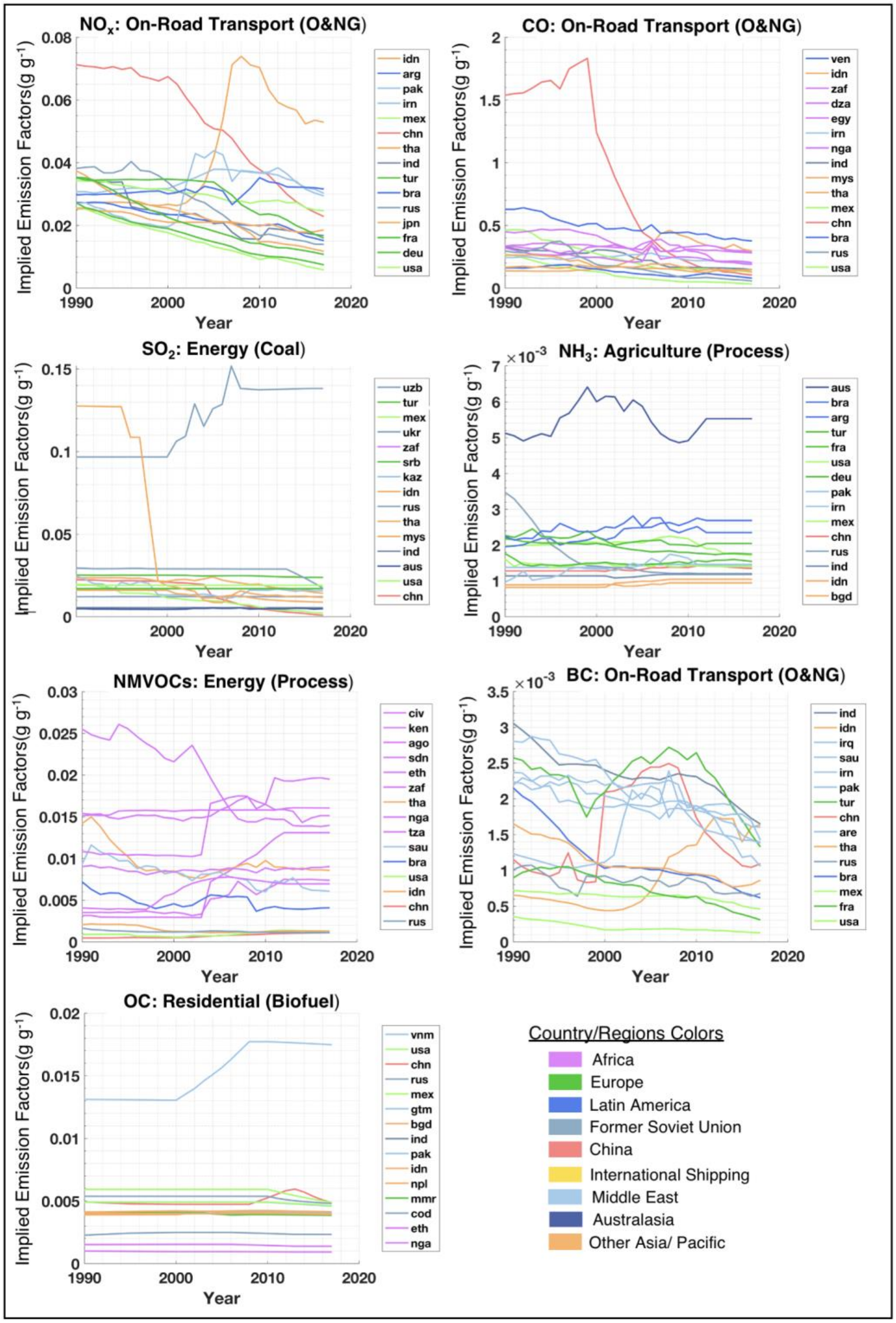

Figure S2. Time-series of implied (post-scaling) emission factors for select fuel and sector combinations that dominantly contribute to global emissions of each compounds. NOx, CO, and BC: oil & natural gas combustion in the on-road transport sector, SO_2: coal combustion in the energy sector, NH_3: agricultural emissions, NMVOCs: process-level energy sources, and OC: residential biofuel combustion. Time series are shown for the top 15 emitting countries, listed by their ISO codes to the right of each panel. Time series are colored by the region of each country.

S2.3.2 Africa Emissions Scaling

As discussed in the main text, new scaling inventories are included in this work for emissions from India and Africa. For African countries, default $\mathrm{CEDS}_{\mathrm{GBD\text{-}MAPS}}$ emissions for residential and road sectors are scaled to the respective values in the DICE-Africa inventory (Marais and Wiedinmyer, 2016) for 2006 and 2013, as a function of diesel, light oil (Table S1), and biofuel use. For years between 2006 and 2013, scaling factors (SFs) from Eq. (2) in the main text are linearly interpolated within the CEDS system. These SFs are held constant before 2006 and after 2013. DICE-Africa OC emissions from cars are additionally scaled by 0.14 prior to the CEDS scaling procedure in order to correct for a previous error in the DICE-Africa OC EFs (http://wiki.seas.harvard.edu/geos-chem/index.php/DICE-Africa_anthropogenic_emissions_inventory#Scale_DICE-Africa_emissions_to_address_errors_in_inventory). Upper and lower bounds of scaling factor are additionally relaxed here to limits of 1000 and 0.001 (100 and 0.01 in CEDSv2019-12-23) to ensure better agreement between DICE-Africa and $\mathrm{CEDS}_{\mathrm{GBD\text{-}MAPS}}$ sectoral totals. In a small number of instances, calculated scaling factors are outside this range, which may reflect differences in sectoral definitions between the two inventories or real uncertainties in the magnitude of sectoral-level emissions in Africa.

As also noted in the main text, DICE-Africa emission estimates from gas flares across Africa and ad-hoc oil refining in the Niger Delta are not included in the $\mathrm{CEDS}_{\mathrm{GBD\text{-}MAPS}}$ scaling procedure (Table S2). Total default $\mathrm{CEDS}_{\mathrm{GBD\text{-}MAPS}}$ emissions in Africa for each compound in 2013 from the 1B2_fugitive_petr_gas (gas flaring) sector are almost always larger than the respective DICE-Africa gas-flaring emissions, suggesting that emissions from this source sector may be accurately represented in default $\mathrm{CEDS}_{\mathrm{GBD\text{-}MAPS}}$ estimates. However, in the event that gas-flaring emissions from the DICE-Africa inventory are not accounted for in the $\mathrm{CEDS}_{\mathrm{GBD\text{-}MAPS}}$ default emissions, the $\mathrm{CEDS}_{\mathrm{GBD\text{-}MAPS}}$ 1B2_fugitive_petr_gas emissions across Africa may be underestimated by up to 28% (or up to < 0.01 Tg) for each compound in 2013 (Table S3).

In addition, DICE-Africa emissions from petrol/diesel use in residential generators, as well as fuelwood use for charcoal production and other commercial activities are not included in the $\mathrm{CEDS}_{\mathrm{GBD\text{-}MAPS}}$ scaling procedure. These sectors are not explicitly represented by the $\mathrm{CEDS}_{\mathrm{GBD\text{-}MAPS}}$ working sectors and are only expected to be represented in the $\mathrm{CEDS}_{\mathrm{GBD\text{-}MAPS}}$ default estimates to the extent that these sources are included in the IEA energy consumption data. Emissions from charcoal production will be allocated to the 1A1bc_Other-Transformation sector, while commercial fuelwood use would be allocated to the 1A4a_Commercial-institutional sector. In the event that these sources are not included in default $\mathrm{CEDS}_{\mathrm{GBD\text{-}MAPS}}$ emissions, the emissions from biofuel use in the CEDS other transformation and commercial sectors in 2013 may be underestimated by up to 100% (or up to 6 Tg) for each compound (Table S5). Similarly, residential generator use may be allocated to the 1A4b_Residential (RCO-R) and/or 1A4c_Agriculture-forestry-fishing (RCO-Other) sectors. In the event that generators are not accounted for in default estimates, CEDS emissions from light oil/diesel use in the residential sectors may be underestimated by up to 84% (or up to 0.25 Tg) for each compound (Table S5). While these maximum possible under-predictions represent large fractions of emissions from individual fuels and sectors, the sum of these potential missing emissions correspond to maximum under-predictions in total 2013 $\mathrm{CEDS}_{\mathrm{GBD\text{-}MAPS}}$ emissions in Africa of less than 11% (or < 10.5 Tg) for each compound (Table S3). Possible under-predictions of <11% are within typical uncertainties of bottom-up emission inventories (Sect. 4.2.3). Table S5, however, does indicate that some emissions from commercial and residential sectors in Africa may be underpredicted in CEDS$_{\text{GBD-MAPS}}$ inventory.

Table S5. Maximum possible under-predictions in sectoral CEDS$_{\text{GBD-MAPS}}$ Africa emissions relative to DICE-Africa

DICE Sectors (Fuels)	**CEDS Sectors (Fuels)**	**NO$_x$**		**SO$_2$**		**CO**		**NMVOC**		**NH$_3$**		**BC**		**OC**	
		Tg[a]	**%[b]**	**Tg[a]**	**%[b]**	**Tg[a]**	**%[b]**	**TgC[a]**	**%[b]**	**Tg[a]**	**%[b]**	**TgC[a]**	**%[b]**	**TgC[a]**	**%[b]**
Gas Flares	1B2_fugitive_petr_gas	0.03	<0.1	-	-	<0.01	<0.1	<0.01	<0.1	-	-	<0.01	14	<0.01	28
Residential Generators (gas/diesel)	1A4b_Residential + 1A4c_Agriculture-forestry-fishing (light oil + diesel oil)	0.25	84	0.01	26	0.05	48	<0.01	2	-	-	<0.01	<0.01	<0.01	0.1
Charcoal production (fuelwood)	1A1bc_Other-transformation (process)	<0.01	16	-	-	6.0	99	2.5	99	0.03	99	<0.01	16	0.02	81
Com. Activity (fuelwood)	1A4a_Commercial-institutional (biomass)	0.09	100	0.03	88	4.5	98	2.0	99	<0.01	68	0.05	68	0.2	68
Sum of above sectors	All CEDS$_{\text{GBD-MAPS}}$ Africa Emissions	0.37	6	0.04	0.7	10.5	11	4.5	9	0.03	0.5	0.05	6.5	0.22	8

[a] Sum DICE-Africa 2013 emissions from each country within the given sector

[b] Potential underprediction in CEDS$_{\text{GBD-MAPS}}$ sectoral emissions, assuming DICE-Africa emissions are not accounted for in default CEDS estimates (i.e., 100* (CEDS$_{\text{GBD-MAPS}}$ Em. + DICE-Africa Em.)/ CEDS$_{\text{GBD-MAPS}}$ Em.)

As discussed in the main text, Fig. 3 compares the scaled CEDS$_{\text{GBD-MAPS}}$ emissions of all compounds in Africa to those from the CEDS$_{\text{Hoesly}}$ inventory. Large differences include the reductions of NO$_x$ and BC emissions from the on-road transport sector in CEDS$_{\text{GBD-MAPS}}$ relative to the CEDS$_{\text{Hoesly}}$ inventory. As discussed in Sect. 2.2, these reductions are largely driven by a difference in EFs used for emissions from diesel vehicles. For the on-road transport sector, the DICE-Africa inventory uses activity data from the UN energy database for total petrol/diesel use in the transport sector, which is then divided into usage for motorcycles and vehicles as described in Marais and Wiedinmyer (2016). Vehicle activity data are not split further, and a single EF is applied to total vehicle activity data to calculate DICE-Africa emissions from all on-road cars. This DICE-Africa EFs for cars are consistent with the default CEDS EFs for on-road gasoline emissions and will be more representative of light vehicles than larger diesel trucks, which have default EFs in CEDS roughly twice as large.

S2.3.2 India Emissions Scaling

We also scale emissions from India to a new 2015 emissions inventory described in Venkataraman et al. (2018) (SMoG-India). Similar scaling sector and fuel definitions are defined as described above. As described in the main text, emissions for NO$_x$, SO$_2$, CO, NMVOCs, OC, and BC are available for 17 sectors and nine fuel types. Scaling mapping files can be found at: https://github.com/emcduffie/CEDS/tree/CEDS_GBD-MAPS/input/mappings/scaling. Scaling factors were calculated for the year 2015 and applied forward and back to the entire 1970 – 2017 timeseries. Due to uncertainties in the sectoral mapping and applicability of 2015 scaling factors over the entire time period, we note the potential misallocation of the SMoG-India 'Informal Industry' sector to the CEDS$_{\text{GBD-MAPS}}$ 1A2c_ind-Comb-Food-tobacco sector (rather than the 1A2g-Comb-Ind-other sector). This misallocation results in CEDS$_{\text{GBD-MAPS}}$ NO$_x$ emissions in India possibly overpredicted by up to ~1 Tg between 1987-2014 (see also Sect. S4). While sectoral misallocations impact the magnitude of sub-sector emissions, total $\mathrm{CEDS}_{\mathrm{GBD\text{-}MAPS}}$ industry emissions in 2015 are equivalent to total industry emissions (information + light + heavy industry) from the SMoG-India inventory.

In addition, there are cases where default CEDS emissions for a specific sector/fuel-type combination equal 0, resulting in emissions of 0 after the scaling process. To avoid missing emissions in these instances, CEDS working fuel types are aggregated into “scaling fuels” (total coal, total liquid fuel, natural gas, and process emissions) in a similar manor to the scaling sectors (as described above in Sect. S2.3), and are later re-allocated to the CEDS working fuel types according to distributions prior to scaling. While this process may result in a slightly different fuel distribution at the most detailed level, final $\mathrm{CEDS}_{\mathrm{GBD\text{-}MAPS}}$ emissions (both gridded and country-level products) are aggregated into contributions from total coal, biofuel, oil and gas, and process emissions.

S2.4 Default BC and OC Emission Scaling Procedure Updates – Additional Details

Relative to CEDS v2019-12-23, BC and OC emissions are now scaled to available regional- and national-level inventories. $\mathrm{CEDS}_{\mathrm{GBD\text{-}MAPS}}$ emissions for OC and BC from countries within each scaling inventory are shown in Fig. S3 and S4. These figures additionally compare these emissions to those from the $\mathrm{CEDS}_{\mathrm{Hoesly}}$, GAINS (ECLIPSE v5a) (Klimont et al., 2017), EDGAR v4.3.2 (Crippa et al., 2018), and scaling inventories. As described above and in the main text, regional inventories and final $\mathrm{CEDS}_{\mathrm{GBD\text{-}MAPS}}$ emissions may not agree depending on the level of overlap between the sectoral emissions included in each scaled inventory. For example, the national emissions from China (Zheng et al., 2018) are lower than the $\mathrm{CEDS}_{\mathrm{GBD\text{-}MAPS}}$ estimates due to waste emissions that are not included in the national-inventory.

It should also be noted that emissions from the metal and chemical industrial sectors in Japan are underestimated in both $\mathrm{CEDS}_{\mathrm{Hoesly}}$ and $\mathrm{CEDS}_{\mathrm{GBD\text{-}MAPS}}$ relative to the country level inventory (preliminary update from Kurokawa et al., 2013). Default CEDS emissions for these sectors are estimated to be zero in CEDS Step 1 and are therefore not scaled to the available inventory emissions. This underprediction is largest for years prior to 1995 (see Fig. S4) and is reduced in recent years due to a decreasing fractional contribution of these sectors to total OC and BC emissions in the Kurokawa et al., 2013 inventory (40% to 28% for OC, 2% to 1.6%. for BC between 1990 and 2010). In addition, $\mathrm{CEDS}_{\mathrm{GBD\text{-}MAPS}}$ emissions are not scaled to EMEP emissions (EMEP, 2019) prior to 2000 due to changes in inventory reporting (Fig. S3).

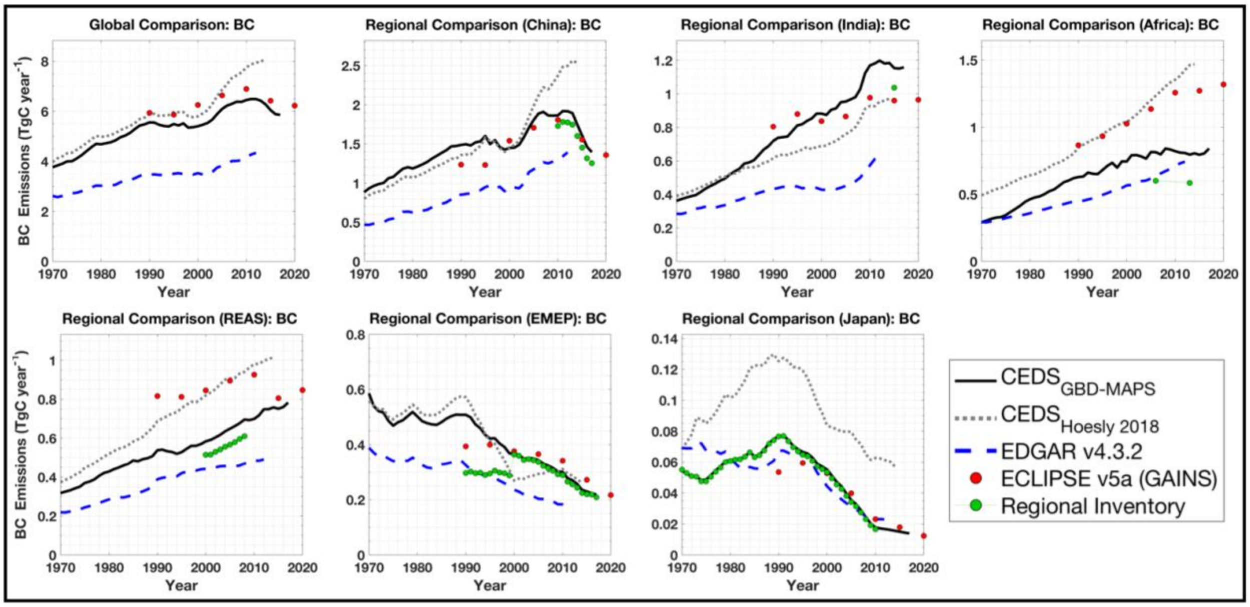

Figure S3. Time series of BC emissions from CEDS$_{\text{GBD-MAPS}}$ (black line), CEDS$_{\text{Hoesly}}$ (gray dashed line), EDGAR v4.3.2 (blue dashed line), and ECLIPSE v5a baseline current legislation (CLE) inventory from the GAINS model (red dots). Each panel shows total annual emissions from each designated country/region. GAINS values for 2015 and 2020 are emission projections. Global inventories show reported emissions from all sectors excluding open burning, shipping, and aviation. Respective regional inventories are shown by green dots/lines and include all reported emissions that are also included in regional CEDS$_{\text{GBD-MAPS}}$ emissions (e.g., do not include open burning, road dust, shipping, aviation, etc). Note: in the regional comparisons, CEDS$_{\text{GBD-MAPS}}$, CEDS$_{\text{Hoesly}}$, and EDGAR v4.3.2 emissions also include inland navigation, while GAINS v5a CLE do not include any shipping emissions. In the global comparison, all available shipping emissions (inland navigation and international shipping) are included in each inventory. REAS and EMEP member countries listed in Table S6.

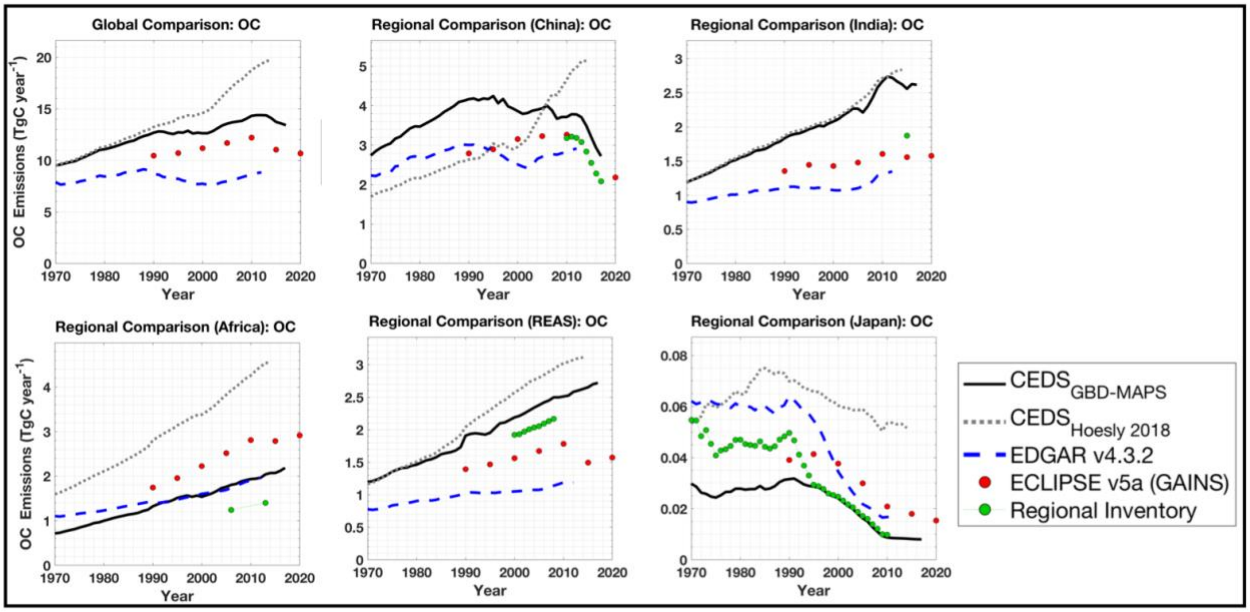

Figure S4. Same as Fig. S3, but for OC emissions.

Table S6. Countries included in REAS and EMEP regions

REAS	Afghanistan	Bhutan	Brunei Darussalam	Cambodia
	Bangladesh	Maldives	DPR Korea	Kyrgyzstan
	Indonesia	Myanmar	Kazakhstan	Mongolia
	Laos	Sri Lanka	Nepal	Singapore
	Malaysia	Turkmenistan	Pakistan	Thailand
	Tajikistan	Vietnam	Philippines	Uzbekistan
	Taiwan			
EMEP	Albania	Armenia	Belgium	Czech Republic
	Belarus	Austria	Cyprus	Estonia
	Bulgaria	Croatia	France	Germany
	Denmark	Finland	Italy	Hungary
	Georgia	Greece	Malta	Kyrgyzstan
	Iceland	Ireland	Montenegro	Latvia
	Luxembourg	Macedonia	Portugal	Netherlands
	Norway	Poland	Slovenia	Romania
	Sweden	Slovakia	Spain	Switzerland
	United Kingdom			

S2.5 Spatial Gridding & Aggregation Updates – Additional Details

Relative to CEDSv2019-12-23, CEDS emissions prior to gridding are now aggregated into 17 intermediate sectors as a function of four fuel categories: total coal (hard coal + brown coal + coal coke), solid biofuel, the sum of liquid fuel (heavy oil + light oil + diesel oil) and natural gas, and all remaining ‘process’ emissions.

CEDS Step 5 then spatially allocates total country-level emission estimates on to a 0.5°×0.5° global grid to facilitate their use in earth system models. The procedure for spatially allocating CEDS total country-level emissions is largely unchanged between CEDSv2019-12-23 and CEDS$_{\text{GBD-MAPS}}$. This process uses normalized spatial distribution proxies that are compound- and sector-specific. In CEDSv2019-12-23, proxy distribution data are primarily from gridded EDGAR emissions (v4.2 and v4.3) (EC-JRC/PBL, 2012, 2016) and HYDE population (Klein Goldewijk et al., 2011) (primarily for historical extension prior to 1970 and waste emissions). In CEDSv2019-12-23, gridding proxies are then held constant after 2008 or 2010 (ROAD transportation only). For the CEDS$_{\text{GBD-MAPS}}$ inventory, we have updated the compound- and sector-specific normalized spatial proxies for 1970 – 2012 to use the most recent release of the EDGAR inventory (v4.3.2) (Table S7). Spatial proxies are then held constant for all years after 2012. These updates extend many of the latest spatial proxies from 2008 to 2012 but may still introduce uncertainty in the gridded CEDS$_{\text{GBD-MAPS}}$ products between 2013 and 2017 for sectoral emissions that have experienced large changes in their normalized spatial distributions within large countries (Sect. 4.2.5). The same sector-specific gridding proxy is also applied to emissions from each fuel group within each sector. This process may introduce additional uncertainties into the gridded CEDS$_{\text{GBD-MAPS}}$ products as discussed in Sect. 4.2. These uncertainties do not impact the final country-level CEDS$_{\text{GBD-MAPS}}$ products because they are not gridded.

As further described in Hoesly et al. (2018), sectors that do not have congruent emissions between CEDS and EDGAR v4.3.2 inventories use population data from HYDE (Klein Goldewijk et al., 2011) and Gridded Population of the World (GPW) (Doxsey-Whitfield et al., 2015) products as backup spatial proxies. Supplemental Table S7 provides a complete list of gridding proxies as a function of sector. All sectors that do not use EDGAR data use the same spatial proxies as in CEDSv2019-12-23. For example, emissions from the waste sector are gridded using yearly estimates of population, which have not been updated relative to CEDSv2019-12-23 and are therefore held constant after the year 2015.

Table S7. Gridding proxies used for spatial allocation, listed by sector.

CEDS final sectors	CEDS intermediate gridding sectors	Spatial Proxy[a]	Years[b]
Agriculture (AGR)	Agriculture	EDGAR v4.3.2 AGR	1970 – 2012
International Shipping (SHP)	International Shipping	ECLIPSE and additional data[c]	1990, 1995, 2000, 2005, 2010, 2015
	International Shipping (tanker loading)	ECLIPSE and additional data[c]	1996
On-Road Transportation (ROAD)	On-Road Transportation	EDGARv4.3.2 ROAD	2010
Non-Road Transportation (NRTR)	Non-Road Transportation	EDGAR v4.3.2 NRTR	1970 - 2012
Residential, Commercial, Other - Residential (RCOR)	Residential, Commercial, Other - Residential	EDGAR v4.3.2 RCO	1970 – 2012
Residential, Commercial, Other - Commercial (RCOC)	Residential, Commercial, Other - Commercial	EDGAR v4.3.2 RCO	1970 – 2012
Residential, Commercial, Other - Other (RCOO)	Residential, Commercial, Other - Other	EDGAR v4.3.2 RCO	1970 – 2012
Energy (ENE)	Oil and gas fugitive/flaring	ECLIPSE FLR[c]	1970 – 2015
	Electricity and heat production	EDGAR v4.3.2 ELEC	1970 – 2012
	Fuel production and transformation	EDGAR v4.3.2 ETRN	1970 – 2012
	Fossil Fuel Fires	EDGAR v4.3.2 FFFI	1970 - 2012
Waste (WST)	Waste	HYDE population, GPW v4 (modified rural population)[c]	1970 – 2015
Industry (IND)	Industrial Combustion	EDGAR v4.3.2 INDC	1970 – 2012
	Industrial process and product use	EDGAR v4.3.2 INPU	1970 – 2012
Solvent production and application (SLV)	Solvent production and application (SLV)	EDGAR v4.3.2 SLV	1970 - 2012

[a] All species and sectors use population as a backup proxy.

[b] Spatial proxies held constant for years not listed. For example, EDGAR v4.3.2 proxies from 2012 are used for years 2012-2017. All sectors use population as a backup proxy (2016-2017 use 2015 population).

[c] Not updated relative CEDS$_{\mathrm{Hoesly}}$ inventory.

After the gridding procedure, the 17 intermediate sectors are then aggregated into 11 final sectors, by effectively splitting the original CEDSv2019-12-23 emissions from the TRA sector into 'On-Road' and 'Non-Road/Other' contributions and splitting the original RCO sector into individual contributions from the Residential, Commercial, and Other sectors. Table 2 contains a complete breakdown of the definitions of CEDS working, intermediate gridding, and final sectors. Figure S5 illustrates the level of detail available in this new CEDS$_{\mathrm{GBD\text{-}MAPS}}$ inventory by illustrating global BC emissions in 2017 from 1) all source sectors, 2) the residential sector only, 3) residential biofuel-use only, and 4) residential coal-use only.

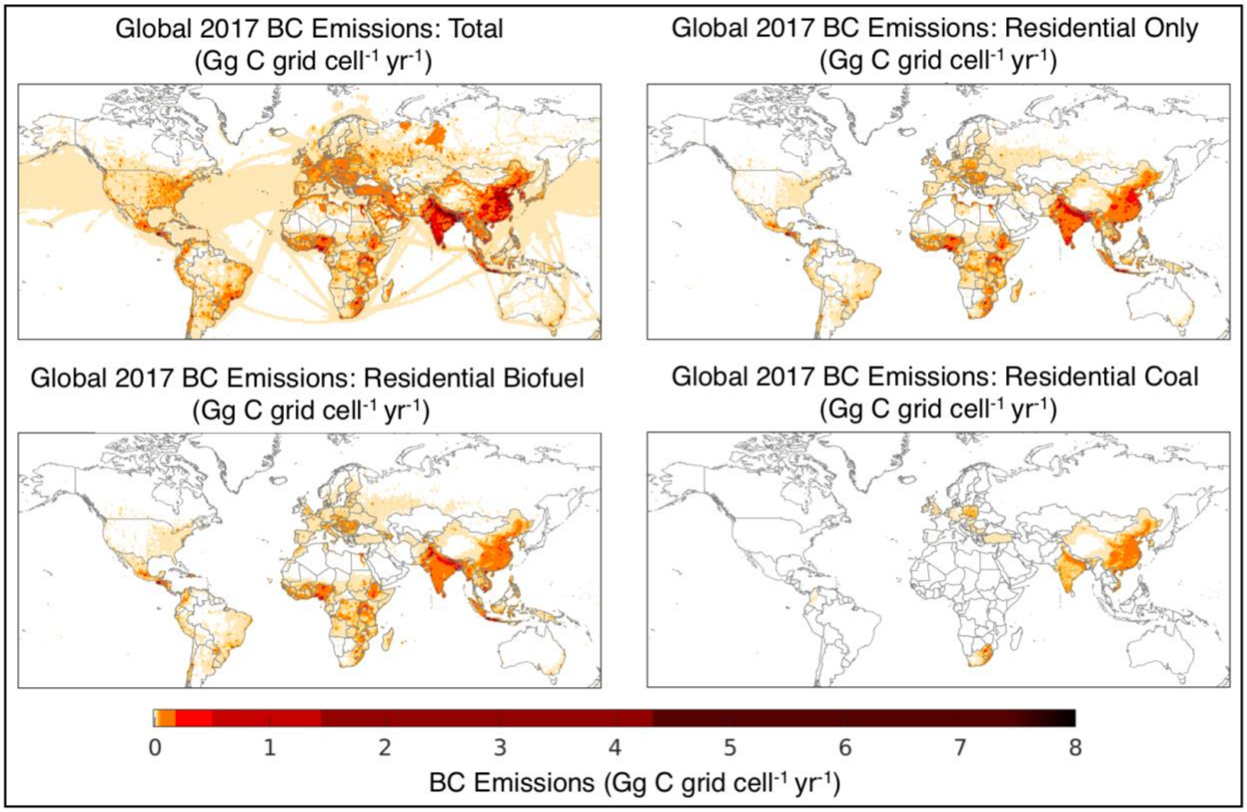

Figure S5. Map of global BC emissions for 2017 from (top left) all sectors, (top right) residential emissions only, (bottom left) residential biofuel only, and (bottom right) residential coal only.

Section S3. Supplemental Results

Table S8. Fractional sectoral and fuel-type contributions to 2017 global emissions of each compound. Sectoral contributions in bold sum to 100% for each compound (i.e., AGR + ENE +… SHP =100%). Fractional contributions of fuel-types within each sector sum to 100% for each compound (i.e., ENE coal + ENE biofuel + ENE Oil+Gas + ENE Process =100%).

Sector	Fuel-Type	NO_x	CO	SO_2	NH_3	NMVOC	BC	OC
AGR	**Total**	**5%**	**-**	**-**	**75%**	**-**	**-**	**-**
AGR	Coal	-	-	-	-	-	-	-
AGR	Biofuel	-	-	-	-	-	-	-
AGR	Oil + Gas	-	-	-	-	-	-	-
AGR	Process	100	-	-	100	-	-	-
ENE	**Total**	**22%**	**11%**	**42%**	**2%**	**36%**	**10%**	**8%**
ENE	Coal	46	10	63	4	<1	3	7
ENE	Biofuel	3	2	<1	3	<1	15	53
ENE	Oil + Gas	35	8	18	6	<1	2	<1
ENE	Process	16	80	19	87	99	80	40
IND	**Total**	**15%**	**14%**	**36%**	**2%**	**6%**	**12%**	**10%**
IND	Coal	49	36	38	5	25	47	17
IND	Biofuel	10	11	1	39	25	24	78
IND	Oil + Gas	36	5	25	11	9	29	5
IND	Process	5	48	36	45	41	-	-
ROAD	**Total**	**23%**	**32%**	**2%**	**1%**	**17%**	**20%**	**7%**
ROAD	Coal	-	-	-	-	-	-	-
ROAD	Biofuel	-	-	-	-	-	-	-
ROAD	Oil + Gas	100	100	100	100	100	100	100
ROAD	Process	-	-	-	-	-	-	-
NRTR	**Total**	**6%**	**1%**	**1%**	**<1%**	**1%**	**1%**	**<1%**
NRTR	Coal	<1	<1	<1	<1	<1	<1	<1
NRTR	Biofuel	-	-	-	-	-	-	-
NRTR	Oil + Gas	100	100	100	100	100	100	100
NRTR	Process	<1	<1	<1	<1	<1	<1	<1
RCOR	**Total**	**3%**	**35%**	**4%**	**6%**	**18%**	**38%**	**54%**
RCOR	Coal	9	13	68	<1	2	13	8
RCOR	Biofuel	57	86	22	96	97	70	92
RCOR	Oil + Gas	34	1	10	3	1	17	<1
RCOR	Process	-	-	-	-	-	-	-
RCOC	**Total**	**1%**	**<1%**	**2%**	**<1%**	**<1%**	**5%**	**4%**
RCOC	Coal	-	47	68	23	16	45	38
RCOC	Biofuel	-	12	1	28	29	28	54
RCOC	Oil + Gas	100	41	31	49	55	27	8
RCOC	Process	-	-	-	-	-	-	-
RCOO	**Total**	**3%**	**3%**	**1%**	**<1%**	**1%**	**6%**	**2%**
RCOO	Coal	2	10	36	12	4	13	22
RCOO	Biofuel	1	21	1	11	23	10	48
RCOO	Oil + Gas	97	69	63	77	73	77	30
RCOO	Process	-	-	-	-	-	-	-
SLV	**Total**	**-**	**-**	**-**	**<1%**	**17%**	**-**	**-**
SLV	Coal	-	-	-	-	-	-	-
SLV	Biofuel	-	-	-	-	-	-	-
SLV	Oil + Gas	-	-	-	-	-	-	-
SLV	Process	-	-	-	100	100	-	-
WST	**Total**	**2%**	**3%**	**<1%**	**14%**	**2%**	**5%**	**13%**
WST	Coal	-	-	-	-	-	-	-
WST	Biofuel	-	-	-	-	-	-	-
WST	Oil + Gas	-	-	-	-	-	-	-
WST	Process	100	100	100	100	100	100	100
SHP	**Total**	**20%**	**<1%**	**12%**	**<1%**	**2%**	**3%**	**1%**
SHP	Coal	-	-	-	-	-	-	-
SHP	Biofuel	-	-	-	-	-	-	-
SHP	Oil + Gas	100	100	100	100	27	100	100
SHP	Process	-	-	-	-	73	-	-

Table S9. Region/Country definitions for main text Fig. 8 and supplemental Fig. S7-S20 (grouped by geographical location)

Region/Country	Member Countries			
Africa	Algeria	Angola	Burundi	Benin
	Burkina Faso	Botswana	Central African Republic	Cote d'Iviore
	Cameroon	Chad	Congo	Comoros
	Cape Verde	DR Congo	Djibouti	Egypt
	Eritrea	Ethiopia	Gabon	Ghana
	Guinea	Gambia	Guinea-Bissau	Equatorial Guinea
	Kenya	Liberia	Libya	Lesotho
	Madagascar	Malawi	Mali	Mauritania
	Mauritius	Morocco	Mozambique	Namibia
	Niger	Nigeria	Reunion	Rwanda
	Sao Tome and Principe	Senegal	Seychelles	Sierra Leone
	Somalia	South Africa	South Sudan	Sudan
	Tunisia	Swaziland	Tanzania	Togo
	Zimbabwe	Uganda	Western Sahara	Zambia
China	China			
Europe	Albania	Austria	Belgium	Bosnia
	Bulgaria	Croatia	Cyprus	Czech Republic
	Denmark	Finland	France	Germany
	Gibraltar	Greece	Greenland	Hungary
	Iceland	Ireland	Italy	Liechtenstein
	Luxembourg	Macedonia	Malta	Montenegro
	Netherlands	Norway	Poland	Portugal
	Romania	Serbia and Montenegro	Slovakia	Slovenia
	Spain	Sweden	Switzerland	Turkey
	United Kingdom			
Former Soviet Union	Armenia	Azerbaijan	Belarus	Estonia
	Georgia	Kazakhstan	Kyrgyzstan	Latvia
	Lithuania	Moldova	Tajikistan	Turkmenistan
	Russia	Ukraine	Uzbekistan	
India	India			
Latin America/Oceania	Antigua and Barbuda	Argentina	Aruba	Bahamas
	Barbados	Belize	Bermuda	Bolivia
	Brazil	British Virgin Islands	Cayman Islands	Chile
	Colombia	Costa Rica	Cuba	Curacao
	Dominica	Dominican Republic	Ecuador	El Salvador
	Faeroe Islands	Falkland Islands	French Guiana	Grenada
	Guadeloupe	Guatemala	Jamaica	Guyana
	Honduras	Haiti	Netherland Antilles	Martinique
	Mexico	Montserrat	Peru	Nicaragua
	Panama	Paraguay	Sint Maarten	Saint Kitts and Nevis
	Saint Lucia	St Pierre and Miquelon	St Vincent and	Suriname
	Trinidad and Tobago	Turks and Caicos Islands	Grenadines	Uruguay
	Venezuela		US Virgin Islands	
North America	United States	Canada	Puerto Rico	
Other Asia/ Pacific	American Samoa	Bangladesh	Bhutan	Brunei Darussalam
	Cambodia	Cook Islands	DPR Korea	FS of Micronesia
	Fiji	French Polynesia	Guam	Hong Kong
	Indonesia	Japan	Kiribati	Laos
	Macao	Malaysia	Maldives	Marshall Islands
	Mongolia	Myanmar	Nepal	New Caledonia
	Niue	Palau	Papua New Guinea	Philippines
	Republic of Korea	Samoa	Singapore	Soloman Islands
	Sri Lanka	Taiwan	Thailand	Timor-Leste
	Tokelau	Tongo	Vanuatu	Vietnam
	Wallis and Futuna Islands			
Australasia	Australia	New Zealand		
Middle East	Afghanistan	Bahrain	Iraq	Islamic Republic of Iran
	Israel	Jordan	Kuwait	Lebanon
	Pakistan	Palestine	Oman	Qatar
	Saudi Arabia	Syria	United Arab Emirates	Yemen

To supplement the results presented in Sect. 3, Fig. S6 provides time series of the contributions of each source sector to global emissions, for each compound. Figures S7-S12 additionally show time series of sectoral emissions of each compound in dominant source regions, including North America, Europe, China, India, Africa, and the Other Asia/Pacific region (Table S9). To highlight the fuel-type information in the CEDS$_{\text{GBD-MAPS}}$ inventory, Fig. S13 also illustrates global emissions of each compound as a function of fuel-group and sector, while Fig. S13-S20 illustrate the fuel-type contributions to emissions from the 11 world regions listed above. Figures S21 and S22 compare CEDS$_{\text{GBD-MAPS}}$ and CEDS$_{\text{Hoesly}}$ emissions. Figures S23 and S24 provide an additional comparison of CEDS$_{\text{GBD-MAPS}}$ global sectoral emissions to sectoral emissions reported from the EDGAR v4.3.2 and GAINS (ECLIPSE v5a) inventories.

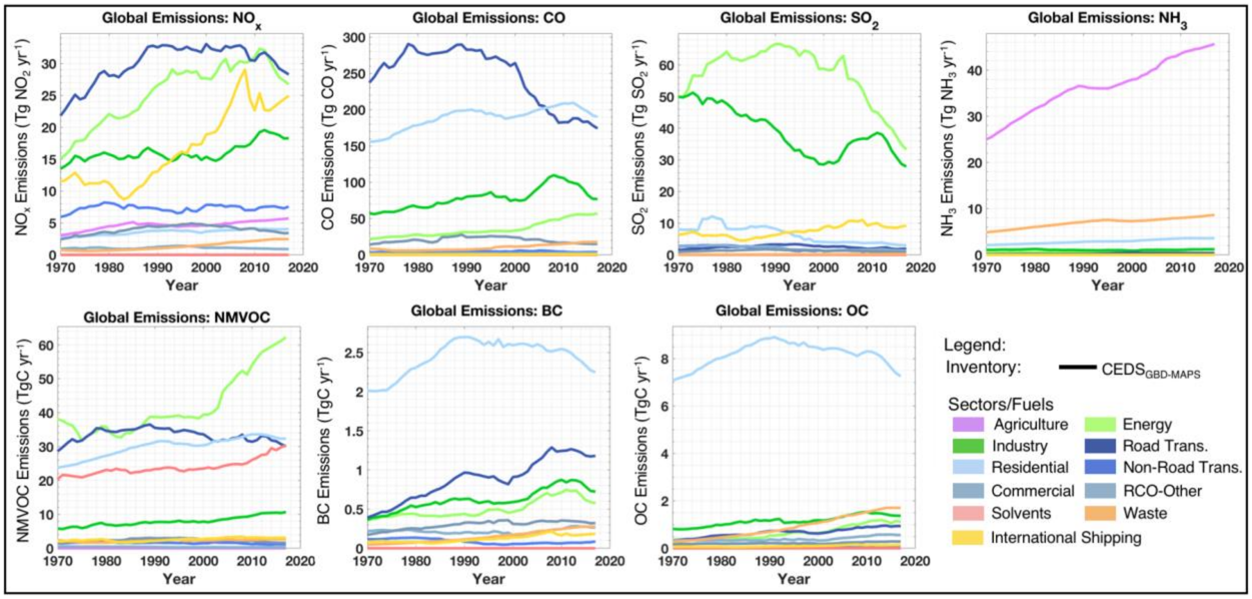

Figure S6. Time series of global emissions for each compound as a function of emission sector (all fuel types shown).

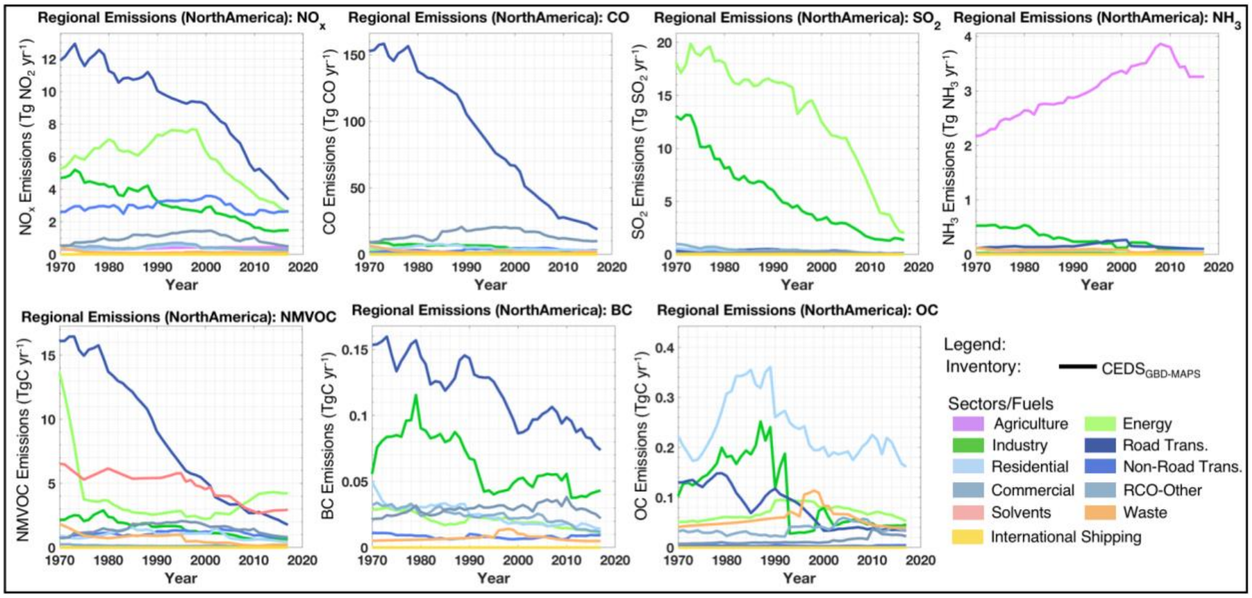

Figure S7. Time series of emissions in North America, as a function of emission sector (all fuel types shown).

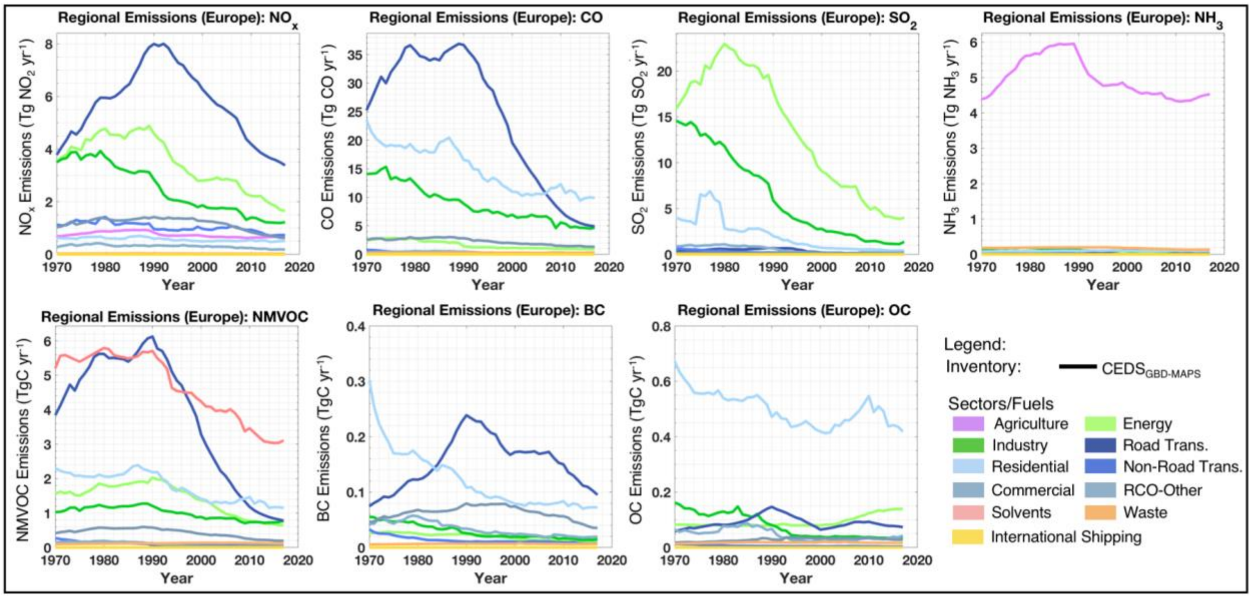

Figure S8. Time series of emissions in Europe, as a function of emission sector (all fuel types shown).

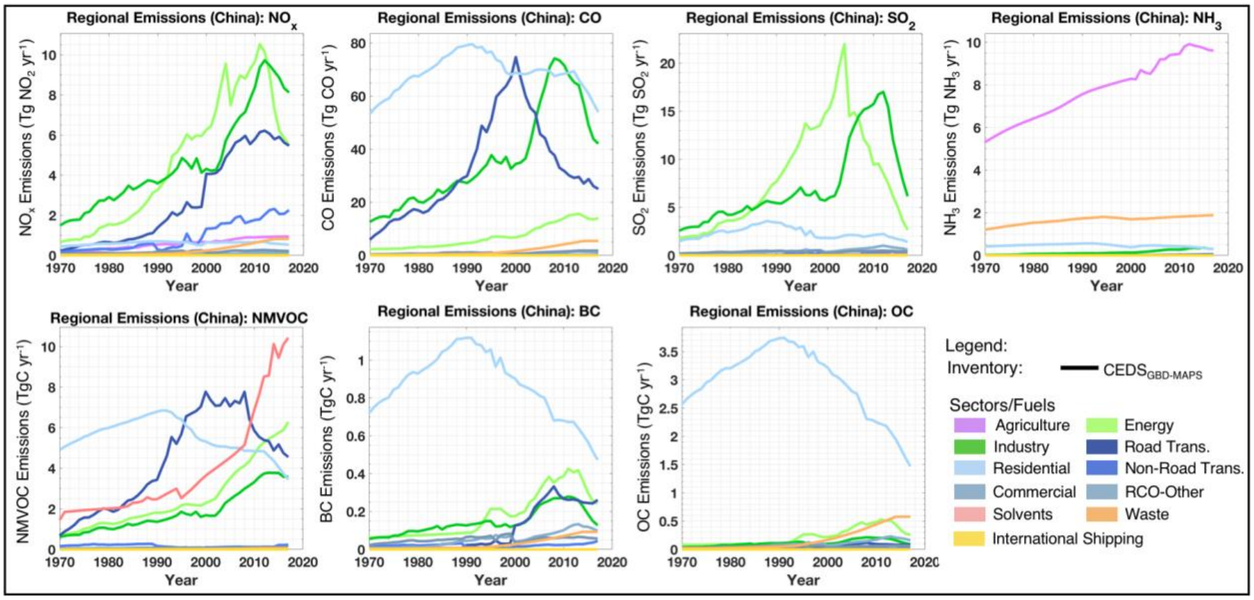

Figure S9. Time series of emissions in China, as a function of emission sector (all fuel types shown).

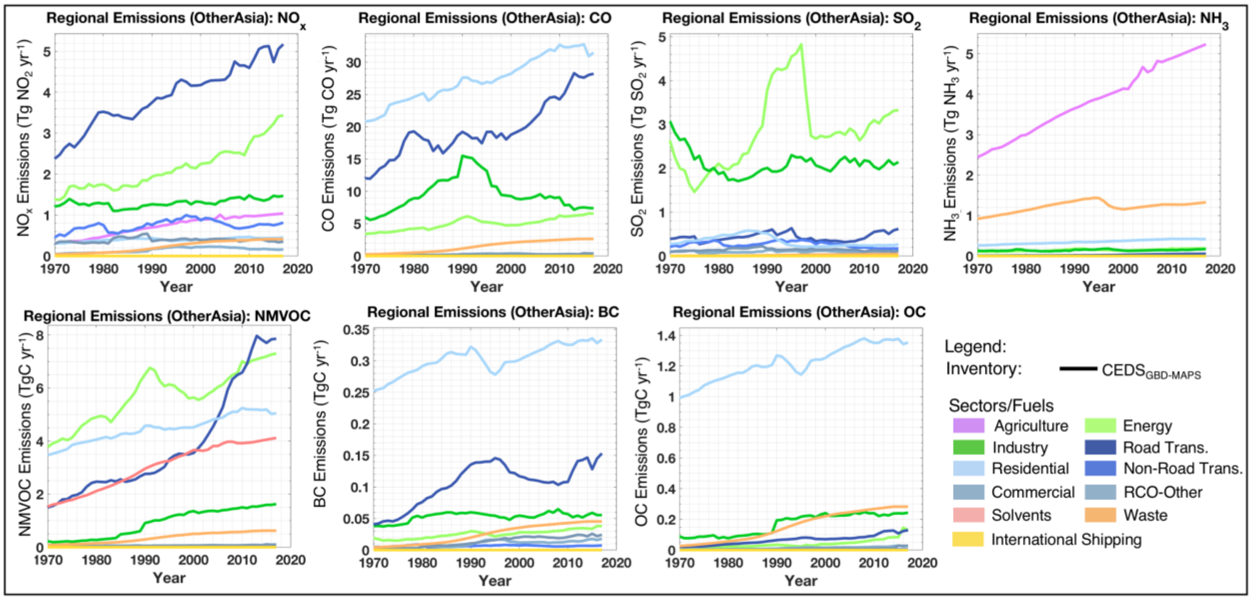

Figure S10. Time series of emissions in the Other Asia/Pacific region (Table S9), as a function of emission sector (all fuel types shown).

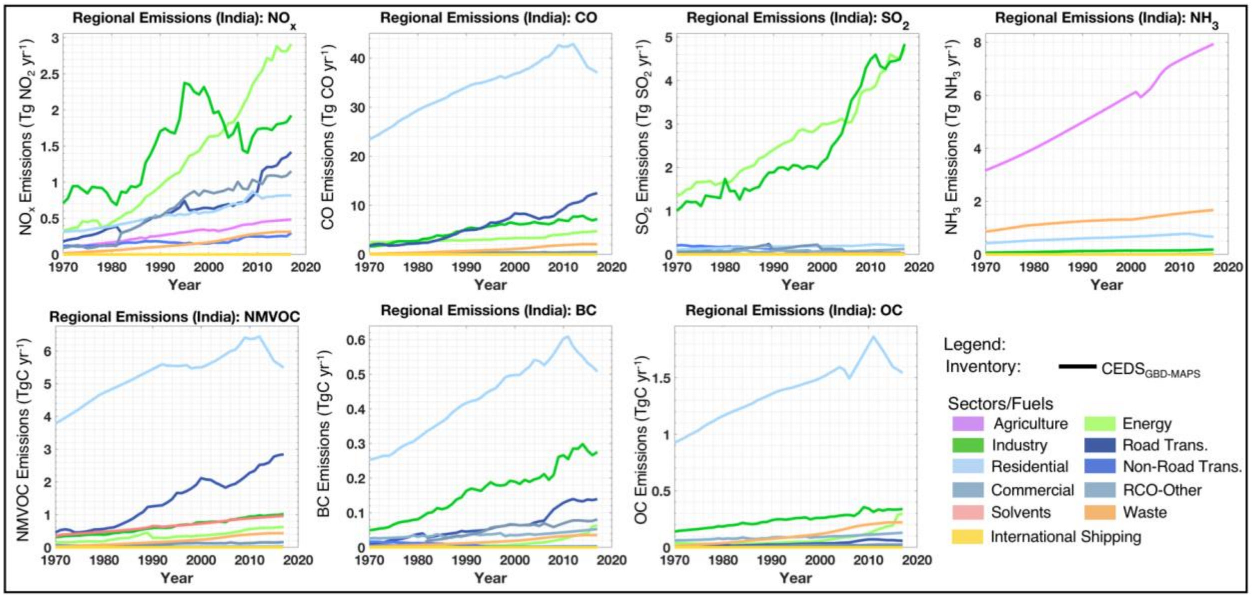

Figure S11. Time series of emissions in India, as a function of emission sector (all fuel types shown).

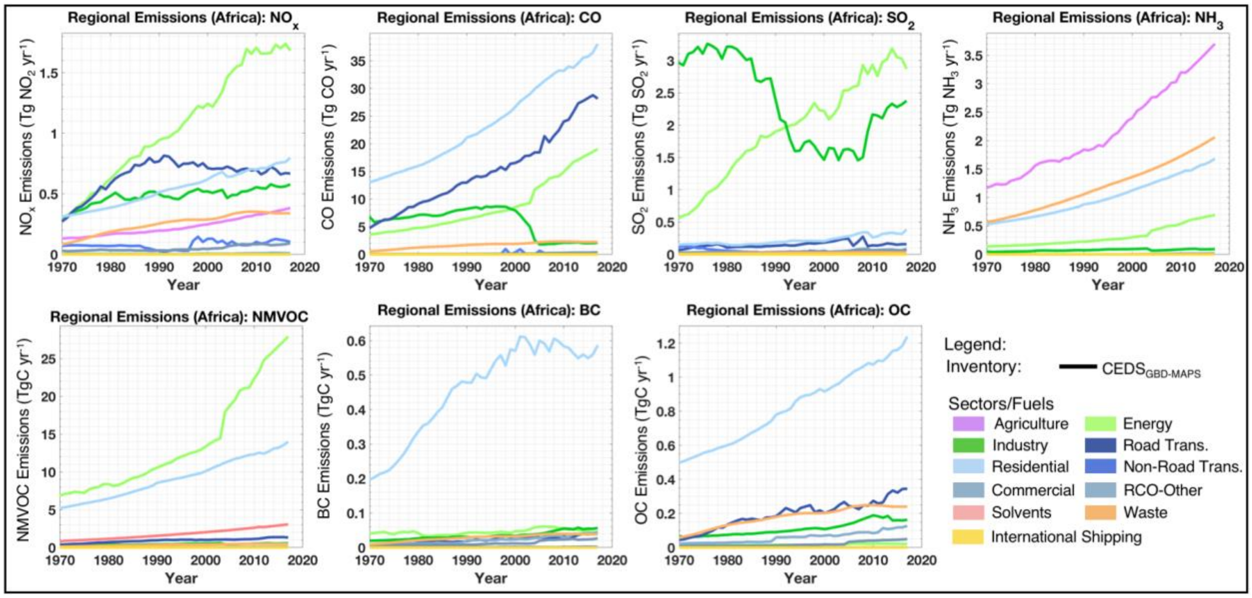

Figure S12. Time series of emissions in Africa, as a function of emission sector (all fuel types shown).

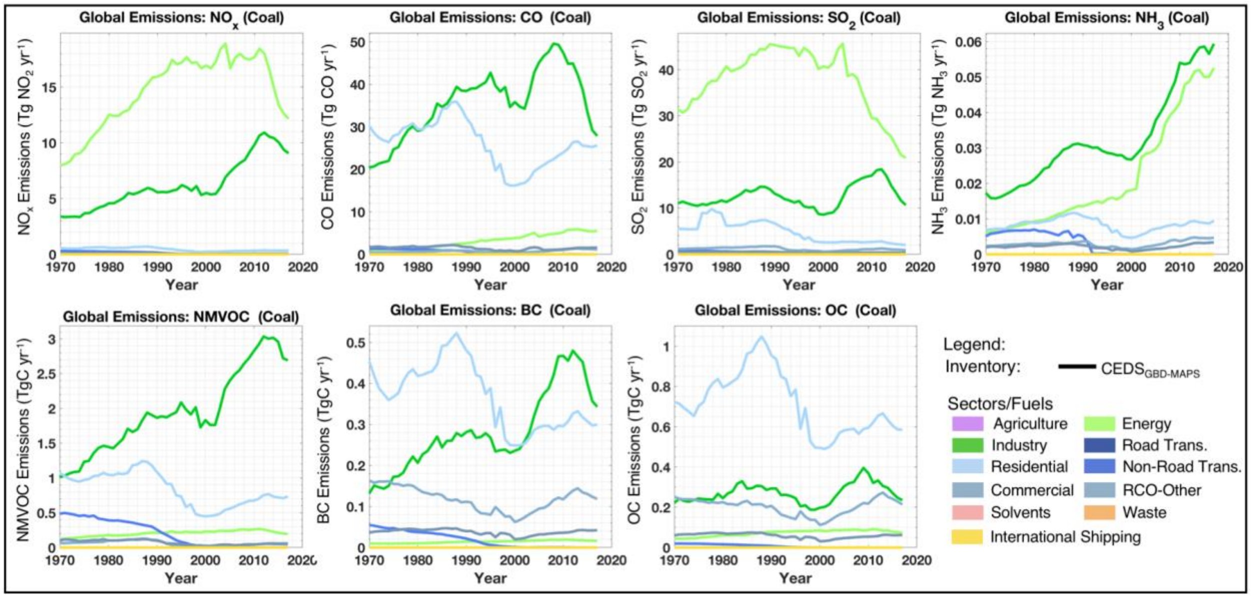

Figure S13. Time series of global sectoral emissions associated with coal combustion.

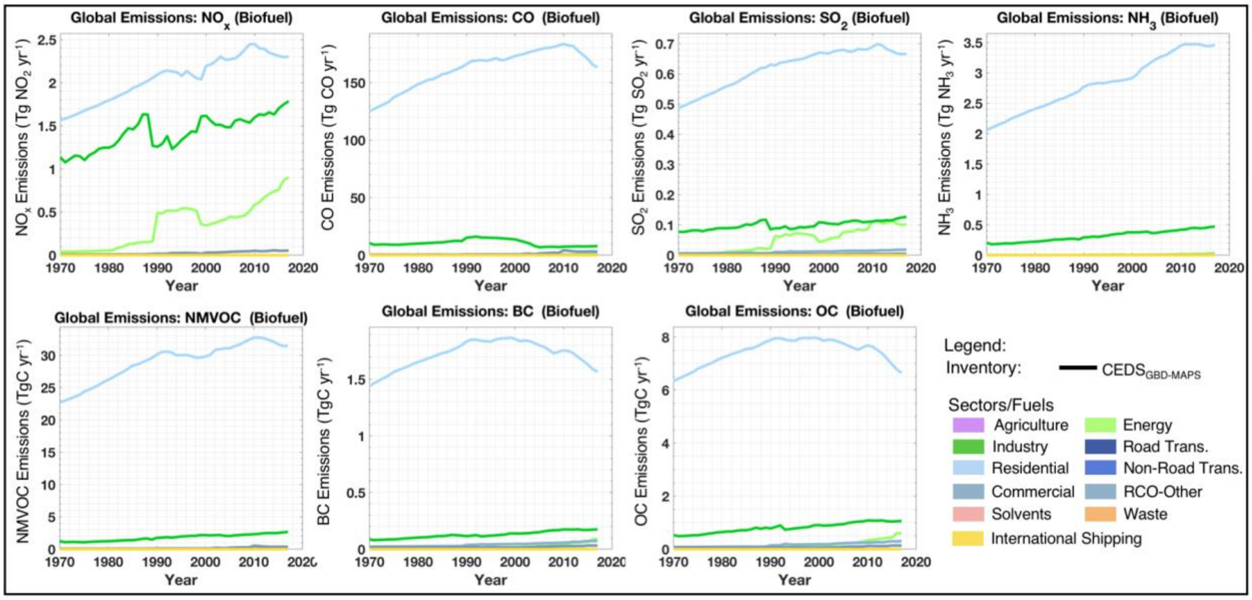

Figure S14. Time series of global sectoral emissions associated with solid biofuel combustion.

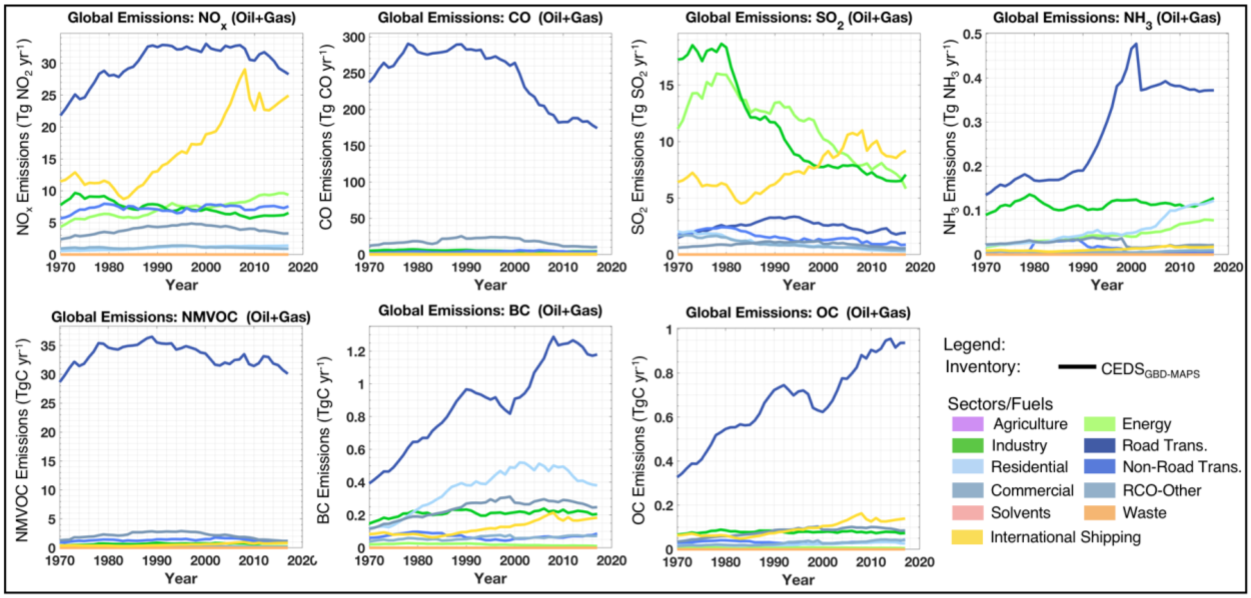

Figure S15. Timeseries of global sectoral emissions associated with the combustion of liquid oil and natural gas.

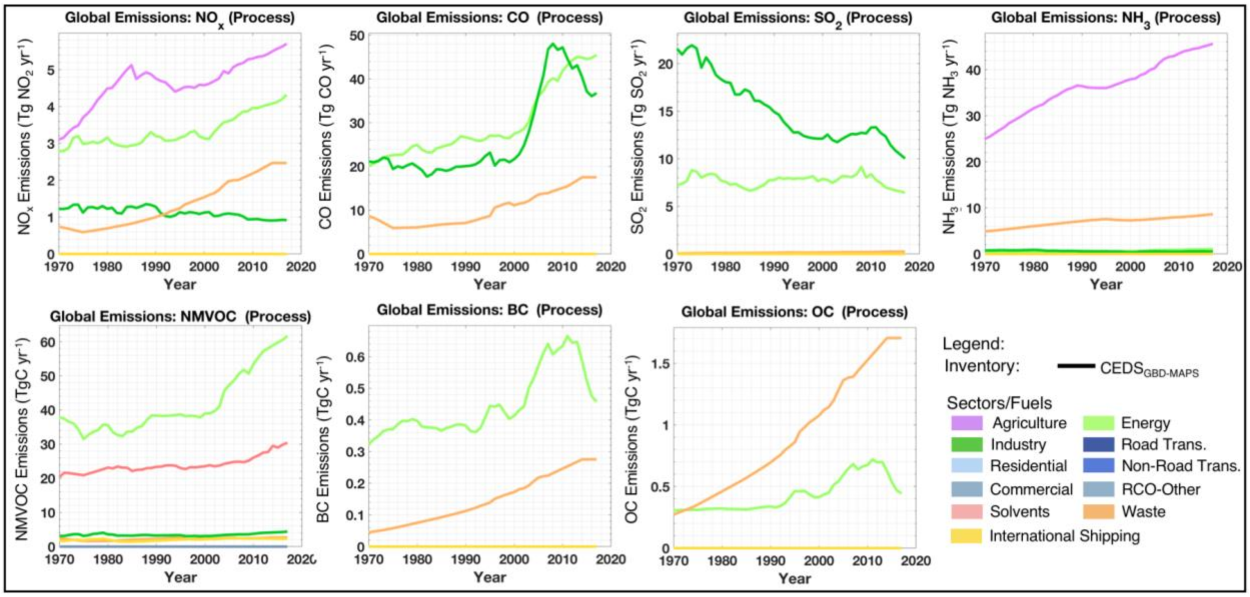

Figure S16. Timeseries of global sectoral emissions associated with CEDS process-level emission sources (Table 2)

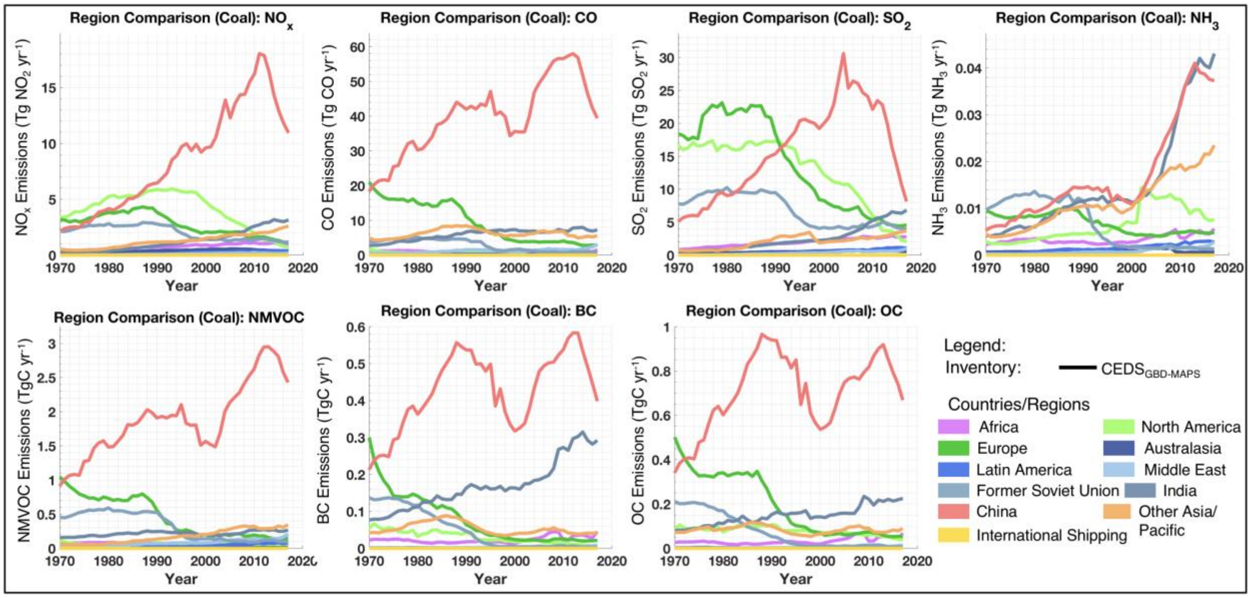

Figure S17. Timeseries of emissions associated with coal combustion, split into contributions from 11 world countries/regions (from coal combustion in all sectors).

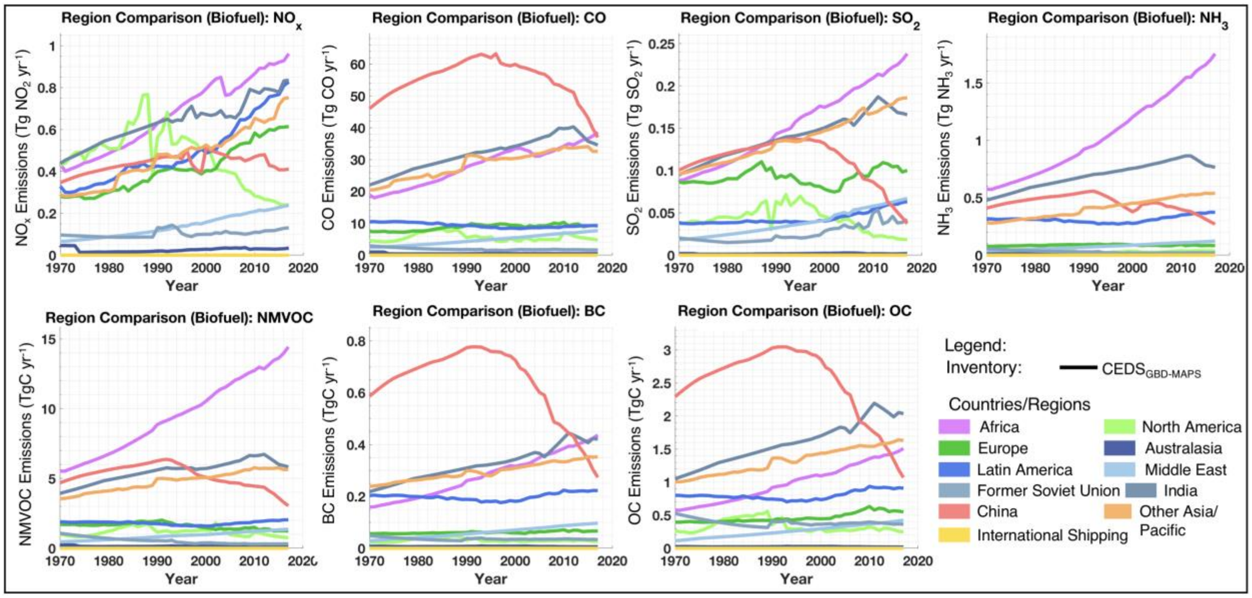

Figure S18. Timeseries of emissions associated with solid biofuel combustion, split into contributions from 11 world countries/regions (from biofuel combustion in all sectors).

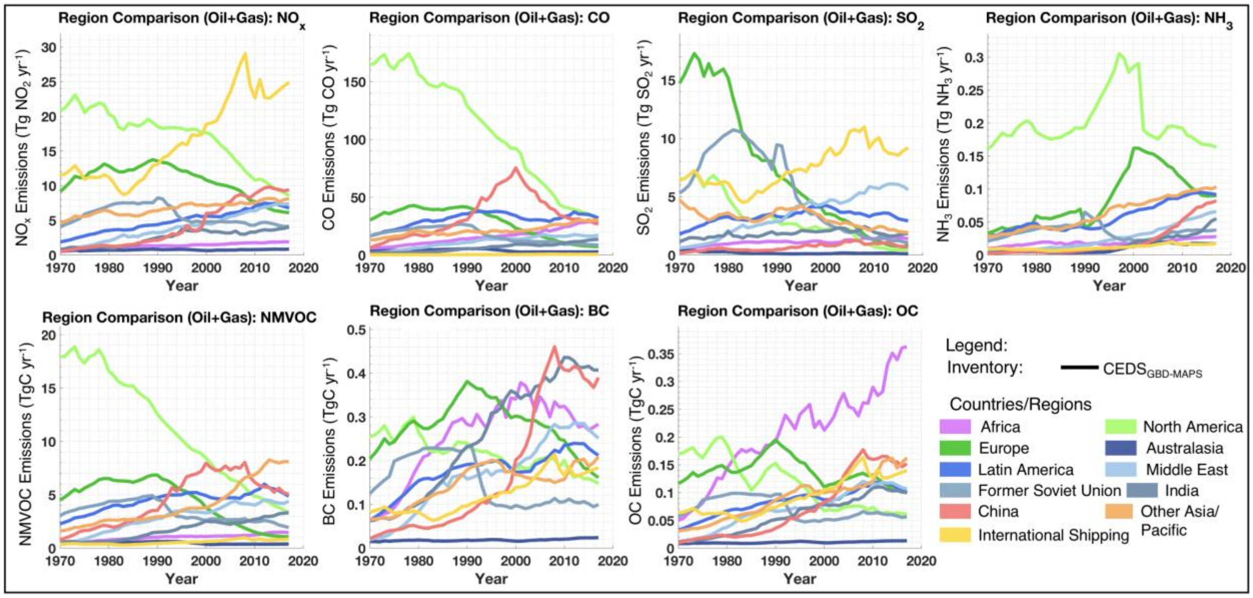

Figure S19. Timeseries of emissions associated with the combustion of liquid oil and natural gas, split into contributions from 11 world countries/regions.

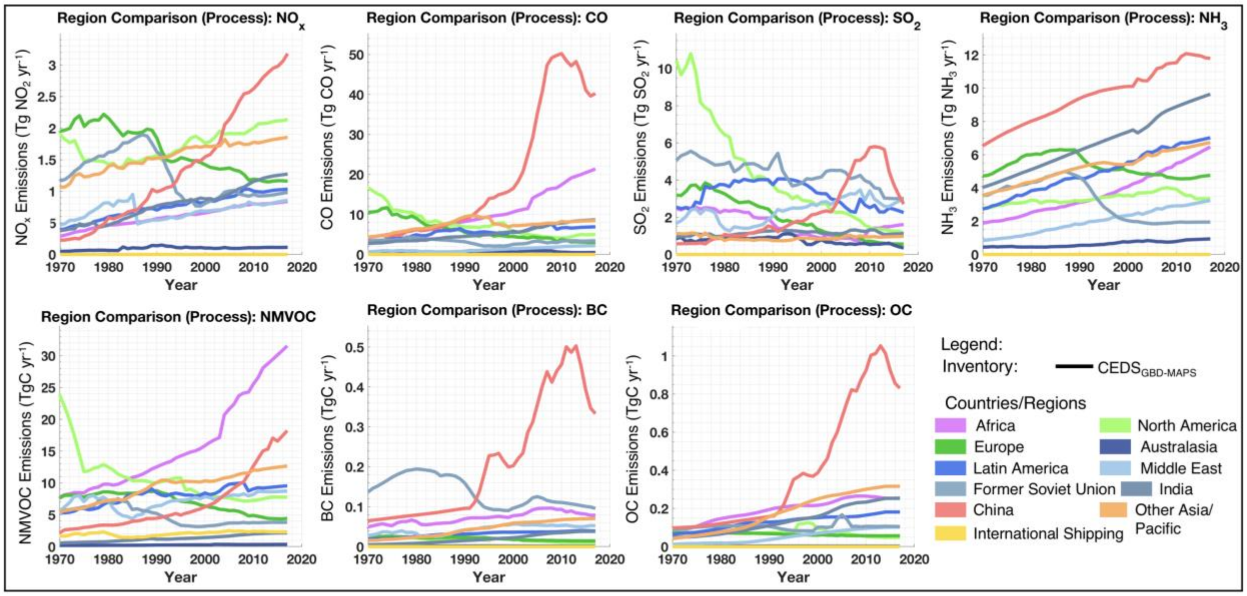

Figure S20. Timeseries of emissions from CEDS process-level sources (Table 2), split into contributions from 11 world countries/regions.

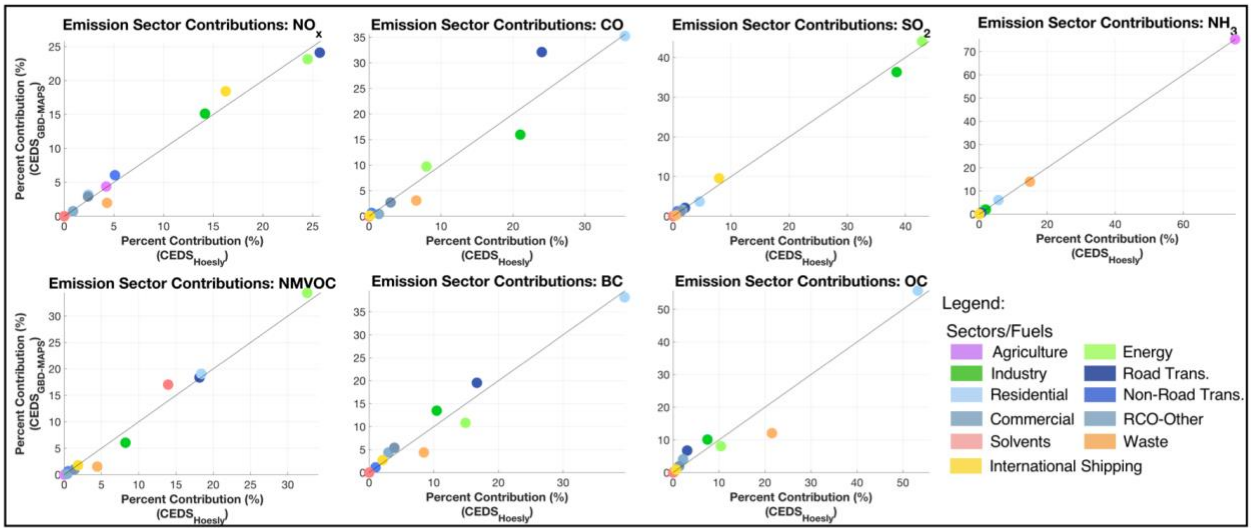

Figure S21. Comparison of CEDS sectoral fractional contributions in the $CEDS_{GBD-MAPS}$ (y-axis) and $CEDS_{Hoesly}$ (x-axis) inventories. Fractional contributions are calculated from global total emissions from all fuel types (= Sector X/ Total global emissions). Black line in the 1:1 line. Points are colored by sector.

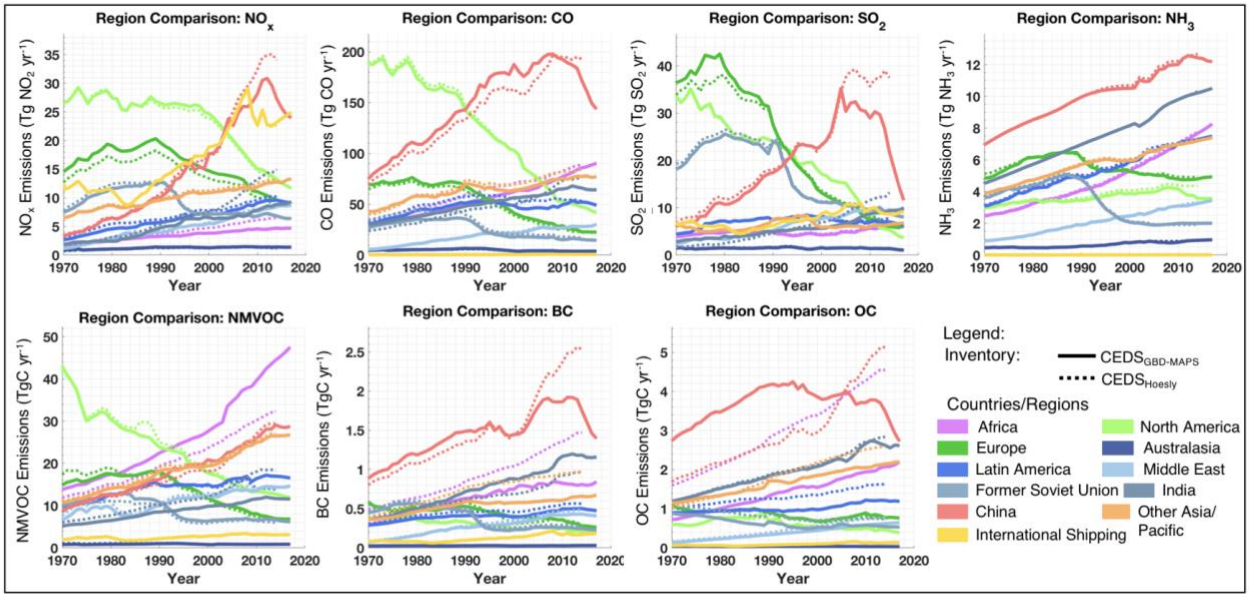

Figure S22. Comparison of CEDS$_{\text{Hoesly}}$ and CEDS$_{\text{GBD-MAPS}}$ emissions as a function of 11 world regions.

Table S10. Mapping between EDGAR v4.3.2, ECLIPSE v5a (GAINS), and CEDS$_{\text{GBD-MAPS}}$ sectors for Fig. S23-S24

Aggregate Figure Sectors	**CEDS$_{\text{GBD-MAPS}}$ Final Sectors**	**EDGAR v4.3.2 Reported Sectors**	**ECLIPSE v5a (gridded data) sectors**
Agriculture	AGR	4A – Enteric fermentation 4B – Manure management 4C – Rice cultivation 4D1/4D2/4D4 – Direct soil emissions	Agriculture – livestock and arable land operations (AGR)
Energy	ENE	1A1a – Public electricity and heat production 1A1bc/1A5 – Other energy industries 1B1 – Fugitive solid fuels 1B2 – Fugitive oil and gas 7A – Fossil fuel fires	Energy – power plants, energy production/ conversion, fossil fuel distribution (ENE)
Industry	IND	1A2 – Manufacturing and Construction 2A1 – Cement Production 2A2 – Lime Production 2A4 – Soda Ash Production 2A7 – Other mineral production 2B – Other Chemical Production 2C – Metal Production 2D – Pulp/paper/food/drink Production	Industrial combustion (IND)
On-road + Non-Road Transportation	ROAD NRTR	1A3b – Road transportation 1A3c – Rail transportation 1A3d – Inland navigation 1A3e – Other transportation	Transport – on-road and non-road (TRA)
Residential + Commercial + Other	RCOR RCOC RCOO	1A4 – Residential and other sectors	Residential and commercial combustion (DOM)
Solvent Use	SLV	3A – Solvent and other product use: paint 3B - Solvent and other product use: degrease 3C - Solvent and other product use: chemicals 3D - Solvent and other product use: other	Solvent use (SLV)
Waste	WST	6A – Solid waste disposal on land 6B – Wastewater handling 6C – Waste incineration 6D – Other waste handling	Waste disposal, including burning (WST)
International Shipping	SHP	1C2 – International shipping	International shipping (SHP)

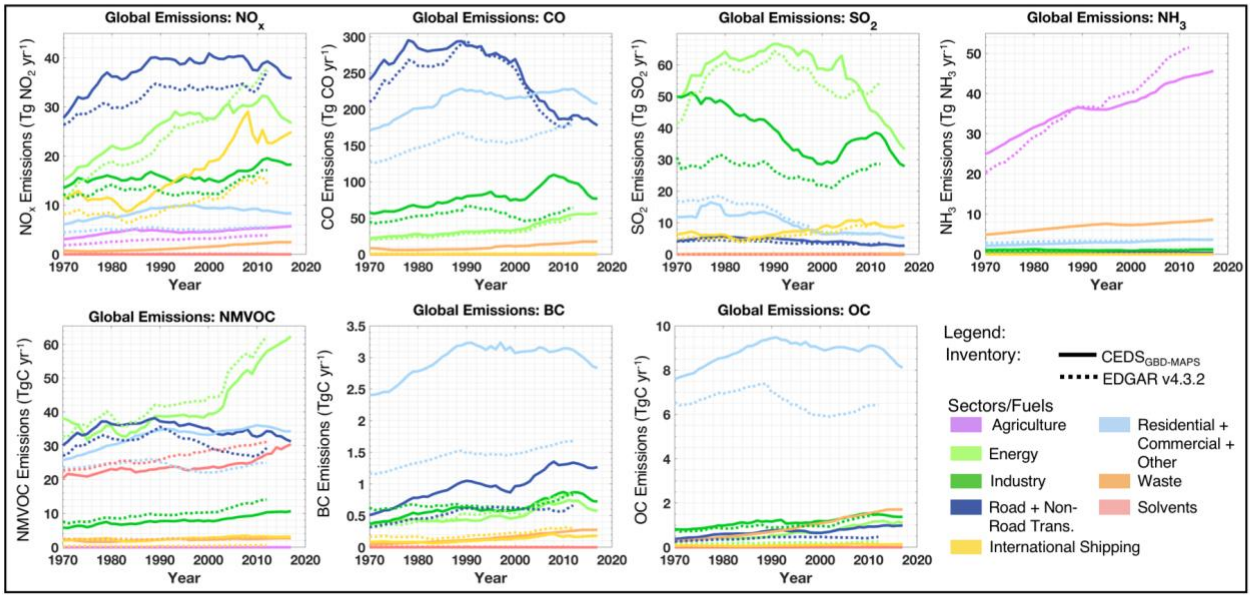

Figure S23. Comparison of sectoral global emissions in CEDS$_{GBD-MAPS}$ and EDGARv4.3.2 inventories. CEDS$_{GBD-MAPS}$ emissions are shown by solid lines, EDGARv4.3.2 data are shown by dashed lines. Sectoral mappings are in Table S10.

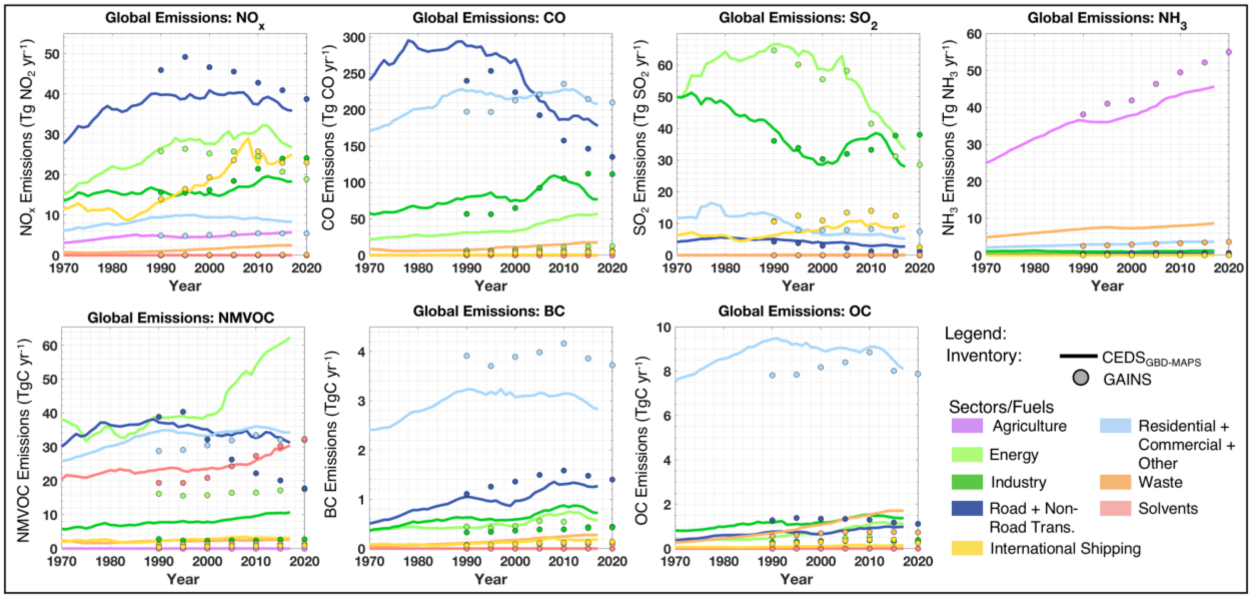

Figure S24. Comparison of sectoral global emissions in CEDS$_{GBD-MAPS}$ and GAINS inventories. CEDS$_{GBD-MAPS}$ emissions are shown by solid lines, GAINS data are shown by dashed lines. Sectoral mappings are in Table S10.

Section S4. Known Inventory Issues

This list is up to date as the submission of the ESSD discussion paper describing the CEDS$_{GBD-MAPS}$ system and the associated data. These issues are in addition to known issues already recognized from the core CEDSv2019-12-23 system (https://github.com/JGCRI/CEDS/issues). New issues after this point will be listed using the issues tracking system on the GitHub repository for both the core CEDS and CEDS$_{GBD-MAPS}$ systems at: https://github.com/JGCRI/CEDS/issues and https://github.com/emcduffie/CEDS/issues.

- SO_2 and NO_x emissions from the energy sector in China are too large between 1978 and 2004. This issue results from an issue in the underlying IEA energy data, which manifests in the spikes in SO_2 and NO_x energy emissions in 2004 that are visible in Fig. S9. This issue may result in up to a 10 Tg overprediction in SO_2 emissions from the energy sector in 2004, which decrease to a maximum possible overprediction of 0.3 Tg by 1978. For NO_x emissions, the maximum overprediction is 4 Tg in 2004, which decreases to 0.1 Tg by 1978.
- As discussed in Sect. S2.3, industrial emissions of NO_x in India may be overpredicted by up to 1 Tg between 1987 and 2014. This results from the potential misallocation of the SMoG-India 'Informal Industry' sector to the $\text{CEDS}_{\text{GBD-MAPS}}$ 1A2c_ind-Comb-Food-tobacco sector, rather than the 1A2g-Comb-Ind-other sector.
- Industry emissions of NO_x and SO_2 in China may not account for emissions from metal smelting due to uncertainties in the MEIC sectoral scaling mapping files for industry sector emissions.
- Residential emissions of SO_2 from the combustion of coal may be over-predicted by up to 4 Tg between 1972 – 1980 (Fig. S13). This sudden increase in emissions from this sector is associated with the $\text{CEDS}_{\text{GBD-MAPS}}$ procedures and not the underlying IEA energy data.

References

Boden, T. A., Marland, G., and Andres, R. J.: Global, Regional, and National Fossil-Fuel CO_2 Emissions, Carbon Dioxide Information Analysis Center, U.S. Department of Energy, Oak Ridge, Tenn., U.S.A., 2016.

Boden, T. A., Marland, G., and Andres, R. J.: Global, Regional, and National Fossil-Fuel CO_2 Emissions, Carbon Dioxide Information Analysis Center, U.S. Department of Energy, Oak Ridge, Tenn., U.S.A., doi: 10.3334/CDIAC/00001_V2017, 2017.

Bond, T. C., Bhardwaj, E., Dong, R., Jogani, R., Jung, S., Roden, C., Streets, D. G., and Trautmann, N. M.: Historical emissions of black and organic carbon aerosol from energy-related combustion, 1850–2000, Global Biogeochemical Cycles, 21, 10.1029/2006GB002840, 2007.

BP: BP Statistical Review of World Energy, bp.com/statisticalreview (last access: 15 January 2018), 2015.

BP: Statistical Review of World Energy: 2019, https://www.bp.com/content/dam/bp/business-sites/en/global/corporate/pdfs/energy-economics/statistical-review/bp-stats-review-2019-full-report.pdf (last access: January 23, 2020), 2019.

Commoner, B., Bartlett, P. W., Eisl, H., and Couchot, K.: Air Transport of Dioxin from North American Sources to Ecologically Vulnerable Receptors in Nunavut, Arctic Canada: Final Report to the North American Commission for Environmental Cooperation., http://www3.cec.org/islandora/en/item/1596-long-range-air-transport-dioxin-from-north-american-sources-ecologically-vulnerable-en.pdf (last access: 25 April, 2020), 2000.

Crippa, M., Guizzardi, D., Muntean, M., Schaaf, E., Dentener, F., van Aardenne, J. A., Monni, S., Doering, U., Olivier, J. G. J., Pagliari, V., and Janssens-Maenhout, G.: Gridded emissions of air pollutants for the period 1970–2012 within EDGAR v4.3.2, Earth Syst. Sci. Data, 10, 1987-2013, 10.5194/essd-10-1987-2018, 2018.

Doxsey-Whitfield, E., MacManus, K., Adamo, S. B., Pistolesi, L., Squires, J., Borkovska, O., and Baptista, S. R.: Taking Advantage of the Improved Availability of Census Data: A First Look at the Gridded Population of the World, Version 4, Papers in Applied Geography, 1, 226-234, 10.1080/23754931.2015.1014272, 2015.

EC-JRC: Emissions Database for Global Atmospheric Research (EDGAR), release EDGARv4.3.2 https://edgar.jrc.ec.europa.eu/overview.php?v=432_AP, https://data.europa.eu/doi/10.2904/JRC_DATASET_EDGAR, (last access: 12 August 2019), 2018.

EC-JRC/PBL: Emission Database for Global Atmospheric Research (EDGAR), release EDGAR v4.2 FT2012, http://edgar.jrc.ec.europa.eu (last access: 15 January 2018), 2012.

EC-JRC/PBL: Emission Database for Global Atmospheric Research (EDGAR), release version 4.3.1, http://edgar.jrc.ec.europa.eu/overview.php?v=431 (last access: 15 January 2018), 2016.

EIA: U.S. Energy Information Administration: Table 10.2a: Renewable Energy Cnsumption, Residential and Commercial Sectors, https://www.eia.gov/totalenergy/data/monthly/#renewable (last access: 26 August 2019), 2019.

EMEP: Officially reported emission data to the European Monitoring and Evaluation Programme: EMEP_NFR14_LEVEL1 data, https://www.ceip.at/ms/ceip_home1/ceip_home/webdab_emepdatabase/reported_emissiondata/(last access: 19 December 2019), 2019.

FAOSTAT: FAOSTAT-Forestry database, http://www.fao.org/forestry/statistics/84922/en/ (last access: 15 January 2018), 2015.

Hoesly, R., O'Rourke, P., Braun, C., Feng, L., Smith, S. J., Pitkanen, T., Siebert, J., Vu, L., Presley, M., Bolt, R., Goldstein, B., and Kholod, N.: CEDS: Community Emissions Data System (Version Dec-23-2019), http://doi.org/10.5281/zenodo.3592073 (last access: March 15, 2020), 2019.

Hoesly, R. M., Smith, S. J., Feng, L., Klimont, Z., Janssens-Maenhout, G., Pitkanen, T., Seibert, J. J., Vu, L., Andres, R. J., Bolt, R. M., Bond, T. C., Dawidowski, L., Kholod, N., Kurokawa, J. I., Li, M., Liu, L., Lu, Z., Moura, M. C. P., O'Rourke, P. R., and Zhang, Q.: Historical (1750–2014) anthropogenic emissions of reactive gases and aerosols from the Community Emissions Data System (CEDS), Geosci. Model Dev., 11, 369-408, 10.5194/gmd-11-369-2018, 2018.

IEA: World Energy Statistics, http://www.iea.org/statistics/ (last access: 15 January 2018), 2015.

IEA: World Energy Statistics 2019 Edition, Database Documentation, http://wds.iea.org/wds/pdf/WORLDBES_Documentation.pdf (last access: 17 September 2019), 2019.

Klein Goldewijk, K., Beusen, A., van Drecht, G., and de Vos, M.: The HYDE 3.1 spatially explicit database of human-induced global land-use change over the past 12,000 years, Global Ecology and Biogeography, 20, 73-86, 10.1111/j.1466-8238.2010.00587.x, 2011.

Klimont, Z., Kupiainen, K., Heyes, C., Purohit, P., Cofala, J., Rafaj, P., Borken-Kleefeld, J., and Schöpp, W.: Global anthropogenic emissions of particulate matter including black carbon, Atmos. Chem. Phys., 17, 8681-8723, 10.5194/acp-17-8681-2017, 2017.

Kurokawa, J., Ohara, T., Morikawa, T., Hanayama, S., Janssens-Maenhout, G., Fukui, T., Kawashima, K., and Akimoto, H.: Emissions of air pollutants and greenhouse gases over Asian regions during 2000–2008: Regional Emission inventory in ASia (REAS) version 2, Atmos. Chem. Phys., 13, 11019-11058, 10.5194/acp-13-11019-2013, 2013.

Marais, E. A., and Wiedinmyer, C.: Air Quality Impact of Diffuse and Inefficient Combustion Emissions in Africa (DICE-Africa), Environ. Sci. Technol., 50, 10739-10745, 10.1021/acs.est.6b02602, 2016.

Meidiana, C., and Gamse, T.: Development of Waste Management Practices in Indonesia, European Journal of Scientific Research, 40, 199-210, 2010.

Nagpure, A. S., Ramaswami, A., and Russell, A.: Characterizing the Spatial and Temporal Patterns of Open Burning of Municipal Solid Waste (MSW) in Indian Cities, Environ. Sci. Technol., 49, 12904-12912, 10.1021/acs.est.5b03243, 2015.

NEI: 2011 National Emissions Inventory (NEI) Data, https://www.epa.gov/air-emissions-inventories/2011-national-emissions-inventory-nei-data(last), 2013.

Reyna-Bensusan, N., Wilson, D. C., and Smith, S. R.: Uncontrolled burning of solid waste by households in Mexico is a significant contributor to climate change in the country, Environmental Research, 163, 280-288, https://doi.org/10.1016/j.envres.2018.01.042, 2018.

Sharma, G., Sinha, B., Pallavi, Hakkim, H., Chandra, B. P., Kumar, A., and Sinha, V.: Gridded Emissions of CO, NOx, SO2, CO2, NH3, HCl, CH4, PM2.5, PM10, BC, and NMVOC from Open Municipal Waste Burning in India, Environ. Sci. Technol., 53, 4765-4774, 10.1021/acs.est.8b07076, 2019.

Stohl, A., Aamaas, B., Amann, M., Baker, L. H., Bellouin, N., Berntsen, T. K., Boucher, O., Cherian, R., Collins, W., Daskalakis, N., Dusinska, M., Eckhardt, S., Fuglestvedt, J. S., Harju, M., Heyes, C., Hodnebrog, Ø., Hao, J., Im, U., Kanakidou, M., Klimont, Z., Kupiainen, K., Law, K. S., Lund, M. T., Maas, R., MacIntosh, C. R., Myhre, G., Myriokefalitakis, S., Olivié, D., Quaas, J., Quennehen, B., Raut, J. C., Rumbold, S. T., Samset, B. H., Schulz, M., Seland, Ø., Shine, K. P., Skeie, R. B., Wang, S., Yttri, K. E., and Zhu, T.: Evaluating the climate and air quality impacts of short-lived pollutants, Atmos. Chem. Phys., 15, 10529-10566, 10.5194/acp-15-10529-2015, 2015.

The World Bank: World Development Indicators, databank.worldbank.org/data/download/WDI_excel.zip (last access: 15 January 2018), 2016.

UN: World Urbanization Prospects: The 2014 Revision, https://esa.un.org/unpd/wup/CD-ROM/WUP2014_XLS_CD_FILES/WUP2014-F01-Total_Urban_Rural.xls (last access: 15 January 2018), 2014.

UN: UN World Population Prospects: The 2015 Revision, http://esa.un.org/unpd/wpp/DVD/ (last access: 15 January 2018), 2015.

UN: World urbanization prospects: The 2018 revision, annual percentage of population at mid-year residing in urban areas by region, subregion, country and area, 1950-2050, https://population.un.org/wup/Download/(last access: 24 July 2019), 2018.

UN: World Population Prospects 2019: Total population (both sexes combined) by region, subregion and country, annually for 1950 to 2100, https://esa.un.org/unpd/wpp/Download/Standard/Population/(last), 2019.

US EPA: An inventory of sources and environmental releases of dioxin-like compounds in the U.S. for the years 1987, 1995, and 2000, U.S. Environmental Protection Agency, Washington DC, EPA/600/P-03/002F, 2006.

Venkataraman, C., Brauer, M., Tibrewal, K., Sadavarte, P., Ma, Q., Cohen, A., Chaliyakunnel, S., Frostad, J., Klimont, Z., Martin, R. V., Millet, D. B., Philip, S., Walker, K., and Wang, S.: Source influence on emission pathways and ambient PM2.5 pollution over India (2015–2050), Atmos. Chem. Phys., 18, 8017-8039, 10.5194/acp-18-8017-2018, 2018.

Wiedinmyer, C., Yokelson, R. J., and Gullett, B. K.: Global Emissions of Trace Gases, Particulate Matter, and Hazardous Air Pollutants from Open Burning of Domestic Waste, Environ. Sci. Technol., 48, 9523-9530, 10.1021/es502250z, 2014.

Zheng, B., Tong, D., Li, M., Liu, F., Hong, C., Geng, G., Li, H., Li, X., Peng, L., Qi, J., Yan, L., Zhang, Y., Zhao, H., Zheng, Y., He, K., and Zhang, Q.: Trends in China's anthropogenic emissions since 2010 as the consequence of clean air actions, Atmos. Chem. Phys., 18, 14095-14111, 10.5194/acp-18-14095-2018, 2018.